JOURNAL OF TELECOMMUNICATIONS AND INFORMATION TECHNOLOGY

Preface

The dynamics of telecommunication sector development and strong competition in this sector in most countries induce telecommunication operators to use new computerized tools. Such tools might help in planning network development, in assessing financial and economic standing, in network design and management, in corporate management including strategic decisions and negotiations of interconnection agreements. The intensive development and decreasing costs of information technology increase the availability of such tools. On July 18–20 2007, the National Institute of Telecommunications in Warsaw, Poland, organized the *6th International Conference on Decision Support for Telecommunications and Information Society* (*DSTIS*), with 68 participants from 7 countries. The aim of DSTIS conference was to bring together international experts and researchers working in decision support and related fields, in order to present diverse methods and tools of decision analysis and support as well as knowledge engineering and knowledge management applied in telecommunications industry and for information society, together with diverse economic and computational aspects related to the main themes. The conference had following session themes: Modeling Fundamentals, Game Theory and Applications, Economics and Decisions, Routing and Traffic Control, Multicriteria Tools, Telecommunication Markets and Knowledge Engineering.

In this issue of our *Journal*, we present selected nine papers from the DSTIS conference, followed by two papers from an earlier ICTON conference also organized by the National Institute of Telecommunications. We hope to present several further papers from DSTIS conference in the next issues.

Andrzej P. Wierzbicki
Guest Editor

Paper

Traffic splitting in MPLS networks – a hierarchical multicriteria approach

José M. F. Craveirinha, João C. N. Clímaco, Marta M. B. Pascoal, and Lúcia M. R. A. Martins

Abstract—In this paper we address a new hierarchical multicriteria routing model associated with a two-path traffic splitting routing method in MPLS networks whereby the bandwidth required by a given node-to-node traffic flow is divided by two disjoint paths. The model has two levels of objective functions and several constraints. An algorithmic approach is presented for calculating non-dominated solutions and selecting good compromise solutions to this problem. Also a number of computational experiments are presented.

Keywords— multicriteria optimization, multicriteria shortest paths, routing telecommunication networks, Internet/MPLS.

1. Introduction

Routing problems in modern multiservice communication networks involve the calculation of paths satisfying various technical constraints (usually quality of service (QoS) related constraints) and seeking simultaneously to "optimize" relevant metrics. The multiplicity of QoS metrics and cost functions which may be involved in the models and the potential conflicts among such metrics/functions make that there are potential advantages in developing multicriteria routing models in this area, which depend on the features of the network functionalities and the adopted routing framework. An overview of applications of multicriteria decision analysis (MCDA) tools to important telecommunications network planning and negotiation problems can be seen in [7]. A state of art review on applications of MCDA to telecommunication network planning and design problems, including a section on routing models is in [1], while an overview and a case study on multicriteria routing models in telecommunication networks is presented in [2].

In particular the multiprotocol label switching (MPLS) platform for IP networks enables the implementation of advanced routing schemes, namely explicit routes satisfying QoS requirements, and is prepared for dealing with multipath routing, including traffic splitting. MPLS is a recent multiservice Internet technology based on the forwarding of packets using a specific packet label switching technique. Among other advanced routing mechanisms the utilization of explicit – routes is characterized by the fact the path, designated as label switched path (LSP), followed by each node-to-node packet stream of a certain type, is entirely determined by the ingress router (corresponding to the originating node). This technological platform is prepared to deal with *multi-path routing*, using the concept of *traffic splitting* that consists of the division of the packet stream of each flow, along two or more disjoint paths such that the sum of the bandwidths available in those paths satisfies the bandwidth requirement of each type of flow, depending on the service class.

In this work we address a new hierarchical multicriteria routing model associated with a two-path traffic splitting routing method in MPLS networks whereby the bandwidth required by a given node-to-node traffic flow is divided by two disjoint paths.

In telecommunication routing models the objective functions are concerned with the necessity of minimizing the consumption of (transmission) resources along a path and to obtain a minimum negative impact on all traffic flows that may use the network. The specific models of these cost functions and of the QoS constraints depend on the type of service associated with the connections which are being routed from origin to destination, as it is the case in the MPLS networks.

The proposed model has two levels of objective functions and several constraints. The formulated multicriteria problem involves the calculation of a pair of disjoint paths for a given node-to-node traffic flow such that the sum of the minimal available bandwidths in the paths (usually designated as "bottleneck bandwidths") is not less than the bandwidth required for that traffic flow (two-path traffic splitting constraint); in the considered problem formulation for real-time traffic a constraint on the maximal number of arcs per path also has to be satisfied. The upper-level objective functions are a "load balancing" cost function that is the sum of the load balancing costs associated with the two paths (the load balancing cost being an additive metric, which seeks to achieve an optimal distribution of traffic throughout the network) and the sum of the number of arcs of both paths (which seeks to optimize the number of used resources and favours path reliability). The two lower-level objective functions are the minimal bottleneck bandwidth in both paths and the maximal estimated delays in the two paths.

An algorithmic approach is presented for calculating non-dominated solutions and selecting good compromise solu-

tions to this problem, taking into account the two optimization levels. The resolution approach begins with the calculation of non-dominated solutions with respect to the first level objective functions by using a new algorithm [4] and includes the definition of preference thresholds for these functions in order to establish a flexible preference system in the first level. The second level objective functions are then just used to obtain bounds for "filtering" a certain number of the most preferred non-dominated solutions of the first level. Also a number of computational experiments were performed with an application model focusing on a video traffic routing application, to show the effectiveness of the proposed algorithm. The application platform used the "GT-ITM Georgia Tech Internetwork Topology Models" software[1] which enabled to generate and analyse a significant variety of randomly generated Internet network topologies, following certain probabilistic laws.

This paper is organized as follows. In Section 2 we describe in detail the proposed multicriteria routing model for two-path traffic splitting and the corresponding mathematical formulation. Section 3 presents the developed resolution approach, including a brief description of the algorithm developed for finding non-dominated pairs of disjoint loopless paths as well as the preference system model. The application model for traffic routing in randomly generated Internet topologies and some computational results are shown in Section 4. Finally in Section 5 we put forward some conclusions and outline future work on this model.

2. Hierarchical multicriteria routing model with traffic splitting

This is an area where there are potential advantages in introducing multicriteria routing approaches, taking into account the network major functional features and the nature of the multiple QoS metrics. Here we will begin by describing the nature and aim of the specific objective functions involved in this new hierarchical multicriteria routing model for MPLS networks with a two-path traffic splitting mechanism.

The first objective function considered in the first optimization level is a "load balancing" cost function that is the sum of the cost associated with the two paths, where the load balancing cost of an arc is a piecewise linear function of the bandwidth used in the arc. This is a function which has been used in previous multicriteria routing models, namely in [8] and in the tricriteria model for MPLS networks in [6].

The minimization of this function aims at minimizing the negative impact on the remaining network flows resulting from the utilization of a given path by the considered node-to-node flow. This function is formalized as follows, for any pair of disjoint simple paths, q and q':

$$\Phi^*(q,q') = \Phi(q) + \Phi(q'), \qquad \Phi(p) = \sum_{(i,j)\in p} \phi_{ij},$$

where ϕ_{ij} is the load balancing cost associated with arc (i,j), given by

$$\phi_{ij} = \begin{cases} o_{ij}, & 0 \le o_{ij}/R_{ij} \le 0.5 \\ 2o_{ij} - \frac{1}{2}R_{ij}, & 0.5 < o_{ij}/R_{ij} \le 0.6 \\ 5o_{ij} - \frac{23}{10}R_{ij}, & 0.6 < o_{ij}/R_{ij} \le 0.7 \\ 15o_{ij} - \frac{93}{10}R_{ij}, & 0.7 < o_{ij}/R_{ij} \le 0.8 \\ 60o_{ij} - \frac{453}{10}R_{ij}, & 0.8 < o_{ij}/R_{ij} \le 0.9 \\ 300o_{ij} - \frac{2613}{10}R_{ij}, & 0.9 < o_{ij}/R_{ij} \le 1\,, \end{cases}$$

where $o_{ij} = R_{ij} - b_{ij}$ is the bandwidth occupied in arc (i,j), and b_{ij} is the available bandwidth in arc (i,j) with capacity R_{ij}.

As for the second objective function in the first level it is simply the sum of the number of arcs in the two paths:

$$h^*(q,q') = h(q) + h(q'),$$

where $h(p)$ denotes the number of arcs of path p. The aim of this function is to seek the minimization of the resources used by the given traffic flow hence favouring the network traffic carrying capability (specially for high loads) as well as the path reliability (under failure of links or arcs).

The optimization of these two function seeks, in an approximate manner, to minimize the negative impact of the use of the two paths, in the remaining traffic flows in the network. Next we will consider two functions for the second priority level which seek to optimize transmission related QoS parameters for the particular node-to-node flow that is being routed through the two paths. The first of these functions is the minimum of the available bandwidths in the links of the two paths (*bottleneck bandwidths*, b), that should be maximized:

$$b^*(q,q') = \min\{b(q), b(q')\} = \min_{(i,j)\in q,q'} \{b_{ij}\};\ b(q) = \min_{(i,j)\in q} \{b_{ij}\}.$$

This function aims at distributing the load of the flow through paths with the least occupied links.

The second function considered in this level is the maximal average delay experienced along the two paths, to be minimized:

$$d^*(q,q') = \max\{d(q), d(q')\};\ \ d(q) = \sum_{(i,j)\in q} d_{ij},$$

where d_{ij} is the average packet delay on link (i,j). This function seeks the choice of pairs of paths with minimal average packet delay.

[1] Available at http://www.cc.gatech.edu/fac/Ellen.Zegura/graphs.html

Concerning the constraints, the first one corresponds to the *traffic-splitting* requirement using two paths, i.e., the sum of the bottleneck bandwidths in the two disjoint paths cannot be less than the bandwidth required by micro-flows (i.e., end-to-end connections with given QoS requirements) of the considered node-to-node flow, $\Delta_{\text{bandwidth}}$:

$$\text{for any } \; q,q' \in \mathcal{P}, \quad b(q)+b(q') \geq \Delta_{\text{bandwidth}}. \qquad (1)$$

The second constraint which may be considered in the model is a "jitter" related constraint, which may be transformed, for certain queueing disciplines (namely for weighted fair queueing discipline), into a constraint on the maximal number of arcs per path, Δ_{jitter}:

$$\text{for any } \; q,q' \in \mathcal{P}, \quad h(q),h(q') \leq \Delta_{\text{jitter}}. \qquad (2)$$

This constraint is important for certain types of QoS traffic flows (i.e., with guaranteed levels of quality of service) as in the case of video traffic considered in the application model and may be eliminated for best effort traffic flows for which there is no such guarantee of QoS.
The considered *hierarchical multicriteria routing problem* can then be formulated, designating by $\mathcal{P}$ the set of feasible paths:

- 1st level
$$\begin{cases} \min\limits_{q,q' \in \mathcal{P}} \Phi^*(q,q') \\ \min\limits_{q,q' \in \mathcal{P}} h^*(q,q'), \end{cases} \qquad (3)$$
- 2nd level
$$\begin{cases} \max\limits_{q,q' \in \mathcal{P}} b^*(q,q') \\ \min\limits_{q,q' \in \mathcal{P}} d^*(q,q'), \end{cases}$$

subject to the constraints (1) and (2).
The addressed hierarchical multicriteria routing problem consists of finding "satisfactory" compromise solutions (q,q'), $q,q' \in \mathcal{P}$, where q and q' are disjoint loopless paths, taking into account the optimization hierarchy.

3. Resolution approach

In general problem (3) does not have an optimal solution (pair of disjoint paths) due to possible conflict between the considered first level functions.
Thus, it will be necessary to consider the set of "non-dominated" solutions, i.e., solutions such that there is no other feasible solution which improves one objective function without worsening the second objective function.
The definition of dominance in terms of two functions c and h (to be minimized) is recalled:

Definition 1: Given solutions a and b, a dominates b ($a_D b$) if and only if $c(a) \leq c(b)$, $h(a) \leq h(b)$ and at least one of the inequalities is strict. Solution b is dominated if and only if there is another solution, say a, such that $a_D b$.
$\mathcal{P}_N$ will denote the set of non-dominated solutions.

The first stage of the developed approach [4] is the creation of a modified network in which a pair of disjoint paths in the original network corresponds to a single path in the new network. This modification of the network is as follows. We will begin by introducing the basic mathematical notation. Let $(\mathcal{N},\mathcal{A})$ be a directed network where $\mathcal{N}$ is the node set and $\mathcal{A}$ denotes the arc (or link) set. A path p from $s \in \mathcal{N}$ to $t \in \mathcal{N}$ is a sequence of the form $p = \langle s = v_0, v_1, \ldots, t = v_{h(p)} \rangle$, where $(v_k, v_{k+1}) \in \mathcal{A}$, for any $k \in \{0,\ldots,h(p)-1\}$; nodes s and t are called the initial and terminal nodes of p, which correspond in our model to ingress and egress MPLS routers; p is a simple (or loopless) path if it has no repeated nodes. $\mathcal{P}_{xy}$ will denote the set of paths from node x to node y and two paths p,q from s to y are node-disjoint iff the only nodes they have in common are x and y.
The steps of the modification of the network topology are then:

- Duplicate the nodes: $\mathcal{N}' = \mathcal{N} \cup \{i' : i \in \mathcal{N}\}$.
- Duplicate the arcs and add a new arc linking t and the new s': $\mathcal{A}' = \mathcal{A} \cup \{(i',j') : (i,j) \in \mathcal{A}\} \cup \{(t,s')\}$.
- Maintain the initial node: s.
- Consider a new terminal node: t'.

Concerning the objective function coefficients $\phi_{i'j'}$ and $h_{i'j'}$ associated with each arc $(i',j') \in \mathcal{A}'$ the new coefficients are:

- $\phi_{i'j'} = \phi_{ij}$, if $(i,j) \in \mathcal{A}$, and $\phi_{t,s'} = 0$,
- $h_{i'j'} = h_{ij} = 1$, if $(i,j) \in \mathcal{A}$, and $h_{t,s'} = 0$.

Each simple path p from s to t' in $(\mathcal{N}',\mathcal{A}')$ corresponds to a pair of paths from s to t in $(\mathcal{N},\mathcal{A})$, i.e., there exist $q \in \mathcal{P}_{st}$ and $q' \in \mathcal{P}'_{s't'}$, such that

$$p = q \diamond (t,s') \diamond q'.$$

Thus, if $q \cap q' = \emptyset$, then q,q' correspond to a pair of disjoint simple paths in $(\mathcal{N},\mathcal{A})$.
Figure 1 illustrates, in a simplified manner, the construction of the modified network.

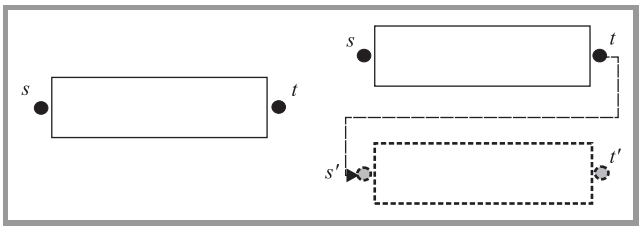

Fig. 1. Original and correspondent augmented networks.

It is also assumed that a transmission capacity $R_{ij} \in \mathbb{R}^+$ (usually expressed in bit/s) and the available bandwidth, b_{ij}, are assigned to each link (i,j).

The first stage of the approach is the resolution of the first level bicriterion problem by calculating the non-dominated solutions set by an adaptation of the algorithm in [3] based on a simple path ranking method by [9].

The resolution is based on the ranking of simple feasible (with respect to constraints (1) and (2)) paths by non-decreasing order of Φ^* in the modified network $(\mathcal{N}',\mathcal{A}')$, until the value of this function is greater than a certain value $\hat{\phi}$. Firstly this value $\hat{\phi}$ (which works as stopping criterion of the algorithm) is obtained by minimising h^*, i.e., it is the value Φ^* when h^* is optimal; if there are alternative optimal solutions to h^*, $\hat{\phi}$ is the least possible value of Φ^* among those solutions. A dominance test is then used to select the non-dominated paths of the augmented network that are calculated as explained above. The dominance test based on [3] is now presented.

Let Φ_{ca} and h_{ca} be the objective function values corresponding to the last candidate to non-dominated path in $(\mathcal{N}',\mathcal{A}')$ as expressed above. Note that the first one, in the initialization of the process, is the optimal path with respect to Φ. If there are alternative optimal paths, the one with the least value of h is selected. Let $p_k = q_k \diamond (t,s') \diamond q'_k$ be the path under test in $(\mathcal{N}',\mathcal{A}')$. Noting that $\Phi^*(q_k,q'_k) = \Phi(p_k)$ and $h^*(q_k,q'_k) = h(p_k)$:

1. If $\Phi(p_k) = \Phi_{\text{ca}}$
   - and $h(p_k) < h_{\text{ca}}$, then p_k dominates the candidate path and it is a new candidate to be non-dominated; update h_{ca};
   - and $h(p_k) = h_{\text{ca}}$, then p_k is added to the candidate path set;
   - and $h(p_k) > h_{\text{ca}}$, then p_k is dominated by the previous candidate.
2. If $\Phi(p_k) > \Phi_{\text{ca}}$
   - and $h(p_k) < h_{\text{ca}}$, then the candidate path remains in the non-dominated candidate path set and p_k is added as a new element of this set; update Φ_{ca} and h_{ca};
   - and $h(p_k) > h_{\text{ca}}$, then p_k is dominated by the previous candidate.

In order to define a system of preferences for the non-dominated solutions of the first level, the next stage of the algorithmic approach is the calculation of preference thresholds corresponding to required (aspiration level) and acceptable (reservation level) values for the objective functions Φ^* and h^*. These thresholds are used to define regions in the first level objective function space, with different priority requirements, which enable the ordering of the candidate solutions in $\mathcal{P}'_N$, the set of non-dominated paths in $(\mathcal{N}',\mathcal{A}')$. It is important to note that the consideration of these preference thresholds is a simple and efficient manner of enabling an automated decision process, as required in this multicriteria routing method.

Preference thresholds can be easily calculated in the modified network in the following manner:

- Required (aspiration level) and acceptable (reservation level) values of h, h_{req} and h_{acc}, respectively:

$$h_{\text{req}} = \text{int}(\overline{m}_p) + 1, \quad h_{\text{acc}} = \text{int}(\overline{m}_p) + \Delta_{\text{arcs}} - 1,$$

  ($\Delta_{\text{arcs}} > 2$), where $\text{int}(x)$ is the smallest integer greater than or equal to x, and $\overline{m}_p$ is the average value of the feasible shortest path lengths for all node pairs in the modified network.

- Required and acceptable values of Φ, Φ_{req} and Φ_{acc}, respectively:

$$\Phi_{\text{req}} = (\overline{\Phi}_{\min} + \Phi_m)/2, \quad \Phi_{\text{acc}} = (\overline{\Phi}_{\max} + \Phi_m)/2,$$

  where $\overline{\Phi}_{\min}$, $\overline{\Phi}_{\max}$ are the average minimal and maximal feasible path costs Φ for all node pairs in the modified network, and $\Phi_m = (\overline{\Phi}_{\min} + \overline{\Phi}_{\max})/2$.

Therefore a region with the highest priority (region A as exemplified in Fig. 2) may be defined by the points for which both the required values Φ_{req} and h_{req} are satisfied. Second priority regions (B_1 and B_2 in Fig. 2) may also be defined by the points for which only one of the requested values is satisfied while the reservation level for the other function is not exceeded. Also a region with third priority (C) may be calculated, such that only the reservation levels for both functions are satisfied, while the aspiration levels are exceeded.

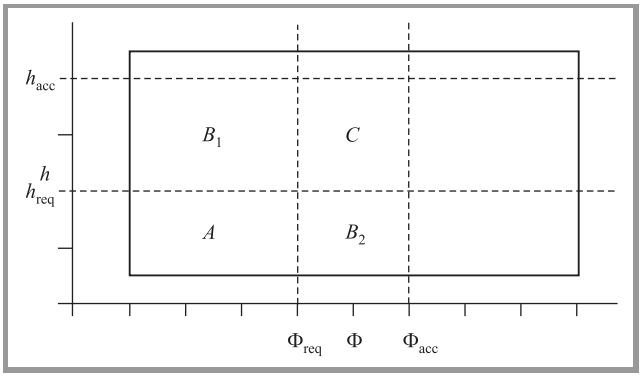

Fig. 2. Priority regions.

The final stage of the resolution approach involves the selection of the non-dominated solutions of the first level, which are filtered according to acceptance bounds defined from the second level objective functions. Therefore these bounds, b_m, a lowerbound on bottleneck bandwidth, and, d_M, an upperbound on delay, work as a filtering mechanism to the non-dominated solutions and are defined as follows.

Let $p = q \diamond (t,s') \diamond q'$, be a path in $(\mathcal{N}',\mathcal{A}')$ (corresponding to a 1st level non-dominated solution). Then:

$$b_m = \min\{b(q^*), b(q'^*)\},$$

where $p^* = \text{argmin}_p\{\max\{d(q), d(q')\} : p = q \diamond (t,s') \diamond q' \in \mathcal{P}'_N\}$, and

$$d_M = \max\{d(q'), d(q'')\},$$

where $p' = \text{argmax}_p\{\min\{b(q), b(q')\} : p = q \diamond (t,s') \diamond q' \in \mathcal{P}'_N\}$.

Finally the solution(s) of the first level with higher priority which satisfy these bounds will be selected as compromise solution(s) to the problem.

Note that it could be considered limitative to analyse exclusively non-dominated solutions of the first level having in mind that there is a second level of criteria evaluation. Also it may be advisable, in some cases, to widen the set of possible compromise solutions to be filtered by the final stage of the resolution approach. So, similarly to the approach in [2] we may consider ε-non-dominated solutions in the first level, the value of ε being tuned according to the specific application environment. Furthermore the consideration of ε-non-dominated solutions, in the upper optimization level enhances the model flexibility. In fact, the widening of the set of solutions under analysis can be accompanied by the tightening of the bounds obtained from the second level or *vice-versa*. Hence the combination of the variation in ε and in the bounds from the second level enables the representation of the relative importance of both levels to be "calibrated", in the solution selection stage. In this manner the flexible nature of our multicriteria model can be reinforced.

4. Application model and computational results

In order to test the hierarchical multicriteria routing model and resolution approach described in the previous sections a C language program implementing such an approach was written and some computational experiments were run for a specific application problem.

The presented model was applied to a video traffic routing problem in a MPLS type network. The network topologies used for that purpose where generated with the "GT-ITM Georgia Tech Internetwork Topology Models" software. This software allows the calculation of randomly generated Internet topologies with different architectures and using various types of laws for defining the probability of occurrence of an edge between any two given nodes, typically as an exponential function of the Euclidian distance between the nodes and some calibrating parameters. These models seek to better reflect the structure of real Internet type networks. Since we wanted to have a control over the average node degree, we used, as the more adequate edge probability distribution, the Doar-Leslie model [5]. This was calibrated, for each given number of nodes, to obtain approximately the desired average node degree. The considered networks had $30, 50, 100, 150, 200$ nodes and an average node degree of 4. For each number of nodes 10 network topologies were generated and for each network 20 source-destination node pairs were considered.

In the video traffic routing problem each node is assumed to be modeled as a queueing system using weighted fair queueing (WFQ) service discipline, enabling the bound on jitter to be represented through a constraint on the number of arcs Δ_{jitter}. Each arc (i,j) was assigned with the available bandwidth b_{ij} and the average packet delay d_{ij}. Values $b_{ij} \in \{0.52, \ldots, 150.52\}$ (in Mbit/s) were randomly generated according to the empirical statistical distribution:

I_0	I_1	I_2	I_3	I_4
50%	20%	15%	10%	5%

,

where I_i are intervals with equal amplitude defined by

$$I_i = \{0.52 + 2k : k = 15i, \ldots, 15(i+1) - 1\},\ i = 0,1,2,3,$$

$$I_4 = \{0.52 + 2k : k = 60, \ldots, 75\},$$

and considering a fixed total link capacity of 155.52 Mbit/s. Values d_{ij} were obtained by an empirical model and depend on the Euclidean distance between the nodes i and j, on the bandwidth capacity $R_{ij} = 155.52$ Mbit/s and on parameters associated with the generation rate of a leaky bucket as in [10].

The constraints for these experiments were $\Delta_{\text{bandwidth}} = 1.5$ Mbit/s, $\Delta_{\text{delay}} = 60$ ms, and $\Delta_{\text{jitter}} = m_p(s,t) + \Delta_{\text{arcs}}$, where $m_p(s,t)$ denotes the minimal number of arcs of a feasible path from s to t in $(\mathcal{N},\mathcal{A})$ and $\Delta_{\text{arcs}} = 6$.

The computational tests performed on the instances generated under the above specifications ran on a core 2 at 1.66 GHz, with 1 MB of cache and 1 Gbit of RAM, running over SUSE Linux 10.2. Figure 3 depicts the solutions found for two problems in 100 node networks and one problem for a 200 node network, respectively. The bullets correspond to the non-dominated solutions of the 1st level set accepted after the 2nd bounds level have been applied, while the points marked with "$\times$" correspond to non-dominated solutions which did not satisfy the bounds of the 2nd level.

Tables 1, 2 and 3 show the function values associated with the solutions, as well as the required and acceptable values for the 1st level objective functions (also represented in the pictures), and the bounds d_M and b_m obtained from the 2nd level and used for filtering the 1st level solutions. Here the best bandwidth and delay values are marked in italic, and the value of the other function, that defines one of the bounds, is shown in bold.

In the first example of the 100 node network (Fig. 3a) all the solutions found at the 1st level, (1), (2) and (3), are accepted through the bounds of the 2nd level. Therefore solution (2) in the higher priority region is selected.

In the example of Table 2 and Fig. 3b (in a network with $n = 100$) only solution (1) was accepted while (2) was

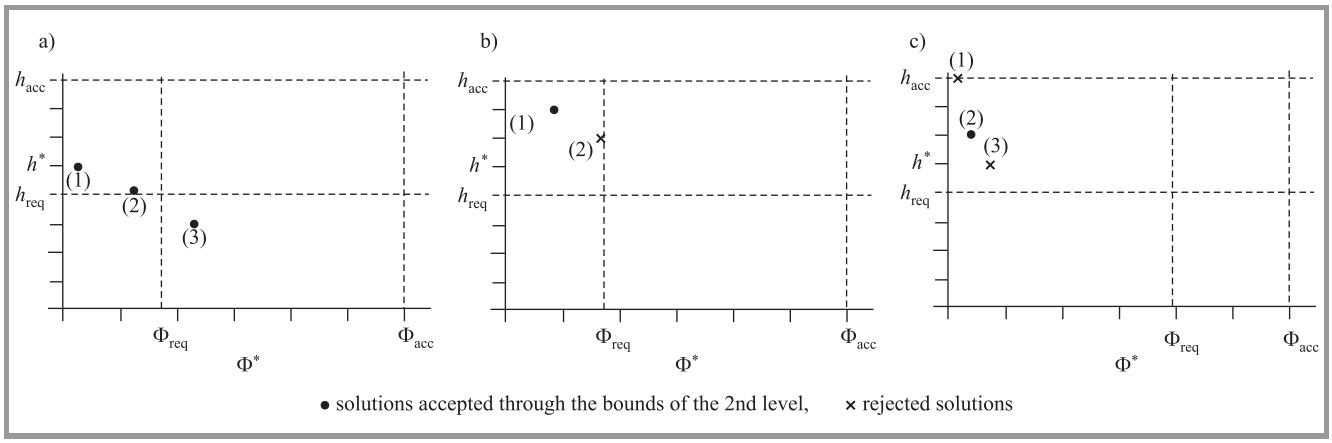

Fig. 3. First level solution for: (a) first and (b) second source-destination pair of 100 node network; (c) of 200 node network.

Table 1
Solutions for the first source-destination pair of nodes ($n = 100$), case Fig. 3a

• 1st level solutions (in the augmented network)

Sol.	Φ^*	h^*	b^*	d^*
(1)	567.24005	5	*72.52*	**6.42697**
(2)	760.20813	4	44.52	4.87697
(3)	940.87207	3	**40.52**	*3.59157*

	h^*	Φ^*
Req.	4	894.10822
Acc.	8	1622.09253

• Solutions accepted through bounds d_M and b_m (in the original network)

Sol.	Path	Φ	h	b	d
(1)	1	267.00003	3	80.52	4.82696
	2	300.24005	2	72.52	6.42697
(2)	1	471.96802	2	44.52	3.09157
	2	288.24005	2	70.52	4.87697
(3)	1	468.90405	2	40.52	3.59157
	2	471.96802	1	44.52	3.09157

	d_M	b_m
Bounds	6.42697	40.52

Table 2
Solutions for the second source-destination pair of nodes ($n = 100$), case Fig. 3b

• 1st level solutions (in the augmented network)

Sol.	Φ^*	h^*	b^*	d^*
(1)	685.24005	7	**62.52**	**6.26236**
(2)	833.14404	6	44.52	6.26236

	h^*	Φ^*
Req.	4	894.10822
Acc.	8	1622.09253

• Solution accepted through bounds d_M and b_m (in the original network)

Sol.	Path	Φ	h	b	d
(1)	1	364.00006	3	82.52	5.96236
	2	321.24002	4	62.52	6.26236

	d_M	b_m
Bounds	6.26236	62.52

Table 3
Solutions for a source-destination pair of nodes ($n = 200$), case Fig. 3c

• 1st level solutions (in the augmented network)

Sol.	Φ^*	h^*	b^*	d^*
(1)	749.72009	9	62.52	7.63314
(2)	787.72003	7	**62.52**	**5.96236**
(3)	861.50409	6	60.52	6.16236

	h^*	Φ^*
Req.	5	1487.28198
Acc.	9	2029.37366

• Solution accepted through bounds d_M and b_m (in the original network)

Sol.	Path	Φ	h	b	d
(2)	1	401.24005	4	62.52	5.96236
	2	386.48007	3	64.52	5.46236

	d_M	b_m
Bounds	5.96236	62.52

rejected. Note that in this case both solutions have the same d^* and we have chosen as bound b_m the most demanding value of b^* (62.52). In the example of Table 3 out of the 3 solutions only solution (2) was accepted through the bounds obtained in the 2nd level, since we have considered (analogously to the previous example) the most demanding value of d^* as bound, for the two solutions (1) and (2) with equal maximal b^*.
Finally, note that when solutions with the same value of one of the metrics appear in the list of selected paths, if required, they can be reordered according to the metric which distinguishes those solutions.

5. Conclusions

A new hierarchical multicriteria routing model associated with a two-path traffic splitting routing method in MPLS networks whereby the bandwidth required by a given node-to-node traffic flow is divided by two disjoint paths, was presented. An algorithmic approach for calculating non-dominated solutions (or ε non-dominated) in the first level and selecting good compromise solutions to this problem, taking into account the objective functions of the second level, was proposed. The resolution approach begins with the calculation of non-dominated solutions with respect to the first level objective functions by using a new algorithm [4] and includes the definition of preference thresholds for these functions in order to establish a flexible preference system in the first level. The second level objective functions are then just used to obtain bounds for "filtering" a certain number of the most preferred non-dominated solutions of the first level. This approach seems highly adequate to an automated decision process, as required by a communication network routing system, having in mind its efficiency and flexibility.
Some computational experiments with an application model focusing on a video-traffic routing problem in randomly generated Internet type topologies were presented, to show the effectiveness of the proposed approach. The calculation of ε non-dominated solutions in the first level combined with variable "filtering" bounds defined in the second level, can be used in the context of the developed procedure in order to increase the flexibility of the approach.

Acknowledgments

Work partially supported by programme POSI of the EC programme cosponsored by FEDER and national funds.

References

[1] J. Clímaco and J. Craveirinha, "Multiple criteria decision analysis – state of the art surveys", in *International Series in Operations Research and Management Science*, J. Figueira, S. Greco, and M. Erghott, Eds. New York: Springer, 2005, pp. 899–951.

[2] J. Clímaco, J. Craveirinha, and M. Pascoal, *Multicriteria Routing Models in Telecommunication Networks – Overview and a Case Study*. Amsterdam: IOS Press, 2007, chapt. 1, pp. 17–46.

[3] J. Clímaco and E. Martins, "A bicriterion shortest path algorithm", *Eur. J. Oper. Res.*, vol. 11, pp. 399–404, 1982.

[4] J. C. N. Clímaco and M. M. B. Pascoal, "Finding non-dominated shortest pairs of disjoint simple paths", Technical Report, no. 3, INESC-Coimbra, 2007.

[5] M. Doar and I. M. Leslie, "How bad is naive multicast routing?", in *INFOCOM (1)*, San Francisco, USA, 1993, pp. 82–89.

[6] S. C. Erbas and C. Erbas, "A multiobjective off-line routing model for MPLS networks", in *Proc. 18th Int. Teletraf. Congr.*, Berlin, Germany, 2003.

[7] J. Granat and A. P. Wierzbicki, "Multicriteria analysis in telecommunications", in *Proc. 37th Ann. Hawaii Int. Conf. Syst. Sci.*, Hawaii, USA, 2004.

[8] J. Knowles, M. Oates, and D. Corne, "Advanced multi-objecive evolutionary algorithms applied to two problems in telecommunications", *British Telecom Technol. J.*, vol. 18, no. 4, pp. 51–65, 2000.

[9] E. Martins, M. Pascoal, and J. Santos, "Deviation algorithms for ranking shortest paths", *Int. J. Foundat. Comput. Sci.*, vol. 10, no. 3, pp. 247–263, 1999.

[10] C. Pornavalai, G. Chakraborty, and N. Shiratori, "Routing with multiple QoS requirements for supporting multimedia applications", *Telecommun. Syst.*, vol. 9, pp. 357–373, 1998.

José Manuel Fernandes Craveirinha is full Professor in telecommunications at the Department of Electrical Engineering and Computers of the Faculty of Sciences and Technology of the University of Coimbra, Portugal, since 97. He obtained the following degrees: undergraduate diploma in electrical engineering science (E.E.S.) – telecommunications and electronics at IST, Lisbon Technical University (1975); M.Sc. (1981) and Ph.D. in E.E.S. at the University of Essex (UK) (1984) and Doct. of Science ("Agregado") in E.E.S. telecommunications at the University of Coimbra (1996). Previous positions were: Associate Professor and Assistant Professor at FCTUC, Coimbra Univ., Telecommunication R&D Engineer (at CET-Portugal Telecom). He coordinated a research group in Teletraffic Engineering & Network Planning at INESC-Coimbra R&D Institute since 1986 and was Director of this institute in 1994–99. He is author and co-author of more than 100 scientific and technical publications in teletraffic modeling, reliability analysis, planning and optimization of telecommunication networks. His main present interests are in reliability analysis models and algorithms and multicriteria routing models for optical and multiservice-IP/MPLS networks.

e-mail: jcrav@deec.uc.pt
Departamento de Engenharia Electrotécnica
e Computadores
Polo II da Universidade de Coimbra
Pinhal de Marrocos
3030-290 Coimbra, Portugal

Instituto de Engenharia de Sistemas
e Computadores – Coimbra
Rua Antero de Quental, 199
3000-033 Coimbra, Portugal

João Carlos Namorado Clímaco is full Professor at the Faculty of Economics of the University of Coimbra, Portugal, and President of the Scientific Committee of the INESC-Coimbra. He obtained the M.Sc. degree in control systems at the Imperial College of Science and Technology, University of London (1978); the "Diploma of Membership of the Imperial College of Science and Technology" (1978); the Ph.D. in optimization and systems theory, electrical engineering, University of Coimbra (1982); and the title of "Agregado" at the University of Coimbra (1989). He was, in the past, Vice-President of ALIO – Latin Ibero American OR Association, Vice-President of the Portuguese OR Society and Member of the International Executive Committee of the International Society on Multiple Criteria Decision Making. Actually he is Member of the IFIP WG 8.3 on Decision Support Systems. He belongs to the editorial board of the following scientific journals: "Journal of Group Decision and Negotiation" (JGDN), "International Transactions in Operational Research" (ITOR), "Investigação Operacional" (IO) – "Journal of the Portuguese OR Society" – and "ENGEVISTA" (a Brazilian journal). He is author and co-author of 95 papers in scientific journals and 30 papers in specialized books. His current major interests of research are: multiple criteria decision aiding, multi-objective combinatorial problems, and management and planning of telecommunication networks and energy systems.

e-mail: jclimaco@inescc.pt
Instituto de Engenharia de Sistemas
e Computadores – Coimbra
Rua Antero de Quental, 199
3000-033 Coimbra, Portugal

Faculdade de Economia da Universidade de Coimbra
Avenida Dias da Silva, 165
3004-512 Coimbra, Portugal

Marta Margarida Braz Pascoal is an Assistant Professor at the Mathematics Department of the Faculty of Science and Technology of the University of Coimbra, Portugal. She obtained the undergraduate diploma in mathematics – specialization in computer science at the University of Coimbra (1995), the M.Sc. degree in applied mathematics at the University of Coimbra (1998) and the Ph.D. in mathematics – specialization in applied mathematics at the University of Coimbra (2005). Her current major interests of research are: ranking solutions of combinatorial problems and multiobjective combinatorial problems.

e-mail: marta@mat.uc.pt
Instituto de Engenharia de Sistemas
e Computadores – Coimbra
Rua Antero de Quental, 199
3000-033 Coimbra, Portugal

Departamento de Matemática
Polo I da Universidade de Coimbra
Apartado 3008
3001-454 Coimbra, Portugal

Lúcia Martins received the Ph.D. degree in electrical engineering (telecommunications and electronics) from the University of Coimbra, Portugal, in 2004. She worked as development engineer for six years in Portugal Telecom public operator. She is an Assistant Professor at the Department of Electrical Engineering and Computers, University of Coimbra, and a Researcher at INESC Coimbra. Her research areas include multiple objective dynamic routing and quality of service analysis in multiservice telecommunications networks.

e-mail: lucia@deec.uc.pt
Departamento de Engenharia Electrotécnica
e Computadores
Polo II da Universidade de Coimbra
Pinhal de Marrocos
3030-290 Coimbra, Portugal

Instituto de Engenharia de Sistemas
e Computadores – Coimbra
Rua Antero de Quental, 199
3000-033 Coimbra, Portugal

Paper

A note on the computation of ordered supported non-dominated solutions in the bi-criteria minimum spanning tree problems

Carlos Gomes da Silva and João C. N. Clímaco

Abstract—This paper presents a new procedure for computing the set of supported non-dominated solutions of bi-criteria minimum spanning tree problems in ordered manner. The procedure is based on the systematic detection of edges which must be replaced in one efficient solution to obtain the adjacent one, in the criteria space. This new approach avoids solving unnecessary problems and makes use of previous computations.

Keywords— minimum spanning tree, supported non-dominated solutions, combinatorial problems.

1. Introduction

The minimum spanning tree problem (MST) is a well-known combinatorial problem that consists of identifying a spanning tree in a weighted connected graph with the smallest sum of costs (weights). The MST has several important practical applications such as physical systems design, reducing data storage, cluster analysis [2]. It is also important because it arises as a subproblem of other complex problems. For instance, in telecommunication multipath models the area of multicast routing (associated with point-multipoint problems) has attracted increasing attention both in terms of quality of service (QoS) routing models, and in terms of explicit consideration of multicriteria in the future. These models are increasingly important as a result of the emergence of multimedia applications such as audio, video services and video-conferencing, specially in the Internet. A typical formulation of multicast routing models in a QoS routing context involves Steiner trees [5]. These problems are in general very difficult to solve. So, it is valuable to point out that in some particular approaches the multicriteria minimal spanning tree models can be useful, and this is a major motivation for our focus on this problem.

A connected graph with n nodes has a maximum of n^{n-2} spanning trees, thus the *brute force* method is useless to solve the MST. The greedy Prim's, Kruskal's and Sollin's algorithm solve efficiently the MST [2].

A natural extension of the MST consists of taking into account more than one criterion function to evaluate feasible solutions. This new problem is known to be NP-complete [3]. The multiple criteria version of the MST is a challenge both from theoretical and practical perspectives, as can be seen in the literature survey by Ehrgott and Gandibleux [6].

A common approach when considering several criteria functions is the computation of the entire set of efficient solutions, also known as Pareto solutions (an efficient solution is a feasible solution such there is no other feasible one that can improve one of the criteria functions without degrading the value of at least one of the others). Some efficient solutions can be found by optimizing weighted-sums of the criteria (*supported efficient solutions*) while others cannot be obtained by this manner (*non-supported efficient solutions*). The supported efficient solutions can also be *extreme* (solutions that correspond to an extreme efficient solution in the *convex-hull* of the feasible region) or *non-extreme*. The image of an efficient solution, by using the criteria functions is called a *non-dominated* solution.

The computation of extreme efficient solutions is much easier when an efficient algorithm exists to optimize the single criterion version of the problem. Due to this fact, the computation of the two types of solutions is frequently made separately. In the MST this approach can be found in [1, 7, 8], for instance. The weighted-sum method is usually used to compute the extreme efficient solutions. It is an iterative procedure which computes, for a given pair of consecutive extreme efficient solutions x', x'' another extreme efficient solution x''' (if there exists any) between the images of x' and x''. This is done by optimizing a weighted-sum function parallel to the line that links the images of x' and x''. The method requires the optimization of several single criterion functions, some of them without producing any new efficient solution.

In this paper we propose an alternative procedure for the bi-criteria minimum spanning tree problems (BMST), which is based on the extension of ideas behind the Kruskal's algorithm. The main features of this procedure are the use of computations made in previous iterations and the fact that it avoids the repetitive resolution of single criterion problems. This is due to the fact that the edges that must leave an efficient MST and the edges that must enter that MST are identified. By removing and inserting these edges, the adjacent non-dominated MST is obtained. In summary, the paper gives a transition rule

from non-dominated solution to the adjacent one. The work by Tarjan [9], related to sensitivity analysis in minimum spanning trees, is useful in the present research.
The paper is organized as follows. In Section 2 it is presented a procedure to find the set of extreme non-dominated solutions in order, in Section 3 it is shown the interactive potential of the proposed approach, and Section 4 is devoted to the main conclusions of this work.

2. Finding supported non-dominated solutions in order

Let $G=(V_n,E)$ be an undirected graph with V_n being the set of n vertices and E being the set of edges of G. Here it is considered the existence of two criteria, hence each edge e_j has associated two costs $c_j^i (i=1,2)$. The criteria, to be minimized, are as follows:

$$z_t(T)=\sum_{j:e_j\in T} c_j^t,$$

where T is a spanning tree on G.

Supported non-dominated solutions optimize weighted sum functions. In the bi-criteria case, these functions are $f_\lambda(T)=\lambda z_1(T)+(1-\lambda)z_2(T)$, with $0\le\lambda\le 1$. When the entire interval $[0,1]$ for λ was analyzed, then all the non-dominated supported solutions were found. Let G^λ be the graph G such that each edge e_j has the cost $p_j^\lambda=\lambda c_j^1+(1-\lambda)c_j^2$.
We are interested in the computation of such a solutions but in an ordered manner, which is a new result considering the available procedures in the literature. The process of obtaining the ordered generation of supported non-dominated solutions is explained below.
A spanning tree is composed of $n-1$ edges, and following the Kruskal's algorithm one has to consider the edges according to non-decreasing costs and select the $n-1$ edges that draw a spanning tree on the given graph.
In the bi-criteria case, the cost of each edge e_j is p_j^λ, which depends on the value of λ. Thus, the minimum spanning tree of $f_\lambda(T)$ also depends on the value of λ. As λ changes in the interval $[0,1]$ some edges also change their relative position, which may lead to a different minimum spanning tree.
According to the path optimality condition [2] a spanning tree T is a minimum spanning tree if and only if every non-tree edge e_j has a cost greater or equal than the cost of any edge in the unique path of T that links the nodes concerning e_j.
Suppose that for a given λ,λ^k, the corresponding minimum spanning tree is T^{λ^k} and the associated supported non-dominated solution is $\left(z_1(T^{\lambda^k}),z_2(T^{\lambda^k})\right)$. This tree remains optimum for every λ which observes the path optimality condition.
Let $P^{\lambda^k}(e_j)$ be the path in T^{λ^k} which links the nodes concerning the non-tree edge e_j. For the non-tree edge e_j the maximum value of λ is given by the solution of the linear problem:

$$\begin{aligned} &\max\ \lambda \\ &s.t.: \\ &p_j^\lambda \ge p_i^\lambda, \forall e_i\in P^{\lambda^k}(e_j) \\ &0\le\lambda\le 1, \lambda>\lambda^k. \end{aligned} \tag{1}$$

The optimal solution of Eq. (1), $\lambda_{\max}^{e_j}$, is given below (if the problem is impossible, which occurs when the cost of two edges never gets equal or when it requires a weight outside the constraints $0\le\lambda\le 1,\lambda>\lambda^k$, it is assumed, for computational reasons, that $\lambda_{\max}^{e_j}$ takes the value $+\infty$):

$$\lambda_{\max}^{e_j}=\min_{e_i\in P^{\lambda^k}(e_j)}\left\{\frac{c_i^2-c_j^2}{\left(c_j^1-c_j^2\right)-\left(c_i^1-c_i^2\right)}:\left(c_j^1-c_j^2\right)-\left(c_i^1-c_i^2\right)<0;+\infty\right\}. \tag{2}$$

In order to preserve the optimality of the spanning tree, the path optimality condition must be observed by every non-tree edge. Thus the overall maximum value is given by $\lambda_{\max}^k=\min_{e_j\notin T^{\lambda^k}}\left\{\lambda_{\max}^{e_j}\right\}$.

Let $N_{\lambda^k}=\left\{e_j\notin T^{\lambda^k}:\lambda_{\max}^{e_j}=\lambda_{\max}^k\right\}$, representing candidates to entering the tree. Introducing e_j in the tree leads to a cycle. Thus, the candidate edges to be removed are the ones belonging to the set

$$C_{\lambda^k}(e_j)=\left\{e_i\in P^{\lambda^k}(e_j):\frac{c_i^2-c_j^2}{\left(c_j^1-c_j^2\right)-\left(c_i^1-c_i^2\right)}=\lambda_{\max}^k, e_j\in N_{\lambda^k}\right\}.$$

If $\lambda=\lambda_{\max}^k$ the current tree is still the optimum tree, but there exists at least another tree with the same weighted cost. Finding all the supported non-dominated solutions with the same weighted cost as T^{λ^k}, requires replacing in the tree every combinations of possible pairs of edges $\left(e_j\in N_{\lambda^k},e_i\in C_{\lambda^k}(e_j)\right)$. Let us note these combinations by $N_{\lambda^k}\otimes C_{\lambda^k}$.

If $\lambda=\lambda_{\max}^k+\varepsilon$ (ε is a small value) the current tree is not the optimum tree of the problem $\min\left\{f_\lambda(T):T\right.$ is a spanning tree on $\left.G\right\}$, since at least one non-tree edge has a smaller weight compared with at least one edge of the associated path in the tree. An optimum tree in this case is the one which has the minimum value for criterion $z_1(T)$ (note that λ is increasing towards the value 1), among all the efficient MST obtained with $\lambda=\lambda_{\max}^k$.

The procedure that generates the supported non-dominated solutions of a bi-criteria MST problem is as follows.

Procedure *SBMST*

Begin

$k \leftarrow 1$;// iterations counter

Compute the first MST, T^{λ^k}, with the cost edges calculated with $\lambda^k = \varepsilon$ (very small positive value);

$H \leftarrow Z(T^{\lambda^k}) = \left(z_1(T^{\lambda^k}), z_2(T^{\lambda^k})\right)$ //set of supported non-dominated spanning trees

Compute $\lambda^k_{\max}$ using expression (2) in T^{λ^k} and define N_{λ^k};

While $\left(\lambda^k_{\max} < 1\right)$ **Do**

Begin

Compute $C_{\lambda^k}(e_j)$ for all $e_j \in N_{\lambda^k}$;

Consider all the possible combinations of edges $N_{\lambda^k} \otimes C_{\lambda^k}$;

Let $T_1^{\lambda^k}, \ldots, T_h^{\lambda^k}$ be the trees obtained from T^{λ^k} by inserting/removing edges considering individually each of the previous combinations of edges;

$H \leftarrow H \overset{h}{\underset{i=1}{\cup}} Z(T_i^{\lambda^k})$ //set of supported non-dominated spanning trees

$k \leftarrow k+1$;

$T^{\lambda^k} \leftarrow \arg\min\{z_1(T) : T \in H\}$;// the tree with the lowest value in criterion z_1;

Compute $\lambda^k_{\max}$ using expression (2) in T^{λ^k} and define N_{λ^k};

End

End

In summary, the procedure starts with the computation of an initial MST, which optimizes criterion z_2 (chosen arbitrarily). The maximum value of λ which maintains the MST is computed as well as the candidates edges to enter the tree, are computed. If the maximum value of λ is greater than or equal to 1 the procedure stops. Otherwise, the leaving edges are identified for each entering candidate. Supported non-dominated trees generated by removing and inserting identified edges are used to update the list of solutions. The tree corresponding to the lowest value of criterion z_1 is the new reference tree and the above steps are repeated.

In order to illustrate the above procedure, let as consider the following example.

Example 1. Let G be the network presented in Fig. 1, where the cost of the edges according to the two criteria are also presented. The purpose is to obtain all the extreme non-dominated minimum spanning trees.

In Fig. 2 the functions $p_j^\lambda, j = 1, ..., |E|$ are represented. The vertical lines correspond to a change in the orders of the costs of the edges.

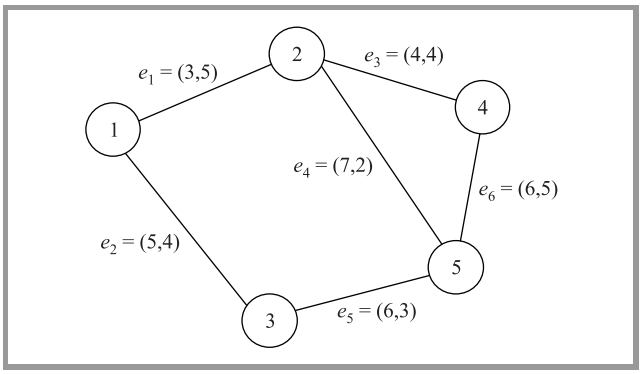

Fig. 1. The starting graph.

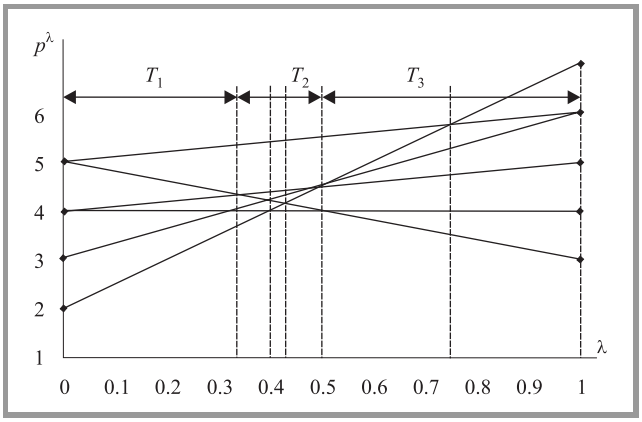

Fig. 2. Functions p_j^λ.

Using the procedure SBMST proposed above, the interval [0,1] for λ is partitioned into 3 relevant sub-intervals, each of them corresponding to a different non-dominated extreme MST.

$Z(T^{\lambda^1}) = (22,13)$; $\lambda^1_{\max} = \frac{1}{3}$; $N_{\lambda^1} = \{e_1\}$; $C_{\lambda^1}(e_1) = \{e_2\}$;

$Z(T^{\lambda^2}) = (20,14)$; $\lambda^2_{\max} = \frac{1}{2}$; $N_{\lambda^2} = \{e_2\}$;

$C_{\lambda^2}(e_2) = \{e_4, e_5\}$.

$N_{\lambda^2} \otimes C_{\lambda^2} = \left\{(e_2, e_4), (e_2, e_5)\right\}$; $Z(T_1^{\lambda^2}) = (18,16)$;

$Z(T_2^{\lambda^2}) = (19,15)$; $T^{\lambda^3} = T_1^{\lambda^2}$; $\lambda^3_{\max} > 1$.

Figures 3, 4 and 5 show three extreme efficient MST of the initial problem. Figure 6 presents the images in the criteria

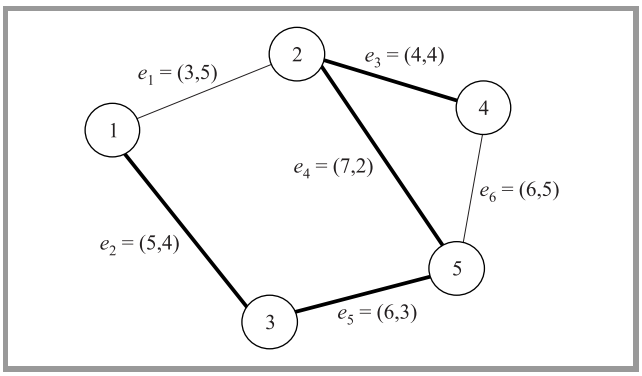

Fig. 3. First extreme eff.MST.

space of each solution (the points are connected for graphic visualization of the Pareto frontier).

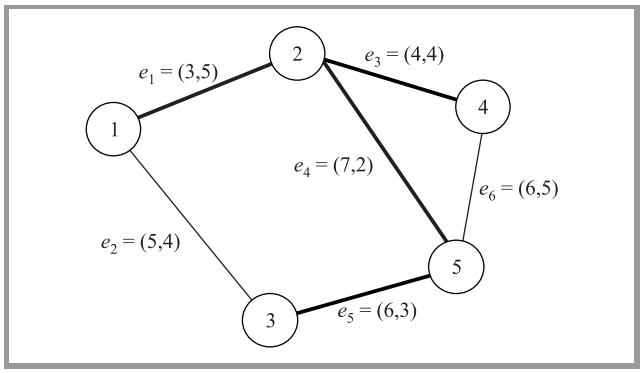

Fig. 4. Second extreme eff.MST.

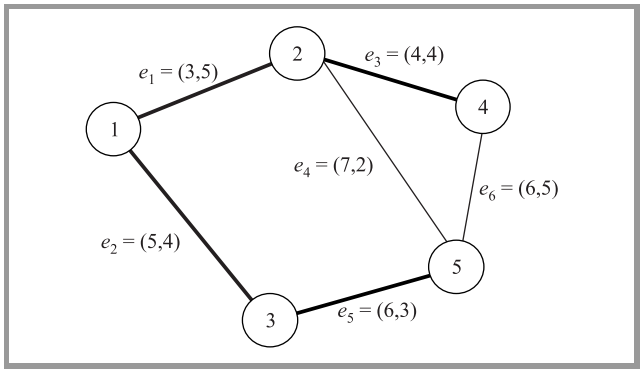

Fig. 5. Third extreme eff.MST.

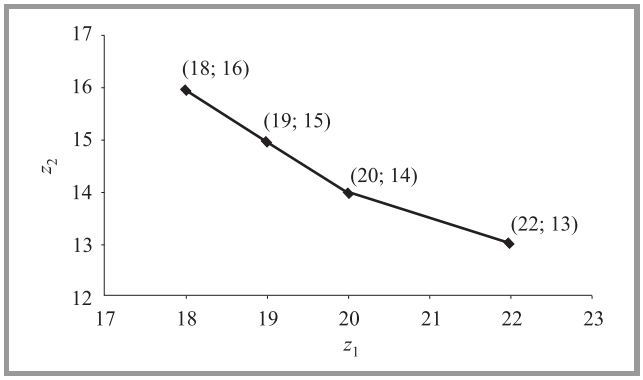

Fig. 6. Pareto front.

Remark. From the previous presentation it is easy to see that if an instance of a BMST observing the two following conditions: 1) $p_i^\lambda < p_j^\lambda, i = 1,...,n-1;\ j = n,...,|E|$ for all $0 \le \lambda \le 1$; 2) then $\{e_1, e_2, e_3, ..., e_{n-1}\}$ are the edges of the single non-dominated spanning tree of the problem.

Instances observing the conditions above are exceptions. In general, the BMST problem has several supported non-dominated solutions.

3. Interactive usefulness

The results presented in the previous section can be useful for building an interactive procedure dedicated to a progressive and selective calculation of the supported non-dominated spanning trees, according to the preferences of the decision maker elicited during the dialogue phase of the interactive process.

A very simple extension of the procedure SBMST, enables the obtainment of the sub-interval of values of λ leading to a same extreme efficient solution. The upper-bound of the sub-interval is obtained as in Eq. (2) and the lower bound, $\lambda_{\min}^k$, is obtained by solving problem Eq. (1) replacing its objective function by min λ and the constraint $\lambda > \lambda^k$ by $\lambda > \lambda_{\max}^{k-1}$. The optimal solution of the latter problem, is given by

$$\lambda_{\min}^{e_j} = \max_{e_i \in P^{\lambda^k}(e_j)} \left\{ \frac{c_i^2 - c_j^2}{\left(c_j^1 - c_j^2\right) - \left(c_i^1 - c_i^2\right)} : \left(c_j^1 - c_j^2\right) - \left(c_i^1 - c_i^2\right) > 0; +\infty \right\}. \quad (3)$$

Thus, $\lambda_{\min}^k = \max_{e_j \notin T^{\lambda^k}} \left\{ \lambda_{\max}^{e_j} \right\}$.

The progressive focus in part, or parts of the original interval of λ, i.e., [0,1], can be achieved by an ad hoc procedure that consists of eliminating the sub-intervals corresponding to efficient solutions already calculated and, possibly, other sub-intervals specified indirectly, for instance, by constraints on the objective function values introduced by the decision maker. This may happen when those constraints intersect edges of the convex hull connecting adjacent extreme non-dominated solutions already calculated.

Alternatively, the progressive focus in part, or parts, of the interval of λ, i.e., [0, 1], can also be achieved using a NISE-like approach (see [4]). Note that, in this case, the combination of the NISE-procedure steps with the progressive calculation of the sub-intervals of λ, corresponding to the extreme non-dominated solution calculated following the NISE approach, enables a faster reduction of the unexploited sub-intervals thereby accelerating the convergence of the process.

Example 2. Let us consider the data from Example 1 and suppose that the decision maker specifies $\lambda = 0.8$. By optimizing the weighted-sum function $f_\lambda(T) = 0.8 z_1(T) + (1-0.8) z_2(T)$, the extreme non-dominated solution $z = (22,13)$ is obtained. This solution is associated with the sub-interval $[0.5, 1]$ thus, in the following iteration, the decision maker is asked to select a weight in the interval $[0,1] \setminus [0.5,1]$.

Extension to the multicriteria case. When there are more than two criterion functions, the above results can be adapted. Given a supported efficient solution of the multicriteria problem, i.e., an optimal solution of the problem $\{\min \lambda_1^0 z_1(T) + \lambda_2^0 z_2(T) + ... + \lambda_q^0 z_q(T) : T$ is a span-

ning tree on G, where $\lambda_1^0 + \lambda_2^0 + ... + \lambda_q^0 = 1$ and $\lambda_j^0 > 0$ $(j = 1, ..., q)$ it still optimizes the weighted-sum functions:

$\{\min \lambda_1 z_1(T) + \lambda_2 z_2(T) + ... + \lambda_q z_q(T) : T$ is a spanning tree on $G\}$, such that $\lambda_1 c_j^1 + \lambda_2 c_j^2 + ... + \lambda_q c_j^q \geq \lambda_1 c_i^1 + \lambda_2 c_i^2 + ... + \lambda_q c_i^q, \forall e_i \in P^{\lambda^0}(e_j), \forall e_j \notin T^{\lambda^0}$.

Thus the feasible region for the weights can be presented to the DM in order to avoid redundant specifications of new weights for the objective functions.

4. Conclusions

A constructive procedure was proposed to compute the entire set of supported non-dominated solutions of the BMST. The procedure relies on the weighted-sum functions of the edges and on the ideas behind Kruskal's algorithm and sensitivity analysis in minimum spanning trees. With this procedure we can identify the edges which must be inserted/deleted from a supported efficient MST, to obtain an adjacent efficient MST. The procedure for finding the weight λ which conducts to the same extreme non-dominated solution was also used to support an interactive framework. The integration of other well-known (potentially interesting) interactive tools was just outlined. The method can also be useful in the multicriteria case.
The exploration of the procedure for finding the non-supported non-dominated solutions is a future line of research.

References

[1] K. Andersen, K. Jörnsten, and M. Lind, "On bicriterion minimal spanning trees: an approximation", *Comput. Oper. Res.*, vol. 23, pp. 1171–1182, 1996.

[2] R. Ahuja, T. Magnanti, and J. Orlin, *Network Flows – Theory, Algorithms And Applications*, New Yersey: Prentice Hall, 1993.

[3] P. Camerini, G. Galbiati, and F Maffioli, "The complexity of multi-constrained spanning tree problems", in *Theory of Algorithms, Colloquium Pecs 1984*, L. Lovász, Ed. Amsterdam: North-Holland, 1984, pp. 53–101.

[4] J. Cohon, *Multiobjective Programming and Planning*. New York: Academic Press, 1978.

[5] J. Clímaco, J. Craveirinha, and M. Pascoal, "Multicriteria routing models in telecommunication networks – overview and a case study", in *Advances in Multiple Criteria Decision Making and Human Systems Management: Knowledge and Wisdom*, Y. Shi, D. Olson, and A. Stam, Eds. Amsterdam: IOS Press, 2007, pp. 17–46.

[6] M. Ehrgott and X. Gandibleux, "A survey and annoted bibliography of multiobjective combinatorial optimazation", *OR Spektrum*, vol. 22, pp. 425–460, 2000.

[7] H. W. Hamacher and G. Ruhe, "On spanning tree problems with multiple objectives", *Ann. Oper. Res.*, vol. 52, pp. 209–230, 1994.

[8] R. M. Ramos, S. Alonso, J. Sicilia, and C. González, "The problem of the optimal biobjective spanning tree", *Eur. J. Oper. Res.*, vol. 111, pp. 617–628, 1998.

[9] R. Tarjan, "Sensitivity analysis of minimum spanning trees and shortest path trees", *Inform. Proces. Lett.*, vol. 14, pp. 30–33, 1982.

Carlos Gomes da Silva received his Ph.D. degree in operational research at University of Coimbra, Portual, in June 2005. He is Professor at Polytechnic of Leiria and a Researcher at INESC-Coimbra. His main research interests are multicriteria combinatorial problems and meta-heuristic resolution procedures.

e-mail: cgsilva@estg.ipleiria.pt
Escola Superior de Tecnologia e Gestão de Leiria
Morro do Lena, Alto Vieiro
2401-951 Leiria, Portugal

INESC-Coimbra
Rua Antero de Quental, 199
3000-033 Coimbra, Portugal

João C. N. Clímaco – for biography, see this issue, p. 10.

Invited paper

Determining hop-constrained spanning trees with repetitive heuristics

Manuela Fernandes, Luis Gouveia, and Stefan Voß

Abstract—The hop-constrained minimum spanning tree problem is the problem of determining a rooted spanning tree of minimum cost in which each path from the root node to any other node contains at most *H* hops or edges. This problem relates to the design of centralized tree networks with quality of service requirements (in telecommunications) and has a close relation with other tree problems. In this paper we investigate the adaptation of some well-known "repetitive" heuristics used for the capacitated minimum spanning tree problem to the hop-constrained minimum spanning tree problem and investigate some simple look ahead mechanisms for enhancing the quality of a savings heuristic. Computational results for a set of benchmark tests with up to 80 nodes are presented.

Keywords— hop-constrained spanning tree problem, meta-heuristics, pilot method, rollout method.

1. Introduction

The hop-constrained minimum spanning tree problem (HMST) is defined as follows. Given a graph $G = (V,E)$ with node set $V = \{0,1,\ldots,n\}$, edge set E as well as a cost c_e associated with each edge $e \in E$ and a natural number H, we wish to find a spanning tree T of the graph with minimum total cost such that the unique path from a specified root node, node 0, to any other node has no more than H hops (edges). The HMST is $\mathcal{NP}$-hard because it contains as a particular case (the case with $H = 2$) an $\mathcal{NP}$-hard version of the simple uncapacitated facility location problem (see [2, 8]). It has been shown by [16] that the HMST is even not in APX, i.e., the class of problems for which it is possible to have polynomial time heuristics with a guaranteed approximation bound. Related theoretical investigations can be found, e.g., in [14]. Special cases are considered, e.g., in [17].

The HMST models the design of centralized telecommunication networks with quality of service constraints. The root node represents the site of a central processor (computer) and the remaining nodes represent terminals that are required to be linked to the central processor. The hop constraints limit the number of hops (edges) between the root node and any other node and guarantee a certain level of service with respect to some performance constraints such as availability and reliability (see, e.g., [22]). Availability refers to the probability that all the transmission lines in the path from the root node to the terminal are working, and reliability corresponds with the probability that a session will not be interrupted by a link failure. In general, these probabilities decrease with the number of links in the path implying that paths with fewer hops have a better performance with respect to availability and reliability. Centralized terminal networks are also usually implemented with multidrop lines for connecting the terminals with the center. In such networks, node processing times dominate over queuing delays and fewer hops mean, in general, lower delays.

Lower bounding schemes for the HMST based on network-flow models have been suggested in [9, 10, 12]. A recent paper [3] summarizes these approaches and proposes new ones (column generation or cut generation) that are based on equivalent formulations, in terms of the corresponding linear programming relaxations. In fact, this survey paper clearly indicates that any type of heuristic solution is needed as optimal solutions for realistic problem sizes are currently out of reach. Lower bounds for an extended version of the problem, i.e., the Steiner tree problem with hop constraints can be found in [10, 19]. Interestingly enough, besides a cheapest insertion and the tabu search method described in [19] for the Steiner version of the problem, and Lagrangean heuristics proposed in [12], not much has been suggested for the HMST in terms of methods for obtaining good quality feasible solutions.

There are many problems that are related to the HMST. Besides the generalization to the Steiner version mentioned in the previous paragraph, we refer to the capacitated minimum spanning tree problem (CMST) (see, e.g., [20] and the references given there) or terminal layout problem that is usually described as the problem of determining a rooted spanning tree of minimum cost in which each of the subtrees off the root node contains at most a given number of K nodes. The connection of the HMST with the CMST is important due to several reasons. While the HMST involves a size (number of nodes or number of edges) constraint on each path leaving the root, the CMST involves a size constraint on the subtrees off the root. Thus, the HMST is an integer relaxation of the CMST and it is natural to assume that some ideas which work well for one problem may also work well for the other. One example of this is given by the fact that reasonably successful approaches for the two problems are based on so-called hop-indexed integer linear programming formulations (see, e.g., [3, 11]). In context of determining feasible solutions (which is more to the point in this paper), straightforward adaptations of minimum spanning tree algorithms for the two problems share a common disadvantage, namely that nodes farther from the root node cannot be linked to the closest nodes due to the additional constraints. Thus, it is natural to think that a savings heuristic that has been suggested and used for the CMST and which overcomes this disadvantage might

also be suitable for the HMST (this is explored in Section 2). This reasoning is extended in Section 3 to repetitive heuristics which are known to successfully improve the savings heuristics for the CMST.
Furthermore, we suggest another heuristic approach which is based on some look ahead feature (Section 4), i.e., a "repetitive" approach superimposed as a guiding process on some construction method. This idea relates to the pilot method developed in the early 90s for the Steiner tree problem in graphs (see [4, 5]). Lateron, similar ideas were developed under different names. The most famous one is the rollout method [1]. For a recent survey on the pilot method and related applications to many combinatorial optimization problems (see [21]).
Computational results in Section 5 show that repetitive methods can improve considerably over the results of the original heuristics, however, for the prize of considerably larger computation times. Furthermore, we observe that we can use the resulting objective function values as good upper cutoff values in available mixed integer programming solvers (such as CPLEX) for determining optimal solutions for previously unsolved problem instances of the HMST. We close with conclusions and directions for further research.

2. Construction heuristics

When trying to solve the HMST an obvious idea is to adapt and modify two algorithms which produce minimum unconstrained spanning trees in an undirected graph. One is the well known Prim [18] algorithm (which for simplicity, we do not describe in the paper). Starting the algorithm from node 0, it is quite easy to modify it in order to guarantee that it produces a feasible solution for the HMST. This algorithm behaves quite poorly for the HMST. In fact it exhibits a disadvantage that is also observed for a modified Prim algorithm for the CMST. As already mentioned in the previous section, the deficiency is that nodes far from the root cannot always be linked to closest nodes due to the additional (hop or capacity) constraints, leading to more expensive solutions.
Thus, we shall follow the literature on the CMST and propose a savings heuristics for the HMST that is quite similar to the well-known Esau-Williams algorithm (EW) [6]. This heuristic usually starts with the star solution (that is, every node linked directly to node 0). The best feasible change, i.e., the change which yields the largest savings, is performed. This is iteratively repeated until no savings can be obtained any more. To be more specific, let χ_i denote the cost of the edge linking the subtree containing node i to the root in the current solution. For each pair of nodes i and j in different subtrees we compute the savings s_{ij} of linking i with j, which is defined as $s_{ij} = \chi_i - c_{ij}$ if the operation of including edge (i, j) and removing the edge linking the subtree containing node i to the root leads to a feasible solution, and $s_{ij} = \infty$, otherwise. The best exchange is performed and the savings are recalculated for the next iteration. The process stops when no positive savings is available any more. The method could easily be applied to other feasible solutions and so it could be classified as improvement procedure, too.

3. Second order algorithms

Second order algorithms are an important class of algorithms following the idea of repetition (also considered to be a multi-pass heuristic). They iteratively apply a so-called first order procedure to different start solutions (where some edges are fixed to be included) and/or modified cost functions (where inhibitively high cost values have been assigned to some edges) thus forcing edges into or out of the solution. Savings procedures like the EW may be applied as "slave" procedures to generate or complete the solution. In each iteration, all possible modifications according to a given rule are checked. The best one is realized and the respective modifications are made permanent for the remaining iterations. The underlying principle is to investigate many good starting points through some greedy procedure and thereby to increase the possibility of finding a good solution on at least one repetition (see, e.g., [13, 15]).

3.1. General scheme

With the main objective of overcoming the typical greediness of simple constructive heuristics, we investigate the class of second order algorithms. As far as we know, this class of heuristics has first been suggested in [15] for the CMST. In such algorithms, several calls of a first order algorithm (which usually is a simple constructive heuristic) are made. At the beginning of each iteration of the algorithm, an adequate set of constraints is added to the problem and the first order algorithm is executed. In general, such constraints force or inhibit edges from being included in the solution. Small modifications on the first order algorithm permit us to obtain such modified solutions. For instance, to prevent an edge (p,q) from being included in the solution, we simply define $c_{pq} = M$, where $M > \max_{(i,j)\in E} c_{ij}$ before running the first order algorithm. For forcing an edge to be in the solution, one can define $c_{pq} = m$, with $m < \min_{(i,j)\in E} c_{ij}$.
A general outline of a second order algorithm is described as follows. Let HEUR denote any first order heuristic for the HMST (e.g., the EW) and let HEUR(S_1, S_2) denote its application to a modification of the data where the edges of S_1 are necessarily included in the solution determined by the algorithm and the edges in S_2 are excluded from it. Let $C(S_1, S_2)$ be the cost of this solution and let *COST* denote the objective function value of the best solution obtained so far. Finally, let *IT* denote the number of iterations of the overall method.

Second order algorithm (Basic scheme)

Initialization: $COST \leftarrow \infty$
Initialize S_1 and S_2
Loop: **for** $i = 1, IT$ **do**
Call HEUR(S_1, S_2)
if $C(S_1, S_2) < COST$ **then**
$COST \leftarrow C(S_1, S_2)$
Modify S_1 and / or S_2

Each iteration of the main loop corresponds to an execution of the first order algorithm after modifying adequately the data / the cost matrix according to the definition of the sets S_1 and S_2. After the IT iterations, $COST$ gives the cost of the best solution. The definition (and rule modification) of the sets S_1 and S_2 may also depend on previous solutions of the main algorithm. One example of such a rule is to prevent two nodes i and j of being in the same subtree (assuming that this has happened in the previous solution) [15]. In this way, we guarantee that the solution obtained in the current iteration is different from the one obtained in the previous iteration. This rule corresponds to inhibiting any edge that connects the two components containing the two nodes, respectively. Thus, S_2 is implicitly defined as containing all such edges.

One way of improving the basic scheme is to repeat it several times. Each time, the best solution obtained so far and the modifications (associated to the corresponding sets S_1 and S_2) are made permanent. To explain this improved version, let SP_1 (SP_2) denote the set of edges which are permanently included in (excluded from) the remaining solutions. Let HEUR(S_1, S_2, SP_1, SP_2) denote the first order algorithm modified in such way that the edges in the set $S_1 \cup SP_1$ must be included in the solution and the edges in the set $S_2 \cup SP_2$ must be excluded from the solution. The cost of such solution is denoted by $C(S_1, S_2, SP_1, SP_2)$. The parameter k identifies the iteration number of the outer loop and $IT(k)$ corresponds to the number of iterations of the inner loop at iteration k of the outer loop. In general, the algorithm stops when all the solutions obtained in the execution of an inner loop do not improve the best solution. In the scheme below, "COND" indicates a general stopping condition.

Second order algorithm (Improved scheme)

Initialization: $COST \leftarrow \infty$
$k \leftarrow 1$
$SP_1 \leftarrow \emptyset$
$SP_2 \leftarrow \emptyset$
Outer Loop: **while not** (COND) **do**
Initialize S_1 and S_2
Inner Loop: **for** $i = 1, IT(k)$ **do**
Call HEUR(S_1, S_2, SP_1, SP_2)
if $(C(S_1, S_2, SP_1, SP_2) < COST)$ **then**
$COST \leftarrow C(S_1, S_2, SP_1, SP_2)$
$A_1 \leftarrow S_1$
$A_2 \leftarrow S_2$
Modify S_1 and / or S_2
$SP_1 \leftarrow SP_1 \cup A_1$
$SP_2 \leftarrow SP_2 \cup A_2$
$k \leftarrow k + 1$

Clearly, different ways and rules to define the sets S_1 and S_2 lead to different second order algorithms. Some of those rules are specified below.

3.2. Inhibiting edges

In this section we only consider inhibitions and thus, the sets S_1 and SP_1 are empty. Several ways of defining the sets S_2 and / or SP_2 are given next.

Simple inhibition (I1). Each edge (not incident to the root) of the previous solution defines the set S_2 in each iteration of the inner loop. (In this case we have $IT(k) = n$ for all k.) The edge leading to the best solution is made permanent and included in SP_2.

Inhibition of pairs of edges (I2). This case is similar to simple inhibition, but now each pair of edges is considered to be included in S_2 (in each iteration). The main idea of this rule is to increase the number of solutions generated by the main body of the algorithm and thus, to increase the possibility of finding a better solution. However, it is clear that this version of the algorithm requires an increased computational time.

The original inhibit in each iteration of the outer loop of the general procedure asks for all edges of the previous solution to be inhibited (I1) or to check for all possible exclusions of two edges at a time (I2). In each iteration of I1 we have a linear number of calls of the first order algorithm and in I2 this number is quadratic.

3.3. Forcing edges

In this section we only consider edge inclusions and thus, the sets S_2 and SP_2 are empty. Several ways of defining the sets S_1 and / or SP_1 are possible.

Join. Here we follow [15] and consider the following two sets of edges:

$$JA_1 = \{(p,q) | c_{pq} = \min_{r=1,\ldots,n} c_{rq}, q = 1,\ldots,n\},$$

$$JA_2 = \{(p,q) | c_{pq} = \min_{r=1,\ldots,n} c_{rq} : c_{0r} \leq c_{0q}, q = 1,\ldots,n\}.$$

The set JA_1 includes for each node the minimum cost edge incident to it. The set JA_2 includes for node q the minimum cost edge incident to it such that the other endpoint is closer to the root node.

In each iteration of the inner loop, S_1 contains exactly one edge from the set $JA_1 \cup JA_2$. Thus, the inner loop will have at most $2n$ iterations (as there may be edges repeated in the two sets and each set has at most n edges). The edge leading to the best solution is made permanent and the algorithm continues.

General join. In this rule we follow the inhibit concept and try to use information from previous solutions to define candidate edges to be included in the next solution. Clearly, all edges not included in the previous solution can be considered as candidates. Thus, one such edge defines a possible set S_1 (edges leading to infeasible solutions when considered together with SP_1 are excluded – this also refers

to edges leading to cycles or edges leading to paths which are too long). However, such an approach is too time consuming as there are many edges to examine. Thus, we consider a variation of the method where we only examine the z least cost edges incident with each node (and not leading to infeasible solutions). In our computational results we shall consider $z = 4$ (this choice results from some experiments reported in [7]).

4. Looking ahead with repetition

Building on a simple greedy algorithm the *pilot method* [4, 5] is a meta-heuristic that builds primarily on the idea of looking ahead for each possible local choice (by computing a so-called pilot solution), memorizing the best result, and performing the according move. One may apply this strategy by successively performing a first order algorithm for all possible local steps (i.e., starting with all incomplete solutions resulting from adding some not yet included element at some position to the current incomplete solution). The look ahead mechanism of the pilot method is related to increased neighborhood depths as the pilot method exploits the evaluation of neighbors at larger depths to guide the neighbor selection at depth one.

Usually, it is reasonable to restrict the pilot process to a given evaluation depth. That is, the pilot method is performed up to an incomplete solution (e.g., partial assignment) based on this evaluation depth and then completed by continuing with a conventional cheapest insertion heuristic. In fact, the general second order algorithm described above is nothing else than a pilot method of depth 1 where the local choice is performed by excluding edges from a given solution, one at a time.

For this paper we use the idea of looking ahead as a motivation for a more general repetitive second order algorithm. As a simple look ahead mechanism motivated by the pilot method we modify I2 as follows (called ILA). In each iteration, for each edge to be inhibited, we calculate a new solution and use all possible edges of that new solution as possible candidates for inhibition. Based on the general stopping criterion imposed by any type of savings heuristic like the EW to stop if no more improvements are possible we have two observations why ILA might have and in fact has larger computation times than I2. First, as intermediate solutions need to be calculated it definitely needs additional time for performing these calculations. Second, as we proceed with the method as long as improvements are possible, there may be an increased number of iterations of the outer loop based on additional improvements found.

5. Computational results

For computational comparisons we use a set of HMST problem instances with 40 and 80 nodes that have previously been used in the literature (see, e.g., [3, 8–10, 12]). We distinguish instances with the root in the center of a rectangle in the Euclidean plane (called TC) and instances with the root in the corner of the rectangle (called TE).

In order to reduce the size of each instance, we have used a simple edge elimination test (see [9]). If $c_{ij} > c_{0j}$, then any optimal solution does not use edge (i, j) and if $c_{ij} = c_{0j} (i \neq 0)$, then there is an optimal solution without edge (i, j). This means that edge (i, j) can be eliminated whenever $c_{ij} \geq c_{0j}$. This edge elimination test is applied to every instance before applying the heuristics. Note that the test is much more effective when applied to instances TC rather than to instances TE. This means that the reduced instances TE are larger than the reduced instances TC suggesting that the TE instances will be much more difficult to solve than the remaining instances. A standard way for reporting numerical results for heuristics found in the CMST literature is to compare with the EW (see, e.g., many of the papers surveyed in [20]).

Computational results for $n = 40$ and $n = 80$ are presented in Tables 1 and 2. In both tables, the first column, denoted by Prob, identifies the problem instance while the second column gives the value of H. For $n = 40$ we know the optimal solutions of all problem instances and they are provided in the third column (OPT). In Table 2 we provide optimal objective function values for the problem instances with $n = 80$ as far as we have been able to compute them based on the CPLEX models of [12] together with the upper bounds taken from Table 2 as upper cutoff values. That is, using the results from our computational study allowed us to compute optimal objective function values that had not been previously known. For the cases with $n = 80$, in case that we do not know an optimal solution from the literature and also cannot provide them with the above mentioned CPLEX models, we provide best known lower bounds *LB* taken from solving the linear programming relaxation of a hop-indexed formulation (see [3, 12]). They are shown in the form (LB).

The next few columns provide the heuristics that we tested. EW gives the upper bound obtained with the Esau-Williams algorithm. I1 and I2 provide the solutions obtained by the inhibition algorithms as described above. That is, I1 represents simple inhibition of edges following [15] and I2 means the case of forbidding two edges at the same time in each iteration of the inhibition procedure. Column ILA gives the results of the simple look ahead modification (applying the inhibition procedure). The column denoted by J shows the results obtained by means of the join procedure, which represents the junction of edges also according to [15]. In column J4 we provide the results for the general join procedure presented above. That is, in this procedure the four cheapest edges incident with each node, except the root, that do not belong to the solution, are candidates. Under the same headings we also provide the CPU times in seconds of the respective procedures. All results are obtained on a Pentium IV, 2.8 GHz following some straightforward implementation. Note that the implementation is straightforward and does not strive to incorporate versatile data structures to improve the CPU times as the major fo-

Table 1

Computational results and CPU times for the instances with $n = 40$

Prob	H	OPT	Upper bounds						CPU times [s]					
			EW	I1	I2	ILA	J	J4	EW	I1	I2	ILA	J	J4
	3	609	653	**612**	**612**	**612**	622	621	0.0	0.8	6.1	14.7	1.5	4.7
TC-1	4	548	594	564	563	**555**	560	563	0.0	0.7	6.5	16.6	1.1	4.3
	5	522	561	**524**	**524**	**524**	**524**	**524**	0.0	0.4	4.3	10.7	1.1	3.6
	3	566	596	572	**566**	**566**	587	575	0.0	0.7	4.5	9.5	1.4	4.8
TC-2	4	519	552	521	521	**519**	521	**519**	0.0	0.4	4.4	10.9	1.2	4.3
	5	496	**497**	**497**	**497**	**497**	**497**	**497**	0.0	0.3	2.3	4.8	1.2	4.0
	3	580	631	586	592	**582**	592	586	0.0	0.8	7.1	18.9	1.2	5.0
TC-3	4	544	585	557	549	**547**	561	550	0.0	0.6	9.6	19.5	1.2	4.4
	5	516	547	**520**	**520**	**520**	**520**	**520**	0.0	0.4	5.9	12.5	1.1	3.9
	3	613	661	624	620	**614**	632	619	0.0	0.5	5.2	13.3	1.4	5.0
TC-4	4	557	601	567	565	**561**	564	564	0.0	0.5	5.7	11.9	1.2	4.6
	5	524	552	543	539	537	536	**529**	0.0	0.4	4.5	11.1	1.1	3.7
	3	599	627	**604**	**604**	**604**	605	**604**	0.0	0.5	4.4	11.3	1.2	4.8
TC-5	4	552	583	560	560	560	**556**	558	0.0	0.7	6.3	13.6	1.1	4.2
	5	522	548	526	526	**522**	526	530	0.0	0.5	4.3	5.9	1.0	3.9
	3	708	834	**709**	**709**	**709**	733	724	0.0	1.0	9.6	20.1	2.7	8.3
TE-1	4	627	686	650	650	650	637	**635**	0.0	0.7	6.7	14.1	2.4	8.2
	5	590	676	627	605	**597**	611	599	0.0	0.6	8.6	20.0	2.2	7.4
	3	710	824	736	736	**730**	744	738	0.0	0.7	7.1	14.6	2.7	9.0
TE-2	4	625	694	653	**625**	628	659	651	0.0	0.8	11.3	27.1	2.3	8.4
	5	581	643	601	599	**593**	599	601	0.0	0.7	7.1	17.4	2.1	7.4
	3	660	779	692	690	**677**	746	686	0.0	0.8	11.1	30.5	2.6	9.3
TE-3	4	581	661	600	600	600	611	**584**	0.0	0.5	4.3	9.1	2.4	7.5
	5	540	602	556	**552**	**552**	562	557	0.0	0.5	6.1	15.2	2.1	7.4
	3	722	779	736	736	**732**	771	743	0.0	0.7	6.8	17.9	2.7	8.6
TE-4	4	625	674	640	**626**	**626**	647	648	0.0	0.7	7.9	16.6	2.2	7.8
	5	585	630	608	597	**591**	594	594	0.0	0.5	8.1	19.2	1.9	7.1
	3	675	791	687	686	**675**	705	682	0.0	1.2	9.0	26.1	2.9	8.6
TE-5	4	614	677	628	621	621	**620**	**620**	0.0	0.5	11.9	21.8	2.5	8.1
	5	571	600	582	580	579	**578**	**578**	0.0	0.7	7.5	15.7	2.1	7.8

cus is solely to investigate whether the solution quality can be enhanced and to which extent. Compared to the literature some of our results are providing new best solutions for these benchmark instances (although we believe that further improvements are possible).

Our results show that the EW performs quite reasonably for the HMST. (We have also implemented the Prim algorithm but do not show the results as they are much worse compared to those of the EW.) Inhibition and join as some simple repetitive mechanism following the idea of applying second order (multi-pass) heuristics clearly improve over the EW results. This is pretty much in line with our expectation and experience gained with respect to the CMST. Also, while not always being the case, the inhibition approach seems to outperform the join approach with respect to the solution quality obtained. This observation is also in line with earlier results from [15] for the CMST. Nevertheless, the computation times for J seem to be higher than those for I1.

Besides the quadratic number of repetitive calls of the first order heuristic (EW) in I2 and ILA for each iteration of the outer loop when compared to I1, an increased solution quality may influence the overall stopping criterion. Therefore, a considerably increased time behavior with respect to the extended algorithms seems obvious and can be clearly taken from the tables. With respect to solution quality the picture seems to be clear in the sense that repetition can really be beneficial. That is, while not always leading to the overall best results the ILA procedure seems to be better or at least as good than the other approaches in most cases. The additional effort for J4 seems to pay compared to J, but J4 seems to outperform ILA only in some cases.

Table 2
Computational results and CPU times for the instances with $n = 80$

Prob	H	OPT	Upper bounds						CPU times [s]					
			EW	I1	I2	ILA	J	J4	EW	I1	I2	ILA	J	J4
	3	1072	1233	1116	1106	1101	**1099**	1106	0.0	44.0	804.3	2011.5	63.9	224.1
TC-1	4	981	1073	1003	**997**	**997**	1011	1001	0.0	40.9	776.0	1796.0	55.6	192.9
	5	922	994	942	930	**929**	948	938	0.0	26.3	511.5	1208.0	48.1	167.7
	3	1054	1183	1115	1088	**1080**	1096	1086	0.0	22.8	801.3	1963.2	56.2	211.6
TC-2	4	967	1070	988	986	**982**	1006	994	0.0	45.9	864.5	2043.2	54.5	171.5
	5	918	993	930	933	**925**	938	936	0.0	33.6	664.1	1307.1	43.6	149.8
	3	1068	1169	1100	1092	**1091**	1100	1098	0.0	40.4	1016.7	2168.6	61.5	230.7
TC-3	4	968	1056	998	986	**982**	1000	997	0.0	36.4	807.6	1941.3	57.7	177.4
	5	912	978	924	920	**916**	930	928	0.0	26.2	641.0	1323.3	44.1	148.4
	3	1071	1168	1114	1110	1104	1111	**1097**	0.0	29.6	698.1	1909.5	65.9	213.1
TC-4	4	968	1049	990	**984**	986	1001	992	0.0	39.9	872.7	1730.3	55.7	184.6
	5	912	980	930	**916**	918	939	926	0.0	33.8	588.6	1399.4	48.1	162.6
	3	1235	1389	1288	**1262**	1268	1297	1274	0.0	21.9	848.3	1271.3	69.9	234.2
TC-5	4	1094	1232	1135	1134	**1126**	1134	1142	0.0	27.3	630.7	1257.1	58.6	206.1
	5	1037	1107	**1052**	**1052**	**1052**	1065	1059	0.0	25.8	426.4	1066.7	48.4	179.8
	3	(1743)	2321	2022	1965	1957	2003	**1928**	0.1	56.2	1044.6	2885.0	123.4	403.1
TE-1	4	(1462)	1953	1698	1666	**1631**	1708	**1631**	0.0	42.7	966.8	2675.1	110.0	372.1
	5	(1349)	1753	1508	**1500**	**1500**	1525	1516	0.0	27.3	601.0	1443.2	90.9	323.2
	3	(1669)	2403	1948	1926	**1845**	2120	1864	0.1	48.2	1082.7	2936.5	162.4	462.6
TE-2	4	(1413)	1814	1636	1548	**1542**	1635	1627	0.0	43.6	954.9	2364.3	133.6	407.6
	5	(1297)	1528	1451	1447	**1441**	1460	1445	0.0	22.2	472.8	1179.0	98.1	345.3
	3	(1672)	2364	1955	1872	**1864**	1960	1893	0.1	37.5	1158.4	2497.8	154.3	452.2
TE-3	4	(1432)	1816	1670	1625	1614	1656	**1601**	0.0	22.5	701.8	1667.1	118.3	365.4
	5	(1308)	1582	1506	1427	**1411**	1429	1426	0.0	22.6	446.5	1141.1	96.5	322.2
	3	(1679)	2409	1900	1864	**1843**	1954	1925	0.1	62.7	888.9	3024.1	141.2	448.7
TE-4	4	(1420)	1967	1704	**1631**	1665	1727	1665	0.1	31.2	1327.0	1831.8	136.5	422.8
	5	(1313)	1638	1499	1490	**1458**	1530	1464	0.0	31.6	981.5	1494.1	111.2	333.9
	3	(1692)	2478	1933	1909	1898	2017	**1892**	0.1	35.8	1435.0	2670.1	137.6	458.5
TE-5	4	(1447)	1775	1643	**1614**	**1614**	1647	1629	0.0	26.1	598.1	1344.3	105.9	387.1
	5	(1325)	1687	1494	1472	**1456**	1490	1458	0.0	10.3	441.1	1226.2	89.0	317.1

6. Conclusions and future research

To conclude with we have seen that the repetition mechanism within a second order algorithm may be worth investigating with respect to solution quality while the computation times are largely increasing. A simple look ahead feature may enhance this picture. With that it seems that results for so-called capacitated tree problems (naming the CMST and the HMST as such) using second order algorithms may be in line with each other. That is, once other capacitated tree problems are considered the use of second order algorithms may be a natural choice within future research.

References

[1] D. P. Bertsekas, J. N. Tsitsiklis, and C. Wu, "Rollout algorithms for combinatorial optimization", *J. Heur.*, vol. 3, pp. 245–262, 1997.

[2] G. Dahl, "The 2-hop spanning tree problem", *Oper. Res. Lett.*, vol. 23, pp. 21–26, 1998.

[3] G. Dahl, L. Gouveia, and C. Requejo, "On formulations and methods for the hop-constrained minimum spanning tree problem", in *Handbook of Optimization in Telecommunications*, M. G. C. Resende and P. M. Pardalos, Eds. New York: Springer, 2006, pp. 493–515.

[4] C. W. Duin and S. Voß, "Steiner tree heuristics – a survey", in *Operations Research Proceedings 1993*, H. Dyckhoff, U. Derigs, M. Salomon, and H. C. Tijms, Eds. Berlin: Springer, 1994, pp. 485–496.

[5] C. W. Duin and S. Voß, "The pilot method: a strategy for heuristic repetition with application to the Steiner problem in graphs", *Networks*, vol. 34, pp. 181–191, 1999.

[6] L. R. Esau and K. C. Williams, "A method for approximating the optimal network", *IBM Syst. J.*, vol. 5, no. 3, pp. 142–147, 1966.

[7] M. Fernandes, "Estudo de limites inferiores e superiores para árvores com restrições de salto". Master thesis, Centro de Investigação Operacional, University of Lisbon, 2002 (in Portuguese).

[8] L. Gouveia, "Using the Miller-Tucker-Zemlin constraints to formulate a minimal spanning tree problem with hop constraints", *Comput. Oper. Res.*, vol. 22, pp. 959–970, 1995.

[9] L. Gouveia, "Multicommodity flow models for spanning trees with hop constraints", *Eur. J. Oper. Res.*, vol. 95, pp. 178–190, 1996.

[10] L. Gouveia, "Using variable redefinition for computing lower bounds for minimum spanning and Steiner trees with hop constraints", *INFORMS J. Comp.*, vol. 10, pp. 180–187, 1998.

[11] L. Gouveia and P. Martins, "A hierarchy of hop-indexed models for the capacitated minimum spanning tree problem", *Networks*, vol. 35, pp. 1–16, 2000.

[12] L. Gouveia and C. Requejo, "A new lagrangean relaxation approach for the hop-constrained minimum spanning tree problem", *Eur. J. Oper. Res.*, vol. 132, pp. 539–552, 2001.

[13] J. P. Hart and A. W. Shogan, "Semi-greedy heuristics: an empirical study", *Oper. Res. Lett.*, vol. 6, pp. 107–114, 1987.

[14] R. Hassin and A. Levin, "Minimum spanning tree with hop restrictions", *J. Algor.*, vol. 48, pp. 220–238, 2003.

[15] M. Karnaugh, "A new class of algorithms for multipoint network optimization", *IEEE Trans. Commun.*, vol. COM-24, no. 5, pp. 500–505, 1976.

[16] P. Manyem and M. Stallmann, "Some approximation results in multicasting", North Carolina State University, 1996.

[17] L. Monnot, "The maximum *f*-depth spanning tree problem", *Inform. Proces. Lett.*, vol. 80, pp. 179–187, 2001.

[18] R. Prim, "Shortest connection networks and some generalizations", *Bell Syst. Tech. J.*, vol. 36, pp. 1389–1401, 1957.

[19] S. Voß, "The Steiner tree problem with hop constraints", *Ann. Oper. Res.*, vol. 86, pp. 321–345, 1999.

[20] S. Voß, "Capacitated minimum spanning trees", in *Encyclopedia of Optimization*, C. A. Floudas and P. M. Pardalos, Eds. Dordrecht: Kluwer, 2001, vol. 1, pp. 225–235.

[21] S. Voß, A. Fink, and C. Duin, "Looking ahead with the pilot method", *Ann. Oper. Res.*, vol. 136, pp. 285–302, 2005.

[22] K. Woolston and S. Albin, "The design of centralized networks with reliability and availability constraints", *Comput. Oper. Res.*, vol. 15, pp. 207–217, 1988.

Manuela Fernandes, born 1969 in Castelo Branco, Portugal, is Assistant Lecturer of the School of Technology at the Polytechnic Institute of Tomar. Previous positions include Assistant Lecturer of the School of Technology at the Polytechnic Institute of Guarda from 1996 to 1999. She holds a B.Sc. degree in mathematics from the University of Coimbra and a M.Sc. degree from the University of Lisbon. Her main interests are heuristics and meta-heuristics for integer programming problems and networks with applications on telecommunications.
e-mail: manuela.fernandes@aim.estt.ipt.pt
School of Technology
Polytechnic Institute of Tomar
Quinta do Contador
Estrada da Serra
2300-313 Tomar, Portugal

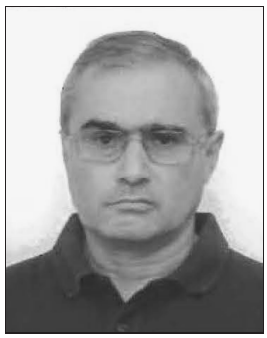

Luis Gouveia, born 1957 in Mozambique, is Associate Professor at the Faculty of Sciences, University of Lisbon and Coordinator of the Operations Research Center at the Faculty of Sciences. He holds degrees in applied mathematics (diploma) from the University of Lisbon and a Ph.D. in operations research. His current research interests are in network design, ILP model reformulation and telecommunications. He is author of numerous papers in various journals. Luis Gouveia serves on the editorial board of some journals including being Associate Editor of "Networks" and "Computers & OR". He is frequently organizing workshops and conferences.
e-mail: legouveia@fc.ul.pt
Faculty of Sciences
University of Lisbon
Cidade Universitária, Bloco C6
Campo Grande, 1749-016 Lisboa, Portugal

Stefan Voß, born 1961 in Hamburg, Germany, is Professor and Director of the Institute of Information Systems at the University of Hamburg. Previous positions include full Professor and Head of the Division of Business Administration, Information Systems and Information Management at the University of Technology Braunschweig, Germany, from 1995 up to 2002. He holds degrees in mathematics (diploma) and economics from the University of Hamburg and a Ph.D., and the habilitation from the University of Technology Darmstadt. His current research interests are in quantitative/information systems approaches to supply chain management and logistics as well as public mass transit and telecommunications. He is author and co-author of several books and numerous papers in various journals. Stefan Voß serves on the editorial board of some journals including being Editor of "Annals of Information Systems", Associate Editor of "INFORMS Journal on Computing" and Area Editor of "Journal of Heuristics". He is frequently organizing workshops and conferences. Furthermore, he is consulting with several companies.
e-mail: stefan.voss@uni-hamburg.de
Institute of Information Systems
University of Hamburg
Von-Melle-Park 5
D-20146 Hamburg, Germany

Paper

Application of bioinformatics methods to recognition of network threats

Adam Kozakiewicz, Anna Felkner, Piotr Kijewski, and Tomasz Jordan Kruk

Abstract— Bioinformatics is a large group of methods used in biology, mostly for analysis of gene sequences. The algorithms developed for this task have recently found a new application in network threat detection. This paper is an introduction to this area of research, presenting a survey of bioinformatics methods applied to this task, outlining the individual tasks and methods used to solve them. It is argued that the early conclusion that such methods are ineffective against polymorphic attacks is in fact too pessimistic.

Keywords— network threat analysis, sequence alignment, edit distance, bioinformatics.

1. Introduction

When biologists discover a new gene, its function is not always apparent. The usual approach is to compare its structure with genes, whose function has already been identified. Comparison (so-called *alignment*) of biological sequences is a basis for bioinformatics, a science focused on theories, algorithms, computational techniques and statistical methods, with the goal of solving problems of biological data analysis [1]. Bioinformatics draws inspiration from many other branches of science and the techniques it provides often have interesting applications outside of biology – including automatic voice and handwriting recognition, but also in computing systems security. This paper focuses on methods of defining the similarity between biological sequences and shows, how similar methods can be applied to the problem of recognition and characterization of computer network threats.

2. Sequence alignment

Sequence alignment is a tool used in bioinformatics to define and visualize a measure of similarity between DNA or protein sequences.

Definition 1 (from [2]) : A (global) *alignment* of two strings S_1 and S_2 is obtained by first inserting chosen spaces (or dashes), either into or at the ends of S_1 and S_2, and then placing the two resulting strings one above the other so that every character or space in either string is opposite a unique character or a unique space in the other string.

For example, in the alignment

```
c  a  c  _  d  b  d
c  a  w  x  _  b  _
```

of strings *cacdbd* and *cawxb*, character *c* is mismatched with *w*, both *d's* and the *x* are opposite spaces, and all other characters are in matches.

Definition 2 (from [2]) : A global *multiple alignment* of $k > 2$ strings $S = S_1, S_2, ..., S_k$ is a natural generalization of alignment for two strings. Chosen spaces are inserted into (or at either end of) each of the k strings so that the resulting strings have the same length, defined to be l. Then the strings are arrayed in k rows of l columns each, so that each character and space of each string is in a unique column.

Alignment is necessary, since evolutionary processes introduce mutations in the DNA and biologists do not know, whether nth symbol in one sequence indeed corresponds to the nth symbol of the other sequence – a shift is probable.

Definition 3 (from [2]) : The *edit distance* between two strings is defined as the minimum number of edit operations – insertions, deletions, and substitutions – needed to transform the first string into the second. For emphasis, note that matches are not counted.

Edit distance is sometimes referred to as *Levenshtein distance* in recognition of the paper [3] by V. Levenshtein where edit distance was probably first discussed.
Sequence alignment is a generalization of an intuitive approach to analysis of similarity between sequences, based on searching for the longest common subsequence (LCS). The LCS is found by inserting gaps in the two sequences, so that they can be aligned with a maximum possible number of matching characters. This operation uses a simple *scoring function*: "+1 for a matching character, 0 otherwise." In real biological applications more complicated *scoring matrices* are used, assigning more points to matching known functional biological sequences, giving points for aligning characters which do not strictly match, but are similar from the point of view of their biological function, and also subtracting points for non-matching characters and gaps in unexpected places. The final score is usually simply a sum of points for all pairs of characters. The alignment is therefore optimal, when the similarity is greatest, resulting in the highest score with the selected scoring matrix [4].
The optimal path leading to the best alignment is found using dynamic programming algorithms. The most well-known dynamic programming algorithm used in bioinformatics for this task is the Needleman-Wunsch algorithm. The goal is to find the best global alignment of two se-

quences of characters. Global alignment answers the question, how similar are the two compared sequences along their entire length. Usually the compared sequences are of similar length, however in some cases the sequences are very different, except for some shorter, similar subsequences. Sometimes it is also necessary to compare sequences of very different lengths. In this case a local alignment algorithm is better. An example of such algorithm is the Smith-Waterman algorithm, a modification of the Needleman-Wunsch algorithm. Given a scoring function, the algorithm is designed to find the most similar pair of subsequences of both sequences. In the local alignment problem the final score is computed only on the pair of subsequences, omitting the rest of the characters. The difference between local and global alignment is illustrated below [5].
Global alignment:

```
--AGATCCGGATGGT--GTGACATGCGAT--AAG--AGGCGTT
    ||| |  |  |  ||||| ||||||  |||  |  | ||
GTCCATCTG--TCTTGGGTGAC-TGCGATACAAGTTA--CCTT
```

Local alignment:

```
--AGATCCGGATGGT--[GTGACATGCGATA]--AG--AGGCGTT
                  ||||| |||||||
GTCCATCTG--TCTTGG[GTGAC-TGCGATA]CAAGTTA--CCTT
```

3. Sequence alignment and network threat recognition

Sequence alignment is a useful tool for network threat recognition in intrusion detection systems, automated threat signature generators and in malware analysis. To recognize a threat it is necessary to compare the new, observed behavior with previously identified or exemplary malicious behavior. The comparison is more useful, if it is not strict – this facilitates the detection of variants of attacks (behaviors) or attempts at masking the attack. Just like in bioinformatics problems, the main task is to find regularities, repeating similar sequences in large datasets.

4. Anomaly detection

One of the first applications of sequence alignment to intrusion detection is mentioned in [5] – with explicit connection to bioinformatics. The authors focused on the problem of detection of masquerading attempts, using logs of the `acct` tool in Unix systems as input data. Masquerading detection involves a *user signature* – a sequence of commands collected from the user, compared with the current session of this user. The main assumption is that an intruder using another user's account will behave in a different way than the rightful owner of the account, and that this difference of issued commands should be detectable. The paper proposes a method of aligning sequences of commands from the current session with the user signature using a modified version of the Smith-Waterman algorithm. The result of the alignment, using a proposed scoring function, is used to detect an intrusion. In the opinion of the authors a local alignment would not be sufficiently effective, as a lot of potentially interesting data would be ignored. Therefore, the authors have used a *semi-global* alignment. In this type of alignment only the suffixes or prefixes of compared sequences are aligned. The scoring function rewards matching commands, but does not penalize the existence of large, non-matching parts of the signature. As in every anomaly detection method, an arbitrary threshold must be chosen to separate a suspected intrusion from a normal, but slightly atypical session of the original user – this threshold was found empirically. The best experimental results show a 75.8% intrusion detection level with 7.7% of false positives. A full description of the algorithm, the scoring function, data preparation method and analysis of results can be found in [5].
Another method of intrusion detection, popular in the literature but rarely used on a wide scale is system call monitoring – the system calls of processes are monitored and compared to typical behavior of a given type of processes. Differences in behavior could indicate a successful attack on the application, resulting in execution of potentially malicious code. A recently proposed extension of this idea is based on *evolutionary distance* between sequences, defined as the sum of costs of substitutions, deletions and insertions. Instead of creating a model of the behavior of the monitored process, a "replica" of the process is created and executed in parallel. A difference in behavior of the two processes may be a symptom of an attack. Since an effect of the same attack on two identical processes on identical platforms must, by definition, be the same, diversification of replicas is necessary. Thus, good candidates for a replica are: the same process running on a different platform (e.g., Windows instead of Linux), or even a different process with the same functionality (e.g., a different WWW server) on a different platform. The authors of the idea assume that even though the processes will use different system calls, the function of those calls will be similar. It is possible to correlate different system calls from different processes/platforms. A description of the method of computing the behavioral distance between processes and of the experimental results can be found in the paper [6]. In the next paper [7] the authors used hidden Markov models for this task.

5. Threat signature generation

Bioinformatics are much more often mentioned in the literature on network threats in the context of threat signature generation systems. This area of research has gained a lot of attention in the recent years. New, unknown threats appear very often. They are initially not recognized by the traditional intrusion detection systems based on threat signatures, since a signature has not been created yet. In this

case a very useful tool is an automatic system, capable of recognizing a new threat and generating its signature, preferably without human intervention.

The first system to automatically generate threat signatures was honeycomb [8], a plug-in for honeyd. While the system itself was not based on bioinformatics methods, it did use some algorithms for detection of repeating similar sequences. The system applied the longest common substring[1] algorithm to find common sequences of bytes in different packets sent to the system. As the system was a part of a honeypot, all incoming packets were by definition suspected to be part of an attack. Unfortunately, the system did not scale well in real honeypot networks, it generated a lot of repeating signatures and was completely useless against polymorphic attacks. Additionally, lack of implemented signature management methods meant that with time it was difficult to tell, which signatures (and attacks) are indeed new.

Honeycomb had many successors, using different methods to recognize repeating sequences in the data stream, using them as the basis for signature generation. However, more advanced bioinformatics algorithms were not proposed until polymorphic attacks were targeted. In a polymorphic attack there are, by definition, few constant substrings (subsequences without gaps), common among all instances of the attack. Furthermore, the longest such substring, if found, is not necessarily the best sequence describing the attack.

For many years identification of a polymorphic attack using signatures expressed as subsequences of the attack was thought impossible. Signature-based intrusion detection systems were expected to disappear soon. However, in paper [9] it was shown, that every polymorphic attack must contain constant, repeating values, allowing the attack to successfully exploit a given vulnerability. Some constants are also required to use a given protocol to communicate with the attacked application. Description of such an attack is, therefore, possible, although difficult – a good description of the attack is neither a single common substring, nor the longest common subsequence, which might contain too many random individual characters. A local alignment is necessary to find a common region in all variants of a polymorphic attack. This approach was suggested in the polygraph system. It is a signature generation system, using information from another system to identify suspect flows. Using a set of such flows a signature is created as a set of short separate character sequences. For example, a signature for the Apache-Knacker exploit was as follows (expressed as a regular expression):

```
GET .* HTTP/1.1\r\n.*:.* \r\nHost:.* \r\n

.*:.*\r\nHost:.*\xFF\xBF.*\r\n
```

To find common characters for the flows the authors used a modified version of the Smith-Waterman algorithm. The modification included rewarding continuous alignment, since such signatures are less likely to cause false positives. Groups of characters were rewarded, while gaps were penalized, where gaps are not only the maximal length of subsequences matched with spaces, but also the maximal length of subsequences of non-matching characters. The penalties were selected so that character sequences were more likely to be aligned if their grouping is typical for a given protocol. In practice this would mean that different scoring functions for different protocols should be developed.

In the experiment carried out by its authors, the system was tested on three real exploits – two for httpd servers (the Apache-Knacker exploit and the ATPhttpd exploit) and one for BIND server (the BIND-TSIG exploit). Clet, a well known tool for polymorphic attack generation was used. It was found, that Clet had many weaknesses – in each variant of the exploit many constant sequences were found. Since the goal of the experiment was to test the system with the assumption of nearly perfect polymorphism, the code of the exploit was manually changed using random values, leaving the sequences necessary for its functioning intact. The signature generator based on the modified Smith-Waterman algorithm produced the correct signature in all tests, giving 0.0008% false positives for Apache-Knacker, and 0% for the BIND-TSIG exploit – verified against a test pool of "proper" traffic. Results for the ATPhttpd exploit were not published. Only 3 samples of the exploit were necessary to reach such a high level of precision. The generated signatures can be used in many modern intrusion detection systems like snort.

Another approach to polymorphic worm detection was used in [10]. Like in the previous case, common regions were searched for – using *Gibbs sampling* and creating signatures based on the frequencies of individual characters. Gibbs sampling is also used in bioinformatics to find *motifs* – unchanged by evolution regions in protein sequences.

6. Honeypot development

Bioinformatics methods can be of great value for honeypot developers. Honeypots are often the main source of information on new threats and a basis for early warning systems. The best honeypots are real systems with real applications. However, their installation and management is complicated and time consuming. This led to the creation of honeypots like honeyd and nepenthes [11], emulating the attacked services. They are easy to deploy and manage, even on a large scale, because the attacks on emulated services are – by definition – never successful, so the honeypots themselves are not infected. The downside of emulation are its limitations – it is never perfect (bug-for-bug compatibility is difficult to attain, especially for unknown bugs), and a honeypot is only as good as the emulation. The problem is how to create new emulation modules for services and their vulnerabilities in a fast and easy way. Automatic tools have been proposed – including ScriptGen,

[1] A *different* term than longest common subsequence (LCS) – it is by definition continuous, while the LCS may contain gaps. The resulting alignment is therefore different – the longest common substring usually is not simply the longest continuous part of the LCS.

which can generate new `honeyd` scripts and aims to add the ability to generate `nepenthes` modules. It functions in three steps:

– running a real system as honeypot, registering incoming traffic;

– traffic analysis without knowing the semantics of the observed protocols, by aligning many sequences of requests and answers and building a state automata based on the result of this analysis;

– creating a `honeyd` script based on the state automata.

A full description of the methods can be found in papers [12] and [13].

7. Summary

Bioinformatics methods are a promising approach to the problem of network threat detection and recognition. However, in most cases their only application are tests in laboratories. It seems that their most promising application from the practical point of view would be the generation of signatures for polymorphic attacks, more general signatures with a low level of false positives, creation of tools for management of automatically generated signatures and for extending the capabilities of honeypots (in tools like `ScriptGen`). An important conclusion is that bioinformatics methods have shown that the popular opinion that polymorphic attacks will make description and detection based on signatures of characteristic sequences obsolete is wrong.

References

[1] N. C. Jones and P. A. Pevzner, *An Introduction to Bioinformatics Algorithms*. Cambridge: MIT Press, 2004.

[2] D. Gusfield, *Algorithms on Strings, Trees, and Sequences: Computer Science and Computational Biology*. Cambridge: Cambridge University Press, 1997.

[3] V. I. Levenshtein, "Binary codes capable of correcting insertions and reversals", *Sov. Phys. Dokl.*, vol. 10, no. 8, pp. 707–710, 1966.

[4] P. Kijewski, "Zastosowanie metod bioinformatyki do rozpoznawania zagrożeń sieciowych", in *SECURE 2006 Bezpieczeństwo – czas na przełom*, Warsaw, Poland, 2006 (in Polish).

[5] S. Coull, J. Branch, B. Szymański, and E. Breimer, "Intrusion detection: a bioinformatics approach", in *Proc. 19th Ann. Comput. Secur. Appl. Conf.*, Washington, USA, 2003.

[6] D. Gao, M. K. Reiter, and D. Song, "Behavioral distance for intrusion detection", in *Proc. 8th Int. Symp. Recent Adv. Intrus. Detect. RAID 2005*, Seattle, USA, 2005.

[7] D. Gao, M. K. Reiter, and D. Song, "Behavioral distance measurement using hidden Markov models", in *Proc. 9th Int. Symp. Recent Adv. Intrus. Detect. RAID 2006*, Hamburg, Germany, 2006.

[8] C. Kreibich and J. Crowcroft, "Honeycomb – creating intrusion detection signatures using honeypots", in *Proc. 2nd Worksh. Hot Top. Netw. Hotnets II. ACM SIGCOMM*, Boston, USA, 2003.

[9] J. Newsome, B. Karp, and D. Song, "Polygraph – automatically generating signatures for polymorphic worms", in *Proc. IEEE Symp. Secur. Priv. SP 2005*, Washington, USA, 2005, pp. 226–241.

[10] Y. Tang and S. Chen, "Defending against Internet worms: a signature-based approach", in *Proc. 24th Ann. Conf. IEEE INFOCOM 2005*, Miami, USA, 2005.

[11] P. Baecher, M. Koetter, T. Holz, M. Dornseif, and F. Freiling, "The nepenthes platform: an efficient approach to collect malware", in *Proc. 9th Int. Symp. Recent Adv. Intrus. Detect. RAID 2006*, Hamburg, Germany, 2006.

[12] C. Leita, K. Mermoud, and M. Dacier, "ScriptGen: an automated script generation tool for honeyd", in *Proc. 21st Ann. Comput. Secur. Appl. Conf. ACSAC 2005*, Tucson, USA, 2005.

[13] C. Leita, M. Dacier, and F. Massicotte, "Automatic handling of protocol dependencies and reaction to 0-day attacks with ScriptGen based honeypots", in *Proc. 9th Int. Symp. Recent Adv. Intrus. Detect. RAID 2006*, Hamburg, Germany, 2006.

Adam Kozakiewicz graduated from the Faculty of Electronics and Information Technology of Warsaw University of Technology, Poland. Currently he works as a Research Associate at Systems and Information Security Methods Team in NASK Research Division and an Assistant at the Institute of Control and Computation Engineering at the Warsaw University of Technology, where he awaits the defense of his Ph.D. thesis in telecommunications. His main scientific interests includes security of information systems, parallel computation, optimization methods and network traffic modeling and control.
e-mail: adam.kozakiewicz@nask.pl
Research and Academic Computer Network (NASK)
Wąwozowa st 18
02-796 Warsaw, Poland

Anna Felkner graduated from the Faculty of Computer Science of Białystok Technical University, Poland. At present she works as a Research Assistant at Systems and Information Security Methods Team in NASK Research Division. She is a Ph.D. student in the Institute of Control and Computation Engineering at the Warsaw University of Technology. Her main scientific interests concerns the security of information systems.
e-mail: anna.felkner@nask.pl
Research and Academic Computer Network (NASK)
Wąwozowa st 18
02-796 Warsaw, Poland

Piotr Kijewski holds an M.Sc. degree in telecommunications from the Warsaw University of Technology. He works for NASK since 2002, as an IT Security Specialist in the CERT Polska team. His main interests in the computer and network security include intrusion detection, honeynets and network forensics. He is the leader of the team that designed, implemented and deployed the nation-wide early warning system based on honeypots in Poland. He has taken part in EU funded security projects (eCSIRT.net, SpotSpam). He is the author of over two dozen papers on security topics, and has spoken on conferences both inside and outside of Poland.
e-mail: piotr.kijewski@cert.pl
Research and Academic Computer Network (NASK)
Wąwozowa st 18
02-796 Warsaw, Poland

Tomasz Jordan Kruk graduated in computer science from Gdańsk University of Technology (M.Sc., 1994) and Warsaw University of Technology (Ph.D., 1999). From 1994 to 2001 he was responsible for supercomputers and services administration in Warsaw University of Technology Computing Centre. Since 1999 he works as an Associate Professor (Adjunct) at the Warsaw University of Technology. Since 2001 also Associate Professor (Adjunct) at Research and Academic Computer Network (NASK). His main areas of interests cover IT security, operating systems and distributed/cluster systems. Currently he heads the Systems and Information Security Methods Team in NASK Research Division.
e-mail: T.Kruk@nask.pl
Research and Academic Computer Network (NASK)
Wąwozowa st 18
02-796 Warsaw, Poland

Paper

A general framework of agent-based simulation for analyzing behavior of players in games

Ichiro Nishizaki

Abstract—In this paper, we give a general framework of agent-based simulation for analyzing behavior of players in various types of games. In our simulation model, artificial adaptive agents have a mechanism of decision making and learning based on neural networks and genetic algorithms. The synaptic weights and thresholds characterizing the neural network of an artificial agent are revised in order that the artificial agent obtains larger payoffs through a genetic algorithm. The proposed framework is illustrated with two examples, and, by giving some simulation result, we demonstrate availability of the simulation analysis by the proposed framework of agent-based simulation, from which a wide variety of simulation settings can be easily implemented and detailed data and statistics are obtained.

Keywords—artificial adaptive agents, simulation, games, behavior of players.

1. Introduction

In games with multiple equilibria, it is difficult to predict which equilibrium will be realized because of uncertainty about actions of opponents. Even in games with a unique equilibrium, it is known that in some special games, the prediction of the Nash equilibrium does not always correspond to reality. To examine human behavior in such games, numerous experiments have been accumulated.

Especially, a considerable number of studies have been made on experiments for examining human behavior in coordination games, generalized matching pennies games, ultimatum bargaining games, market entry games and so forth [3, 9, 16, 17, 19, 20, 21, 22]. Although in experimental studies, situations in accordance with game models are formed in laboratories and human subjects are motivated by money, for such experimental environments with human subjects there exist limitations with respect to the number of trials, the number of subjects, variations of parameter settings and so forth.

In most of mathematical models in economics and game theory, it is assumed that players are rational and maximize their payoffs, and they can discriminate between two payoffs with a minute difference. Such optimization approaches are not always appropriate for analyzing human behavior and social phenomena, and models based on adaptive behavior can be alternatives to such optimization models. Recently as complements of conventional mathematical models, a large number of adaptive behavioral models have been proposed [1, 4, 6, 7, 8, 13, 17, 18, 21, 23].

It is natural that actions of artificial agents in simulation systems are described by using adaptive behavioral rules, and simulation can be a promising approach to modeling situations where it is difficult to assume hyperrational behavior of decision makers. We suppose that simulation is a complement to experiments with human subjects because an extensive range of treatments can be easily performed by varying values of the parameters characterizing games in simulation systems while there exist the above mentioned limitations in experiments with human subjects. As concerns such approaches based on adaptive behavioral models, Holland and Miller [12] interpret most of economic systems as complex adaptive systems, and point out that simulation using artificial societies with adaptive agents is effective for analysis of such economic systems. Axelrod [2] insists on the need for simulation analysis in social sciences, and states that purposes of the simulation analysis include prediction, performance, training, entertainment, education, proof and discovery.

In this paper, we give a general framework of agent-based simulation for analyzing behavior of players in various types of games. In our simulation model, the decision mechanism of an artificial agent is based on a neural network with several inputs, and the agent chooses a strategy in accordance with the output of the neural network. The synaptic weights and thresholds characterizing the neural network are revised so that an artificial agent obtains larger payoffs through a genetic algorithm, and then this learning mechanism develops artificial agents with better performance. In Section 2, we describe the agent-based simulation system with decision and learning mechanisms based on neural networks and genetic algorithms. In Section 3, we provide some simulation result of the coordination games to demonstrate availability of the simulation analysis. Finally in Section 4, to conclude this paper, we make some remarks.

2. Simulation model

In this section, a general framework of agent-based simulation is presented together with two applications to specific games: the minimum strategy coordination game and the generalized matching pennies game [14, 15]. An artificial adaptive agent in our simulation system has a mecha-

nism of decision making and learning based on neural networks (see, e.g., Hassoun [11]) and genetic algorithms (see, e.g., Goldberg [10]).

2.1. Decision making by a neural network

Artificial agents repeatedly play a game; agents obtaining larger payoff are likely to be reproduced in the next period, and conversely agents obtaining only a little payoff are likely to be weeded out. In our model of an artificial genetic system embedded in the agent-based simulation model, the whole population is divided into m game groups, and in each game group the game is played by n agents. The number of agents, n, depends on setting of a game.

An artificial agent corresponds to a neural network, which is characterized by synaptic weights between two nodes in the neural network and thresholds which are parameters in the output function of nodes. In our simulation model, an action of an artificial agent is determined by a vector of outputs from a nonlinear function with several input data that the agent can know after playing a stage game. This decision mechanism is implemented by a neural network. The synaptic weights and thresholds characterizing the neural network are revised so that the artificial agent obtains larger payoffs through a genetic algorithm, and then this learning mechanism develops artificial agents with better performance.

Because a structure of neural networks is determined by the number of layers and the number of nodes in each layer, an artificial agent is prescribed by the fixed number of parameters if the numbers of layers and nodes are fixed. In our model, we form a string compound of these parameters which is identified with an artificial agent, and the string is treated as a chromosome in an artificial genetic system embedded in the simulation model.

2.2. Evolutionary learning through a genetic algorithm

In a simulation system, the game is played by n artificial agents in each of m game groups. Therefore, there are m agents for each type of players. There are s alternative strategies, and each of the agents chooses one among them. Mixed strategies can be implemented by some simple devises if necessary. The payoffs of artificial agents are determined by outcomes of the game. Repeatedly playing the game, agents obtaining larger payoffs are likely to survive; if this is not the case, such agents are culled out in time. In our simulation model, genetic algorithms are employed as an evolutionary learning mechanism. Because a fitness in the artificial genetic system is calculated by the obtained payoffs, agents obtaining larger payoffs are likely to survive. The general structure of simulation model is shown in Fig. 1.

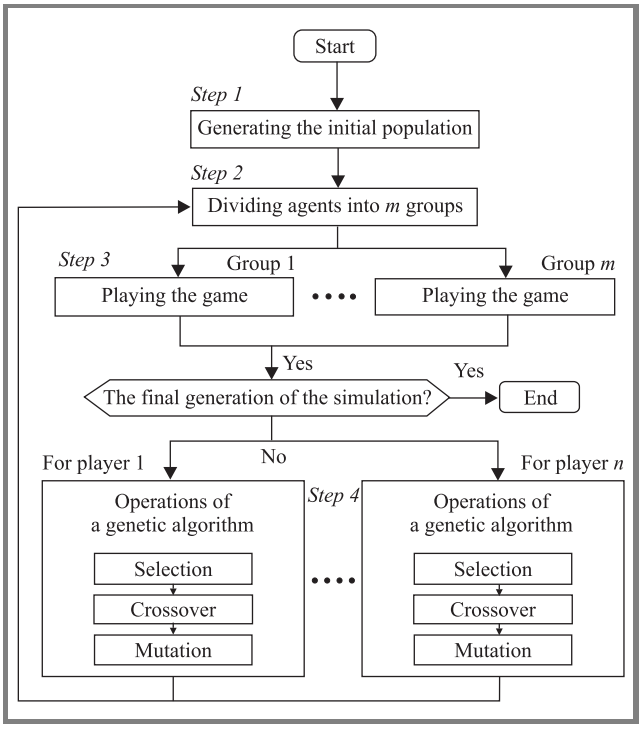

Fig. 1. Flow of the simulation.

The procedure of the simulation is summarized as follows.

Step 1: **Generating the initial population**. Let the number of players in the game and the number of groups for playing the game be n and m, respectively. Then, the whole population of mn artificial agents is initialized by assigning random numbers in the interval $[-1, 1]$ to the parameters of the synaptic weights and the thresholds characterizing the neural network.

Step 2: **Forming groups for playing the game**. The whole population with mn agents is divided into m groups for playing the game.

Step 3: **Playing the game**. Each agent chooses a strategy in accordance with the output of the neural network, and the game is played in each of the groups. The strategy of each agent is determined by the output of the neural network; an agent selects the strategy corresponding to the node with the largest output in the neural network. If the number of generations in the genetic algorithm reaches the final period of the simulation, the procedure stops.

Step 4: **Performing genetic operations**. The ith subpopulation is formed by gathering the ith players (agents) from the m groups; there are n subpopulations. The genetic operations are separately executed to each subpopulation consisting of m agents.

Step 4-1: **Reproduction**. Let π_i denote a payoff of agent i in the present period. The fitness of agent i is calculated as a function of π_i. As a reproduction operator, a certain method such as the roulette wheel selection is adopted. If the roulette wheel selection, by a roulette wheel with slots sized by the probability $p_i^{selection} = f_i / \sum_{i=1}^{mn} f_i$, each chromosome is selected into the next generation.

Step 4-2: **Crossover**. A certain crossover method such as the single-point crossover operator is applied to any pair of chromosomes with the probability of crossover p_c. If the single-point crossover operator is employed, a point of crossover on the chromosomes is randomly selected and then two new chromosomes are created by swapping subchromosomes which are the right side parts of the selected point of crossover on the original chromosomes. A new population is formed by exchanging the population in which the crossover operation is executed for the present generation with a given probability G. The probability G is called the generation gap. An agent keeps the history of obtaining payoffs in the past games, and the payoffs are divided between two offsprings in the proportion of sizes of the swapped subchromosomes.

Step 4-3: **Mutation**. With a given small probability of mutation p_m, each gene which represents a synaptic weight or a threshold in a chromosome is randomly changed. The selected gene is replaced by a random number in $[-1, 1]$.

2.3. Applications

So far, we have given the general framework of agent-based simulation for analyzing behavior of players in variety types of games. In this subsection, the proposed framework is illustrated with two examples: the minimum strategy coordination game and the generalized matching pennies game [14, 15].

Minimum strategy coordination game. Based on the proposed framework, agent-based simulation systems can be developed for a wide variety of games, and we can perform an extensive range of treatments of the corresponding simulation by using the system. For instance, we develop an agent-based simulation system [14] for analyzing the coordination game treated in the experimental investigation by Van Huyck *et al.* [22]. Because this coordination game is characterized by the minimum values of the strategies selected by players, we refer to it as the minimum strategy coordination game.

Before describing the specific structure of the neural network for artificial agents, we give the outline of the minimum strategy coordination game. Let the set of players be $N = \{1, \ldots, n\}$. All the players have the common set of strategies: $S = \{1, \ldots, \bar{s}\}$. Let $x_i \in S$ denote a strategy of player i. Then, the payoff function of player i is represented by

$$\pi(x_i, \underline{x_i}) = a \min(x_i, \underline{x_i}) - b x_i + c,$$
$$\underline{x_i} = \min(x_1, \ldots, x_{i-1}, x_{i+1}, \ldots, x_n),\ a > b > 0,\ c > 0. \tag{1}$$

The payoff of player i decreases with a strategy x_i of self, and increases with the minimum $\underline{x_i}$ among strategies of the others. To guarantee positive payoffs, the constant c is added.

An artificial agent as a player in the minimum strategy coordination game can be implemented by a neural network which is characterized by synaptic weights and thresholds. The structure of the neural network is depicted in Fig. 2.

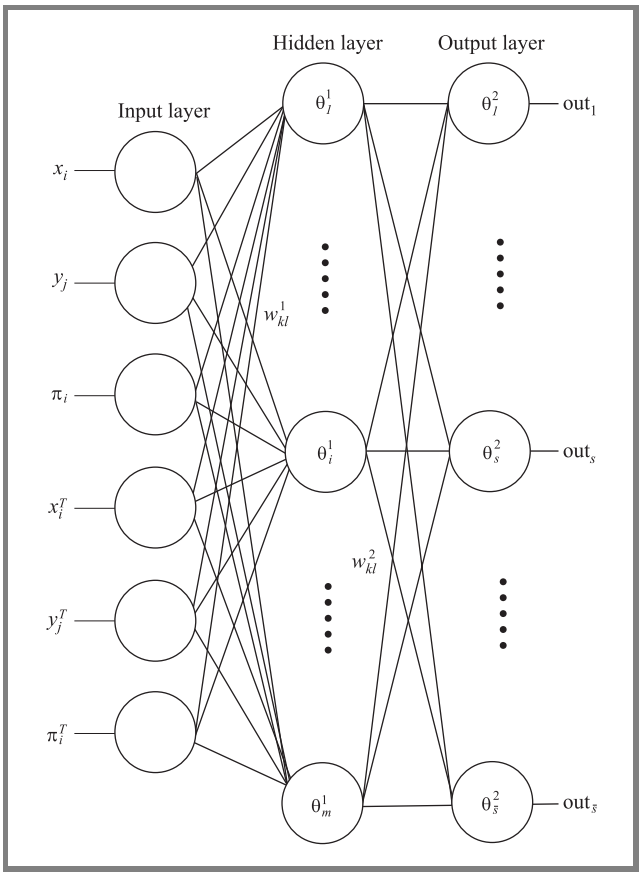

Fig. 2. The structure of the neural network for the minimum strategy coordination game.

There are six inputs in the neural network. In the following information of the inputs, the subscript i, $i = 1, \ldots, n$ means player i and the subscript j, $j = 1, \ldots, m$ means game group j. Thus, the subscript ij identifies a particular agent in the agent-based simulation system. For inputs 1 and 2, because human subjects in the experiment are informed of the minimum strategy at the last game, and it is supposed that they remember the strategies selected by

themselves, the strategy x_{ij} of agent ij and the minimum strategy y_j in game group j are given as inputs of the neural network; the payoff π_{ij} obtained by agent ij at the last period is also given as input 3. Supposing that a player does not remember an exact history of strategies in the past periods, but the player remembers at least the most frequent strategy in the past periods, we provide the weighted most frequent strategy x_{ij}^T in the last T periods as input 4 to the neural network. In the definition of x_{ij}^T, assuming that old memory is apt to decay, the discount factor w, $0 < w < 1$ is introduced. Similarly, as inputs 5 and 6, the weighted most frequent minimum strategy y_j^T and the weighted sum of obtained payoffs in the last T periods are also given.

An algorithm for evolutionary learning through the genetic algorithm is modified if necessary. In the experiment conducted by Van Huyck *et al.* [22], subjects understand the payoff table defined by the payoff function (1), and it is not true that they start to play the game without any prior knowledge of the game. Therefore it is natural for artificial agents in our system to have some knowledge of the game before playing it. To do so, by using the error back propagation algorithm (see, e.g., Hassoun [11]) with the teacher signals, the parameters of the synaptic weights and the thresholds in the neural network are adjusted ahead.

Generalized matching pennies game. We provide another application of the proposed framework of agent-based simulation to the generalized matching pennies game treated in the experiment by Ochs [16]. The payoff table of the generalized matching pennies game is shown in Table 1. In this game, the row player has the two choices U and D and the column player also has the two choices L and R. When an outcome is (U,L) or (D,R), the row player receives a positive payoff of a or 1, respectively. When an outcome is (U,R) or (D,L), the column player receives a positive payoff of 1. For the payoff a of the row player with respect to the outcome (U,L), we assume that $a \geq 1$. When $a = 1$, the game is symmetric, and when $a > 1$, it is asymmetric. It is known that, in the generalized matching pennies game, there does not exist any Nash equilibrium with pure strategies but there exists only a unique Nash equilibrium with strict mixed strategies.

Table 1
A generalized matching pennies game

Row player	Column player	
	L	R
U	$(a,0)$	$(0,1)$
D	$(0,1)$	$(1,0)$

Let p denote a probability of choosing strategy U for the row player, and let q denote a probability of choosing strategy L for the column player. Then, expected payoffs π_R and π_C of the row player and the column player, respectively, are represented by

$$\pi_R = apq + (1-p)(1-q), \tag{2}$$

$$\pi_C = (1-p)q + p(1-q), \tag{3}$$

and the corresponding Nash equilibrium is $(p^{\text{Nash}}, q^{\text{Nash}}) = (1/2, 1/(a+1))$. Because this game is not a zero-sum game, the maximin strategy is different from the Nash equilibrium. The maximin strategies of the row player and the column player are given by $\arg\max_p \min_q \pi_R(p,q)$ and $\arg\max_q \min_p \pi_C(p,q)$, respectively, and therefore the pair of the maximin strategies is $(p^S, q^S) = (1/(a+1), 1/2)$.

Artificial agents playing the generalized matching pennies game can be implemented by a neural network in a way similar to in the previous application of the minimum strategy coordination game. The structure of the neural network is depicted in Fig. 3.

The inputs of the neural network include not only payoffs of self obtained in the past periods but also payoffs of an opponent, and the set of inputs consists of five values. Let $x_i(j)$ be a payoff of player i at period j. Then, the total payoff of player i at period t is represented by

$$x_i^{\text{total}}(t) = \sum_{j=1}^{t} \phi_i^{t-j} x_i(j). \tag{4}$$

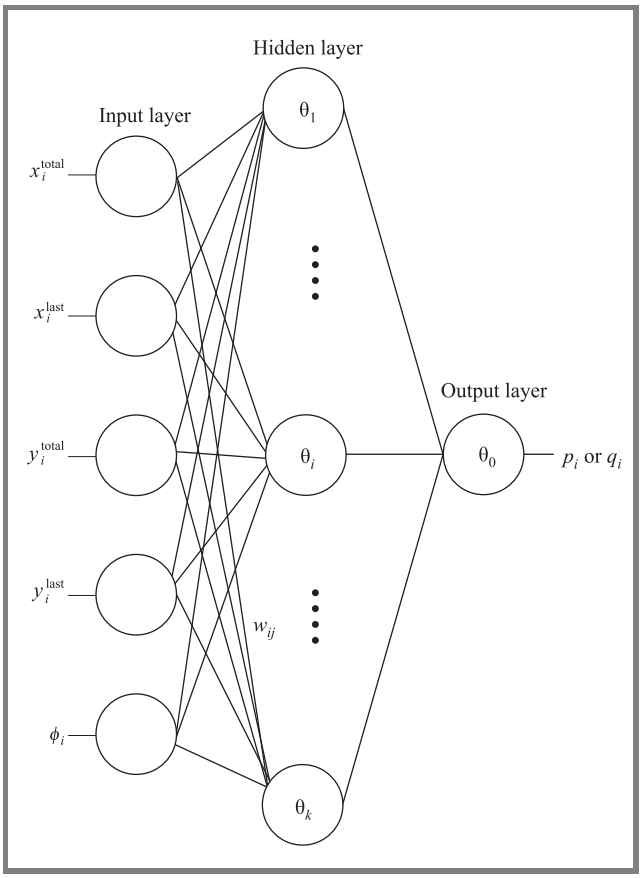

Fig. 3. The structure of the neural network for the generalized matching pennies game.

On the assumption that a decision of the artificial agent is affected by the payoff obtained before, though the previous payoff is reduced by $(1-\phi_i)$, the total payoff x_i^{total} is used as an input 1 of the neural network. In the extended reinforcement model by Erev and Roth [7], a similar parameter is incorporated. In the experiment by Ochs [16], it is found that there exist some players who take an outcome of the previous game into account and make a decision. From this viewpoint, we employ the payoff x_i^{last} obtained at the last game as input 2 of the neural network. Furthermore, Duffy and Feltovich [5] claim that choices of players are influenced by the behavior or payoff of the others, and therefore in our model the payoffs y_i^{total} and y_i^{last} of an opponent as well as the payoffs of self are incorporated as inputs 3 and 4 of the neural network. The value of $(1-\phi_i)$ can be interpreted as the rate of forgetting. On our model, the value of ϕ_i as input 4 to the neural network is fixed for each agent and it is randomly assigned to each agent at the beginning of the simulation.

The output of the neural network is a probability that the artificial agent chooses strategy U if the agent is the row player or strategy L if the agent is the column player.

Because the generalized matching pennies game is a two-person game, the number of players is $n=2$. For development of an agent-based simulation system to this game, we slightly modify the procedure of the simulation to allow artificial agents to use mixed strategies. Furthermore, to examine effect of error in decisions and risk attitude of players, the fitness of an artificial agent is defined as a function of the payoff and the parameters of error and risk attitude in the genetic algorithm embedded in the simulation system.

Although we have shown only two examples, our general framework of agent-based simulation can be applicable to various games and economic situations such as the ultimatum bargaining game, the market entry game, and so forth.

3. Analysis of simulation data

In this section, by giving a part of the simulation result of the minimum strategy coordination game, we demonstrate availability and effectiveness of the simulation analysis by the proposed framework of agent-based simulation, from which a wide variety of simulation settings can be easily implemented and detailed data and statistics are obtained.

In this example, a variety of treatments are performed by varying values of some parameters characterizing the game; the three different simulations are arranged: *simulations coefficients*, *information*, and *size*.

If the coefficient b of the second term in the payoff function (1) is positive, it follows that players who select larger strategies than the minimum strategy pay the penalty. If the coefficient b is equal to zero, the coordination problem such as coordination failure and disequilibrium is eliminated. In the experiment by Van Huyck *et al.* [22], when $b=0$, the payoff dominant equilibrium is observed; when $b=0.1$, the subjects avoid risky strategies and choices of the subjects settle into the secure equilibrium. From this result, it is reasoned that by making the value of b larger from zero, outcomes of the game shift from the payoff dominant equilibrium to the secure equilibrium. In *simulation coefficient*, two treatments are performed, varying the values of the coefficients b and a. Moreover, after putting artificial agents in experiencing the payoff dominant equilibrium in case of $b=0$, the agents play the games with $b\neq 0$. By examining the choices of agents and the realization rate of equilibria in this simulation, we investigate the relation between the penalty and the behavior of artificial agents.

In the experiment with human subjects by Van Huyck *et al.* [22], two types of treatments of information on outcomes of the game are performed: one treatment where the subjects are informed only of the minimum strategy, and the other treatment where the subjects are informed of the distribution of strategies selected by all the players. Comparing the two treatments, they conclude that informing the subjects of the distribution of the strategies accelerates the convergence of behavior of the subjects. In *simulation information*, artificial agents are provided three types of information on outcomes of the game: the minimum strategy, the minimum and the maximum strategies, and the distribution of strategies. We examine the effect of information given to artificial agents on the choices of them and the realization rate of equilibria.

In the experiment, it is also observed that when the number of players is two, in comparison with the case of 14 or 16 subjects, it is likely to realize the payoff dominant equilibrium. In *simulation size*, varying the number of artificial agents as well as the value of b representing the degree of the penalty, we investigate influence of the number of agents on their behavior in the game and outcomes of the game.

In this paper, as an example, we provide detailed analysis of only one treatment of *simulation coefficients*. In general as the value of b is made larger and the risk of paying the penalty increases, the payoff of an artificial agent selecting a large strategy such as the payoff dominant strategy 7 becomes a small value, and therefore it is likely to fail in coordination. However, the risk-free game with $b=0$ is not the case. In this treatment, fixing the value of a at $a=0.2$, the value of the penalty coefficient b is varied; it is set at $b=0.0, 0.005, 0.006,\ 0.007, 0.008, 0.009,\ 0.01, 0.02, 0.03,\ 0.04, 0.05, 0.1$. From the data observed in the treatment, we investigate transitions and steady states of the choice rate of each strategy, the realization rate of each individual equilibrium, and so forth.

Figures 4, 5, 6, and 7 show the choice rate of each strategy, the minimum strategy rate of each strategy, the means of selected strategies and the minimum strategies, and the normalized average payoff, respectively. For comparison, in Figs. 4 and 5, the data from the experiment with human subjects by Van Huyck *et al.* [22] are provided by outline symbols. Moreover, the realization rate of each individual equilibrium and the gross realization rate of equilibria are given in Figs. 8 and 9, respectively.

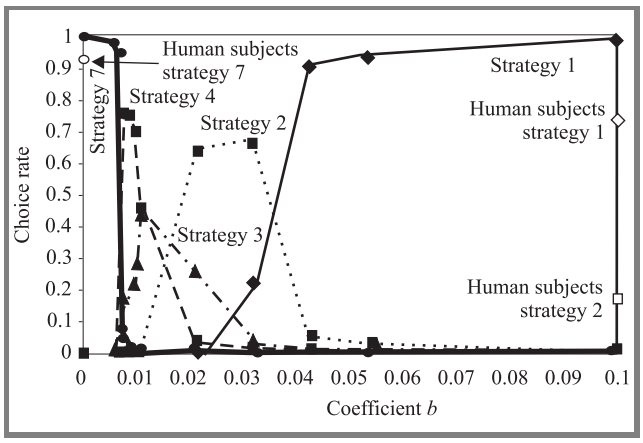

Fig. 4. Choice rate of each strategy in treatment *b*.

In Fig. 4, the choice rate of each strategy at the steady state is given. When the penalty is relatively large, i.e., $b \geq 0.04$, the secure strategy 1 is likely to be selected. Namely, most of the artificial agents avoid the risk of paying a large penalty and select the most secure strategy. As the value of b decreases and therefore the penalty becomes small, the modal strategy, which is the most frequently selected strategy, grows large from the strategy 1 to the strategy 4 one by one. When b is smaller than around 0.006, the modal strategy jumps straight to the strategy 7, and strategies 5 and 6 do not become modal.

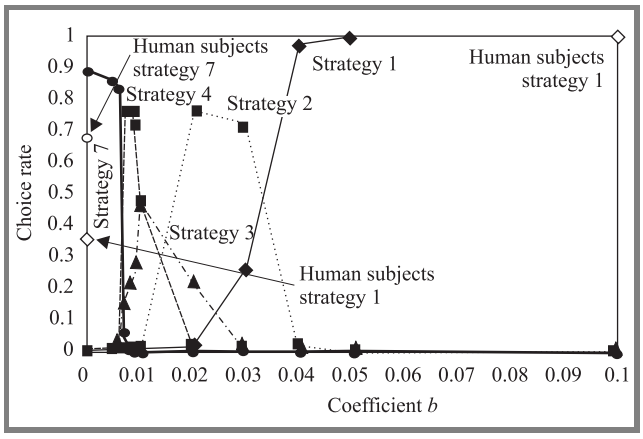

Fig. 5. Minimal strategy rate of each strategy in treatment *b*.

In Fig. 5, the minimum strategy rate of the strategy s means the rate that the strategy s is the minimum in the game. From the fact that Fig. 5 is highly similar to Fig. 4, it follows that the modal strategy in the steady state is almost the same as the minimum strategy. For the strategy 1, when $b \geq 0.04$, although the choice rate of the strategy 1 shown in Fig. 4 decreases little by little as the value of b becomes small, the minimum strategy rate of the strategy 1 shown in Fig. 5 is almost 1.0. Contrary to the strategy 1, when $b = 0$, the choice rate of the strategy 7 is almost 1.0, but the minimum strategy rate falls below 0.9 because the other strategies are selected on rare occasions.

Compared with the result of the experiment with human subjects, when $b = 0.1$, the choice rate of the secure strategy 1 of the artificial agents, 0.99, is larger than that of the human subjects, 0.72; for the minimum strategy rate, both of them get the highest rate, 1.0. For the case of $b = 0$, in the experiment with human subjects, the value of the gain coefficient a is set at $a = 0.1$, which is slightly different from the setting of the simulation. The choice rate of the payoff dominant strategy 7 of the artificial agents is 0.99 which is close to the result of the human subjects, 0.956; the minimum strategy rate of the artificial agents, 0.891, is larger than that of the human subjects, 0.667. All in all, the result of the simulation is similar to that of the experiment with human subjects, and therefore the result of the simulation supports that of the experiment with human subjects. To be more precise, in the both results, the secure strategy is dominant when the risk of paying a large penalty is high; in the absence of such risk, the payoff dominant strategy is likely to be chosen. From the other perspective on this similarity, the simulation system successfully emulate the human behavior in the game.

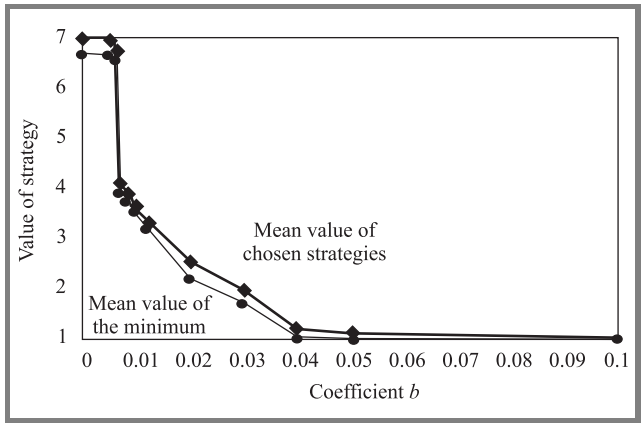

Fig. 6. Means of selected strategies and the minimal strategies in treatment *b*.

In Fig. 6, the means of the chosen strategies and the minimal strategies are shown; it can be found that these values are very similar. This fact means that at the steady state, most of the artificial agents choose the minimal strategies.

From Fig. 7, the payoff obtained by an agent decreases as the value of b increases from $b = 0$. At the point of $b = 0.04$, the payoff is equal to the payoff of the secure strategy 1. Because when $b \geq 0.04$, the payoff of the secure strategy 1 grows large with the value of b, we can understand that most of the artificial agents choose strategy 1 in such a situation.

The realization rate of each individual equilibrium is given in Fig. 8. When $b = 0.1$, the secure equilibrium $(1,\ldots,1)$ is realized at the rate of 0.89 in the steady state. Although as the value of b decreases, the realization rate of the secure equilibrium decreases, it should be noted that in the interval $0.04 \leq b \leq 0.1$, only the secure equilibrium $(1,\ldots,1)$ is realized. As the value of b still decreases over 0.04,

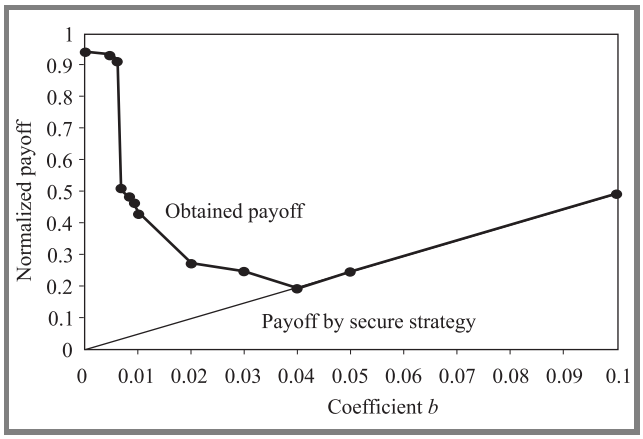

Fig. 7. Normalized average payoff in treatment b.

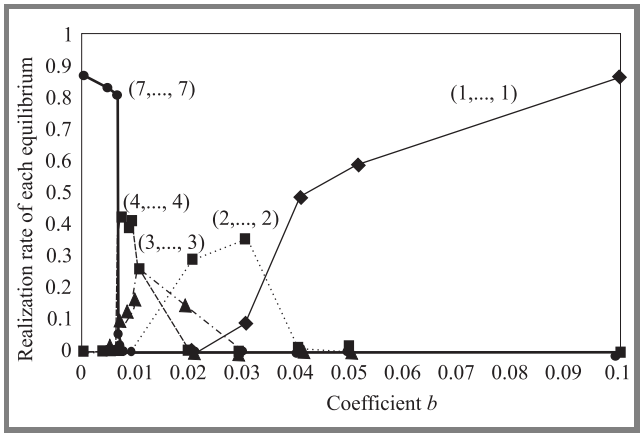

Fig. 8. Realization rate of each individual equilibrium in treatment b.

the consecutive equilibria, $(2,\ldots,2)$, $(3,\ldots,3)$, and $(4,\ldots,4)$, can be found, but the realization rates of these equilibria do not exceed 0.5. When $b \leq 0.006$, the payoff dominant equilibrium $(7,\ldots,7)$ is realized at the rate larger than 0.8.

The gross realization rate of equilibria is shown in Fig. 9; it is found that at both ends of the horizontal axis, $b = 0$ and $b = 0.1$, the equilibria are likely to be realized. In the intermediate cases where effectiveness of the risk of paying the penalty is not clear, it becomes difficult for artificial agents to coordinate their strategies, and therefore the gross realization rate of equilibria descends, compared with the cases of $b = 0$ and $b = 0.1$.

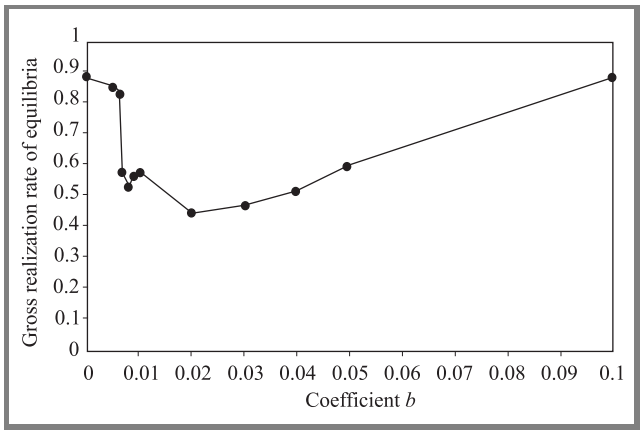

Fig. 9. Gross realization rate of equilibria in treatment b.

As described above we have examined the result of the treatment on change of the coefficient b, and several characteristics of behavior of agents in the game can be found through the agent-based simulation based on the proposed general framework. Although only the two cases of $b = 0$ and $b = 0.1$ are performed in the experiment with human subjects, we conduct various runs of the treatment in the agent-based simulation and we obtain the following observations and findings.

1. In the games without the risk of paying any penalty, the artificial agents successfully coordinate their strategies and the payoff dominant equilibrium is realized.
2. In the games with the risk of paying a substantial penalty, coordination among the artificial agents is failed, but they suitably predict strategies of the opponents and the secure equilibrium forms.
3. The games with the risk of paying the intermediate penalty are likely to bring outcomes of disequilibria.
4. As the value of b decreases, artificial agents shift choices of strategies stepwise from the secure strategy 1 to the payoff dominant strategy 7.
5. While the payoff dominant equilibrium is sensitive to increase of the value of b, the secure equilibrium is not so sensitive to decrease of the value of b.

4. Conclusions

In this paper, we have given a general framework of agent-based simulation for analyzing behavior of players in various types of games and economic situations. In our simulation model, the decision mechanism of an artificial agent is based on a neural network with several input data that the agent can know after playing a stage game, and the artificial agent chooses a strategy in accordance with the output of the neural network. The synaptic weights and thresholds characterizing the neural network of an artificial agent are revised so that the artificial agent obtains larger payoffs through a genetic algorithm, and then this learning mechanism develops agents with better performance. Finally, by giving a part of the simulation result of the minimum strategy coordination game, we demonstrate availability and effectiveness of the simulation analysis by the proposed framework of agent-based simulation.

References

[1] J. Andreoni and J. H. Miller, "Auctions with artificial adaptive agents", *Games Econom. Behav.*, vol. 10, pp. 39–64, 1995.

[2] R. Axelrod, "Advancing the art of simulation in the social sciences", in *Simulating Social Phenomena*, R. Conte, R. Hegselmann, and R. Terna, Eds. Berlin, Heidelberg: Springer-Verlag, 1997, pp. 21–40.

[3] G. E. Bolton and R. Zwick, "Anonymity versus punishment in ultimatum bargaining", *Games Econom. Behav.*, vol. 10, pp. 95–121, 1995.

[4] R. E. Dorsey, J. D. Johnson, and M. V. Van Boening, "The use of artificial neural networks for estimation of decision surfaces in first price sealed bid auctions", in *New Directions in Computational Economics*, W. W. Cooper and A. B. Whinston, Eds. Dordrecht: Kluwer, 1994, pp. 19–40.

[5] J. Duffy and N. Feltovich, "Does observation of others affect learning in strategic environments? An experimental study", *Int. J. Game Theory*, vol. 28, pp. 131–152, 1999.

[6] I. Erev and A. Rapoport, "Coordination, "magic", and reinforcement learning in a market entry game", *Games Econom. Behav.*, vol. 23, pp. 146–175, 1998.

[7] I. Erev and A. E. Roth, "Predicting how people play games: reinforcement learning in experimental games with unique, mixed strategy equilibria", *Amer. Econom. Rev.*, vol. 88, pp. 848–881, 1998.

[8] D. Fundenberg and D. K. Levine, *The Theory of Learning in Games*. Cambridge: The MIT Press, 1998.

[9] J. K. Goeree, C. A. Holt, and T. R. Palfrey, "Risk averse behavior in generalized matching pennies games", *Games Econom. Behav.*, vol. 45, pp. 97–113, 2003.

[10] D. E. Goldberg, *Genetic Algorithms in Search, Optimization, and Machine Learning.* Reading: Addison Wesley, 1989.

[11] M. H. Hassoun, *Fundamentals of Artificial Neural Networks*. Cambridge: The MIT Press, 1995.

[12] J. H. Holland and J. H. Miller, "Adaptive intelligent agents in economic theory", *Amer. Econom. Rev*., vol. 81, pp. 365–370, 1991.

[13] M. Leshno, D. Moller, and P. Ein-Dor, "Neural nets in a group decision process", *Int. J. Game Theory*, vol. 31, pp. 447–467, 2002.

[14] I. Nishizaki, H. Katagiri, T. Hayashida, and N. Hara, "Agent-based simulation analysis for equilibrium selection and coordination failure in coordination games characterized by the minimum strategy", Mimeo, 2007.

[15] I. Nishizaki, T. Nakakura, and T. Hayashida, "Agent-based simulation for generalized matching pennies games", in *Proc. 3nd Int. Conf. Soft Comp. Intell. Syst. 7th Int. Symp. Adv. Intell. Syst. SCIS & ISIS 2006*, Yokohama, Japan, 2006, pp. 1530–1535.

[16] J. Ochs, "Games with unique, mixed strategy equilibria: an experimental study", *Games Econom. Behav.*, vol. 10, pp. 202–217, 1995.

[17] A. Rapoport, D. A. Seale, and E. Winter. "Coordination and learning behavior in large groups with asymmetric players", *Games Econom. Behav.*, vol. 39, pp. 111–136, 2002.

[18] A. E. Roth and I. Erev, "Learning in extensive form games: experimental data and simple dynamic models in the intermediate term", *Games Econom. Behav.*, vol. 8, pp. 163–212, 1995.

[19] A. Roth, V. Prasnikar, M. Okuno-Fujiwara, and S. Zamir, "Bargaining and market behavior in Jerusalem, Ljubljana, Pittsburgh, and Tokyo: an experimental study", *Amer. Econom. Rev*., vol. 81, pp. 1068–1095, 1991.

[20] D. Schmidt, R. Shupp, J. M. Walker, and E. Ostrom, "Playing safe in coordination games: the role of risk dominance, payoff dominance, and history of play", *Games Econom. Behav.*, vol. 42, pp. 281–299, 2003.

[21] J. A. Sundali, A. Rapoport, and D. A. Seale, "Coordination in market entry games with symmetric players", *Organiz. Behav. Hum. Decis. Process.*, vol. 64, pp. 203–218, 1995.

[22] J. B. Van Huyck, R. C. Battalio and R. O. Beil, "Tacit coordination games, strategic uncertainty, and coordination failure", *Amer. Econom. Rev*., vol. 80, pp. 234–248, 1990.

[23] H. P. Young, *Individual Strategy and Social Structure*. Princeton: Princeton University Press, 1998.

Ichiro Nishizaki is Professor at Department of Artificial Complex Systems Engineering, Graduate School of Engineering of the Hiroshima University, Japan. His research and teaching activities are in the area of systems engineering, especially game theory, multiobjective decision making and agent-based simulation analysis.

e-mail: nisizaki@hiroshima-u.ac.jp
Department of Artificial Complex Systems Engineering
Graduate School of Engineering, Hiroshima University
1-4-1 Kagamayama, Higashi-Hiroshima, 739-8527, Japan

Paper

Artificial adaptive agent model characterized by learning and fairness in the ultimatum games

Tomohiro Hayashida, Ichiro Nishizaki, and Hideki Katagiri

Abstract—This paper examines the result of the experimental research on the ultimatum games through simulation analysis. To do so, we develop agent-based simulation system imitating the behavior of human subjects in the laboratory experiment by implementing a learning mechanism involving a concept of fairness. In our agent-based simulation system, mechanisms of decision making and learning are constructed on the basis of neural networks and genetic algorithms.

Keywords—artificial adaptive agents, simulation, games, behavior of players.

1. Introduction

In this paper, we develop a multi-agent simulation system for analyzing behavior of players in the ultimatum games. In the subgame perfect equilibrium of the ultimatum game, player *1* who is a proposer obtains almost all the payoff which is divided between players *1* and *2*, and player *2* accepts the offer of player *1*. It is known from the results of the experimental investigations of the past that the subgame perfect equilibrium does not accurately forecast the ultimatum play, and the payoff is divided almost equally. A diversified range of experiments have been accumulated in order to examine why outcomes of the games deviate from the subgame perfect equilibrium [4, 8, 11, 13, 14, 15, 17, 20, 21], where the following issues are focused on: fairness of players, the number of rounds of the game, difference in nations or races, the right to be player *1*, the structural power of player *1*, anonymity of play, punishment for unfair proposals, magnitude of payoff, and so forth.

Bolton [2] tries to explain the experimental results by using a utility function of a player which is influenced not only by a payoff of the player but also by a payoff of the opponent; the utility function is defined by the payoff of the player and the ratio of the payoff of the player to that of the opponent. Moreover, Bolton and Ockenfels [3] extend this model to games with incomplete information. Rabin [18] define a fairness equilibrium by using a utility function of the payoff of self and the kindness to the opponent, and consider some economic examples. Fehr and Schmidt [7] consider fairness, competition and cooperation in the economic environment by using a utility function defined by the payoff of self and a difference between the payoff of self and that of the opponent. Costa-Gomes and Zauner [5] attempt to explain the experimental data of Roth *et al*. [20] by a utility function with the payoffs of two players and a random disturbance term.

Concerning approaches without any utility function, Roth and Erev [19] propose a simple learning model based on reinforcement learning. Gale *et al*. [9] show that replicator dynamics leads not to the subgame perfect equilibrium, but to the Nash equilibria; they suggest that researchers should give attention to not always the subgame perfect equilibrium but also the Nash equilibria in evaluating the experimental data. Incorporating the quantal response equilibria (QRE) model [16], Yi [22] attempts to explain the experimental result of the ultimatum games.

Abbink *et al*. [1] compare an approach based on the utility function with an approach based on adaptive learning; they argue the abilities and limitations of both approaches. From these research results, it seems to be desirable to incorporate both concepts of fairness and learning for modeling the behavior of players in the ultimatum game. In this paper, we develop a simulation system with artificial adaptive agents which have a decision making and learning mechanism based on neural networks (e.g., [12]) and a genetic algorithm (e.g., [10]). By employing the utility function proposed by Fehr and Schmidt [7] as a fitness function of the genetic algorithm, fairness is incorporated in the learning mechanism of the artificial agents. In our system for simulation of the ultimatum games, an action of an agent is determined by a vector of outputs from a nonlinear function with several input data that agents can know after playing a stage game; this decision mechanism is implemented by a neural network. The artificial agents with chromosomes consisting of the synaptic weights and thresholds characterizing the neural network are evolved so as to obtain larger payoffs through a genetic algorithm, and then this learning mechanism develops agents with better performance.

To imitate the behavior of human subjects in a laboratory experiment and examine the result of the experiment by using the agent-based simulation system, we use the data from the experiment by Roth *et al*. [20], and identify the standard set of the parameters in the utility function incorporating fairness by Fehr and Schmidt [7]. Moreover, by varying the values of the parameters, we evaluate the effect of each individual parameter on the behavior of the artificial agents.

The organization of this paper is as follows. In Section 2, we describe the ultimatum game and briefly review the experimental result of the ultimatum game by Roth *et al*. [20]. Section 3 is devoted to describing the agent-based simulation system with the learning mechanism and the utility function incorporating fairness. In Section 4, we exam-

ine the results of the simulations; finally in Section 5, we give a summary of the simulations and some concluding remarks.

2. The ultimatum game

We deal with an ultimatum game in which two players divide \$10. In this game, player *1* who is the first mover makes an offer $(x_1, x_2 = 10 - x_1)$, $x_2 \in \{1, \ldots, 10\}$, and player *2* who is the second mover accepts or rejects the offer (x_1, x_2); if player *2* accepts, players *1* and *2* obtain $\pi_1 = x_1$ and $\pi_2 = x_2$, respectively; otherwise they obtain nothing, $\pi_1 = \pi_2 = 0$. It is noted that the offer of 0 by player *1* is removed from a list of possible offers; this setting is also used in the ultimatum game in [6]. In Fig. 1, a game tree of the ultimatum game is depicted. Because player *2*'s payoff by acceptance is larger than that by rejection in any of player *2*'s nodes, the subgame perfect equilibrium is player *1*'s offer of $(\$9, \$1)$ and acceptance of player *2*; the pair of the equilibrium payoffs is $(\$9, \$1)$.

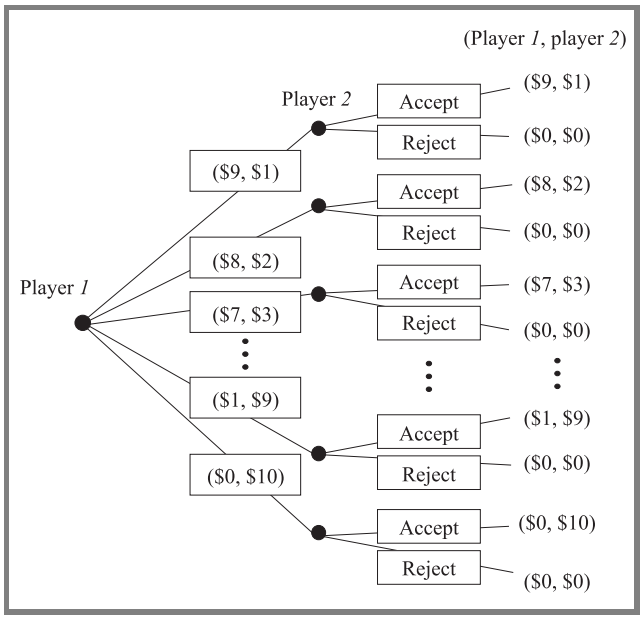

Fig. 1. Game tree of the ultimatum game.

We review and summarize the result of the experiment by Roth *et al*. [20], where the experiment about bargaining and market behavior is conducted in four countries: Israel, Japan, the United State, and Yugoslavia. As a practical matter, in the experiment \$10 is represented as 1000 tokens, and all offers are made in multiples of 5 tokens. There are three sessions of the ultimatum game; in each session, about 20 subjects are recruited and the game is played 10 rounds; a pair of players are randomly matched at each round. Because any offer is available only in increments of \$1 in our simulation, we use the discretized data of the experiment shown in [5] and we take the average after pooling all the data of the four countries. The result of the experiment compatible with the setting of our simulation is shown in Fig. 2, where the data of \$1 correspond to offers from 0 token to 150 tokens, the data of \$2 correspond to offers from 155 tokens to 250 tokens, and so forth, because the minimum offer is set to \$1 in our setting.

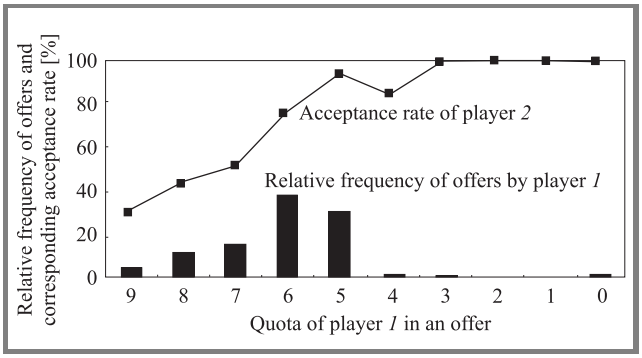

Fig. 2. Summary of the result of the experiment with human subjects.

As can be seen in Fig. 2, only about 4% of all the offers correspond to the subgame perfect equilibrium and the rate of acceptance for the corresponding offers is 31%. This fact is not consistent with the subgame perfect equilibrium prediction. The offers of \$4 or \$5 account for 68% of all the offers, and therefore player *1* seems to be making relatively fair offers. The rate of acceptance by player *2* for offers larger than or equal to \$4 is over 75%.

Although any offers by player *1* a quota of player *2* of which is smaller than or equal to \$1 brings a positive payoff to player *2*, player *2* rejects it at the rate of 70%. This behavior can be interpreted as punishment for unfair proposals by player *1*. By using utility functions defined by not only the payoff of self but also the payoff of the opponent, explanations of such behavior have been attempted [2, 3, 5, 7, 18].

3. Agent-based simulation model

In this paper, because it is supposed that human behavior is adaptive, we employ a simulation model which is a natural framework to implement the adaptive behavior of individuals. In our simulation model, each agent has a decision making mechanism built by a neural network (e.g., [12]) and a learning mechanism based on a genetic algorithm (e.g., [10]).

3.1. Decision making by a neural network

An agent corresponds to a neural network which is characterized by synaptic weights between two nodes in the neural network and thresholds which are parameters for the output function of nodes. Because a structure of neural networks is determined by the number of layers and the number of nodes in each layer, an agent is prescribed by the fixed number of parameters if these numbers are fixed. Forming a string consisting of these parameters which is identified

with an artificial agent, we think of the string as a chromosome of the agent in an artificial genetic system of our simulation model. In our simulation model for analyzing behavior of players in the ultimatum games, two types of agents are required. The first one which is called agent *1* corresponds to player *1* who makes an offer to player *2*; the second one which is called agent *2* corresponds to player *2* who accepts or rejects the offer by player *1*.

3.1.1. Decision making of agent *1*

The structure of a neural network of agent *1* is depicted in the diagram of Fig. 3a. Agent *1* makes an offer corresponding to the largest output among all the ten outputs of the neural network, where the outputs out_s, $s = 1, \ldots, 10$ correspond to from the offer $(9,1)$ to the offer $(0,10)$; the offer $(10-s^*, s^*)$ with the largest output out_{s^*} is chosen as the next offer of agent *1*.
Inputs of the neural network for agent *1* is summarized as follows.

[Input 1] an offer by agent *1* in the last game: $x_1 \in \{9,8,\ldots,0\}$[1] .

[Input 2] a payoff obtained by agent *1* in the last game: $\pi_1 \in \{9,8,\ldots,0\}$.

[Input 3] agent *2*'s choice between acceptance and rejection in the last game: $y_2 \in \{0,1\}$; 0 means rejection, and 1 means acceptance.

[Input 4] a payoff obtained by agent *2* in the last game: $\pi_2 \in \{1,2,\ldots,10\}$.

[Input 5] the average payoff obtained by agent *1* in the past all games: $\bar{\pi}_1 \in [0,9]$.

[Input 6] the average payoff obtained by agent *2* in the past all games: $\bar{\pi}_2 \in [0,10]$.

[Input 7] the average offer of agent *1* in the past all games: $\bar{x}_1 \in [0,9]$.

[Input 8] the average rate of acceptance by agent *2* for the offers in the past all games: $\bar{y}_2 \in [0,1]$.

It should be noted that the average payoff $\bar{\pi}_1$ and the average offer $\bar{x}_1$ are memorized and updated by agent *1*, and similarly the average payoff $\bar{\pi}_2$ and the average rate of acceptance $\bar{y}_2$ are memorized and updated by agent *2*.

3.1.2. Decision making of agent *2*

Agent *2* also makes a decision in a way similar to agent *1*; 8 inputs of all the 9 inputs of the neural network for agent *2* are the same as those of agent *1*, and the other one is an offer by agent *1* in the current game. The output layer of the neural network of agent *2* consists of two nodes which correspond to the choices of acceptance and rejection for the offer. The structure of the neural network of agent *2* is depicted in the diagram of Fig. 3b. Inputs of the neural network for agent *2* are summarized as follows.

[Inputs 1–8] the same as the inputs of agent *1*.

[Input 9] an offer by agent *1* in the current game: $\hat{x}_1 \in \{9,8,\ldots,0\}$.

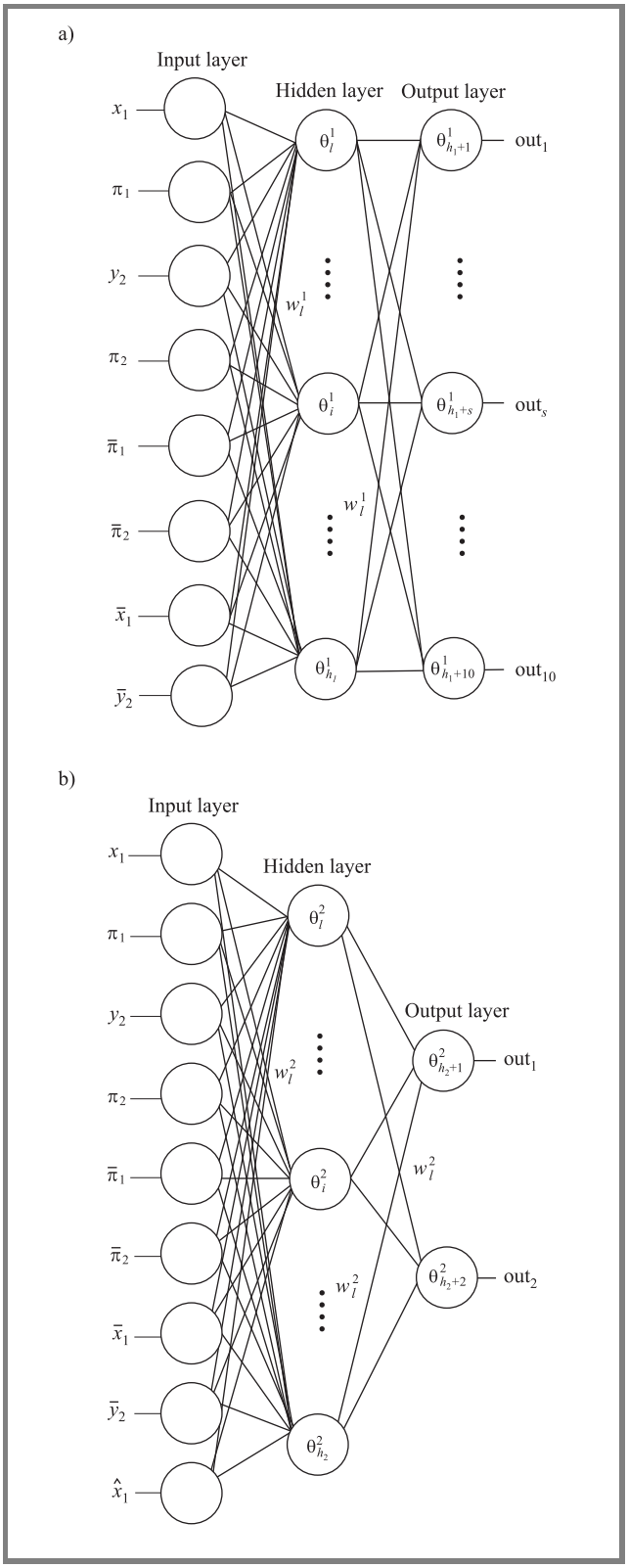

Fig. 3. Neural networks for (a) agent *1* and (b) agent *2*.

[1]Although an offer is represented by a pair (x_1, x_2) in the previous section, the offer (x_1, x_2) is identified only with x_1 because $x_2 = 1 - x_1$.

3.2. Utility function incorporating fairness

For modeling the behavior of players in the ultimatum game, we consider that it is appropriate to incorporate both learning and fairness in the artificial adaptive agent model simultaneously. To implement the concept of fairness, we use utility function as a fitness function in the genetic algorithm which is the basis of the learning mechanism of our agent-based simulation system. As a utility function appropriate for this purpose, we employ the utility function proposed by Fehr and Schmidt [7]; the parameters of the function seems to be easy to interpret because the function is linear, and the excess of the payoff of the opponent over that of self and the reciprocal excess are separated.

When players i and j obtain payoffs π_i and π_j, respectively, the utility u_i of player i is represented as

$$u_i(\pi_i,\pi_j) = \pi_i - \alpha_i \max\{\pi_j-\pi_i,0\} - \beta_i \max\{\pi_i-\pi_j,0\}, \quad i,j=1,2,\ i\neq j, \tag{1}$$

where α_i and β_i are coefficients; the utility $u_i(\pi_i,\pi_j)$ of player i consists of the payoff of self, the penalty for the excess of the payoff of the opponent over that of self, and the penalty for the reciprocal excess. When the payoff of self exceeds that of the opponent, i.e., $\pi_i > \pi_j$, $u_i(\pi_i,\pi_j) = \pi_i - \beta_i(\pi_i-\pi_j)$; when the payoff of the opponent exceeds that of self, i.e., $\pi_j > \pi_i$, $u_i(\pi_i,\pi_j) = \pi_i - \alpha_i(\pi_j-\pi_i)$.

3.3. Evolutionary learning through the genetic algorithm

An agent is prescribed by the fixed number of parameters in our agent-based simulation system. Forming a string consisting of these parameters, we use the string as a chromosome in an artificial genetic system. As we mentioned above, for agent *1*, there are the 8 units in the input layer and the 10 units in the output layer. Let h_1 be the number of units in the hidden layer. Then because the number of links between nodes is $18h_1$ and the number of units in the hidden and the output layers is h_1+10, the neural network corresponding to an agent can be governed by the synaptic weights w_l^1, $l=1,\ldots,18h_1$ and the thresholds θ_l^1, $l=1,\ldots,h_1+10$. Similarly, for agent *2*, the neural network is also governed by the synaptic weights w_l^2, $l=1,\ldots,11h_2$ and the thresholds θ_l^2, $l=1,\ldots,h_2+2$, where h_1 and h_2 are the numbers of nodes in the hidden layers. These parameters and the input values determine an action of the agent, and the synaptic weights and the thresholds are adjusted through the genetic algorithm so that the initial population evolves into the population of agents obtaining larger payoffs.

We separately arrange two subpopulations of agents *1* and *2*; there are N agents in each subpopulation. One agent is selected from each subpopulation, and two agents make a pair for playing the game. Agents repeatedly paly the ultimatum game, and accumulate the payoffs obtained in each stage game. Because the value of the utility Eq. (1) is directly used as a fitness in the artificial genetic system, agents obtaining larger utilities are likely to survive.

We start by describing how the parameters prescribing an agent are initialized. In the experiment, because experimenters explain a procedure of the ultimatum game, subjects should understand the payoff structure of the game. Thus, it is not appropriate that artificial agents start to play the game without any prior knowledge of the game; we give the artificial agents some knowledge of the game before playing it. We implement this by adjusting the parameters of the neural network which are the synaptic weights and the thresholds through the error back propagation algorithm (e.g., [12]) with the teacher signals.

A chromosome of agent *1* consists of the synaptic weights w_l^1, $l=1,\ldots,18h_1$ and the thresholds θ_l^1, $l=1,\ldots,h_1+10$, and that of agent *2* consists of the synaptic weights w_l^2, $l=1,\ldots,11h_2$ and the thresholds θ_l^2, $l=1,\ldots,h_2+2$. Initial values of the parameters w_l^i and θ_l^i are set to random values in $[-1,1]$ before the adjustment by the error back propagation algorithm.

We give teacher signals to the neural network for agent *1* so as to make offers yielding larger payoffs of self. Because the outputs $\text{out}_1^1,\text{out}_2^1,\ldots,\text{out}_{10}^1$ of the neural network for agent *1* correspond to the offers $(9,1),(8,2),\ldots,(0,10)$, the teacher signals of $1,8/9,\ldots,0$ are given to the outputs $\text{out}_1^1,\text{out}_2^1,\ldots,\text{out}_{10}^1$ for any set of the inputs given at random.

For agent *2*, based on the experimental results, the parameters of the neural network is adjusted by using the error back propagation algorithm such that the possibility of ac-

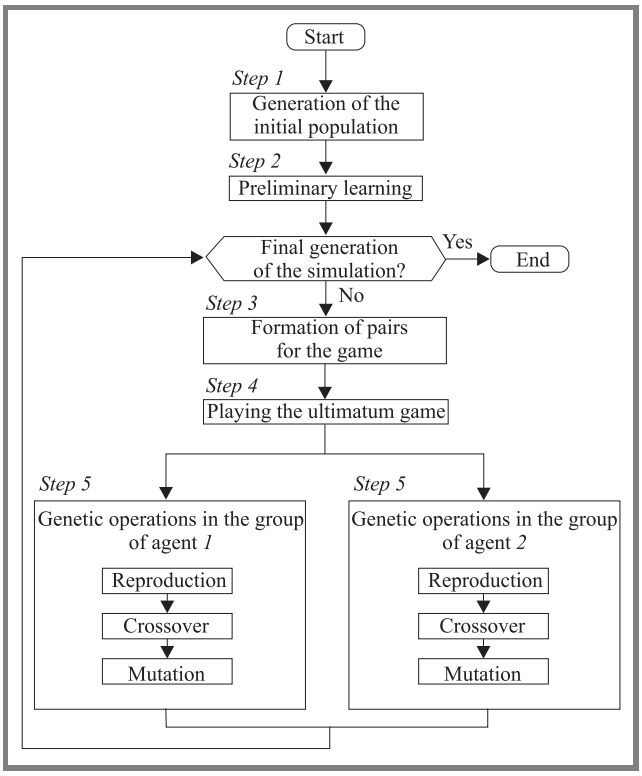

Fig. 4. Flowchart of the agent-based simulation model.

ceptance is equal to that of rejection for the most unfair offer $(10,0)$, the possibility of acceptance increases as the payoff of agent *2* in an offer becomes larger, and agent *2* perfectly accepts the profitable offers with agent *2*'s quotas larger than 6. To be more precise, when input 9 corresponding to agent *1*'s quota in an offer is $\hat{x}_1$ and inputs 1 to 8 are randomly given, the teacher signal, $\frac{1}{12}(10-\hat{x}_1)+0.5$, is given to the output out_1^2 corresponding to acceptance of an offer, and the teacher signal to the output out_2^2 is a complement of $\frac{1}{12}(10-\hat{x}_1)+0.5$ on 1.

We arrange 30 sets of the teacher signals for each of agents *1* and *2*, and the parameters of the neural networks are adjusted by the error back propagation algorithm. In our agent-based simulation system, there are two subpopulations of N agents for agents *1* and *2*, and one agent from the subpopulation of agent *1* and one from the subpopulation of agent *2* are randomly chosen, and then one pair for playing the game is formed. The game is played by N pairs of agents *1* and *2* according to the above mentioned decision making mechanism. The utilities of agents *1* and *2* are determined by Eq. (1) depending on the outcome of the game; these utilities are directly used as the fitness in the genetic algorithm. Because it is known that the algorithm works effectively by enlargement and reduction of the values of the fitness [10], in our system the fitness is linearly scaled. A procedure of the simulation model is summarized in the following and is diagrammatically shown in Fig. 4.

Step 1: **Generation of the initial population**. For each of agents *1* and *2*, N individuals are generated.

Step 2: **Preliminary learning**. By using the error back propagation algorithm with given teacher signals, the parameters of the neural network for each individual are adjusted.

Step 3: **Formation of pairs for the game**. A pair for playing the game is formed by selecting one agent from each of the subpopulations of agents *1* and *2*; by repeating this operation, N pairs are formed.

Step 4: **Playing the ultimatum game**. In each of the N pairs, the ultimatum game is played; the decision of each agent is determined by the outputs of the neural network; and artificial agents obtain their utilities depending on an outcome (π_1,π_2) of the game.

Step 5: **Genetic operation**. The two subpopulations for agents *1* and *2* are formed again by gathering the same type of artificial agents from the N pairs for playing the game; the genetic operations are executed to each subpopulation consisting of N individuals. The utility Eq. (1) of agent *1* or *2* is directly used as the fitness of an artificial agent in the genetic algorithm, and the fitness is linearly scaled.
If the number of periods reaches a given final generation of the simulation, the procedure stops.

Step 5-1: **Reproduction**. As a reproduction operator, the roulette wheel selection is adopted. By a roulette wheel with slots sized by the probability

$$p_{ij}^s = \frac{f_{ij}}{\sum_{j=1}^N f_{ij}}, i = 1,2, \tag{2}$$

each chromosome is selected into the next generation, where f_{ij} is the fitness of the jth individual of agent i.

Step 5-2: **Crossover**. A single-point crossover operator is applied to any pair of chromosomes with the probability of crossover p^c. Namely, a point of crossover on the chromosomes is randomly selected and then two new chromosomes are created by swapping subchromosomes which are the right side parts of the selected point of crossover on the original chromosomes.
For offsprings of agent *1*, the average payoff and the average offer are given by averaging those of the parents with the probabilities corresponding to the sizes of the swapped subchromosomes; similarly, for agent *2*, the average payoff and the average rate of acceptance are calculated.

Step 5-3: **Mutation**. With a given small probability of mutation p^m, each gene which represents a synaptic weight or a threshold in a chromosome is randomly changed. The selected gene is replaced by a random number in $[-1,1]$.

4. Results of the simulations

We develop the artificial agents in this agent-based simulation system so as to imitate the behavior of human subjects in a laboratory experiment by Roth *et al*. [20], and examine the result of the experimental research through the simulation analysis. First, we identify the standard set of the four parameters α_1, β_1, α_2, β_2 in the utility function (1) by minimizing the error of mean square between the result of the simulation and that of the experiment. After identified the the standard set of the parameters, we examine effect of the parameters characterizing the behavior of the human subjects.
Artificial adaptive agents have mechanisms of decision making and learning based on a neural network and a genetic algorithm, and the parameters of the neural network and the genetic algorithm are set to the following values:

- the number of nodes in the neural network for agent *1*:
  8 in the input layer, 10 in the hidden layer, 10 in the output layer;
- the number of nodes in the neural network for agent *2*:
  9 in the input layer, 11 in the hidden layer, 2 in the output layer;

– the size of subpopulations for agents *1* and *2*: $N = 100$;
– the maximal generation of the genetic algorithms: $MaxGen = 3000$;
– the parameters of genetic operations: crossover $p^c = 0.5$, mutation $p^m = 0.001$, generation gap $g = 0.8$.

In this paper, the simulation system is executed 100 runs for each setting of the parameters. Because all preparatory runs converge at certain level until 2500 periods, we set the maximal generation of the simulation to 3000 periods. Numerical data of the simulation are given by averaging each observed value in the last 150 generations of the 100 runs.

4.1. Identification of the standard set of the parameters

By varying values of the parameters, we find the standard set of the parameters approximating the behavior of human subjects. There are four parameters α_1, β_1, α_2 and β_2 in the utility function, and especially, the parameter β_2 is the penalty coefficient for the excess of the payoff of player *2*'s self over the payoff of the opponent in the utility function of player *2*. When player *1* makes an offer such that the payoff of player *2* is larger than the payoff of player *1*'s self, i.e., (x_1, x_2), $x_1 < x_2$, this penalty is valid. Although it is true that such an offer is unfair, it is not natural that player *2* is penalized for accepting the offer. From this reason, fixing the value of β_2 at $\beta_2 = 0$, the values of α_1 and β_1 are varied from 0 to 1 at intervals of 0.1, and the value of α_2 is varied from 0 to 2.
In order to find the standard set of the parameters imitating the behavior of human subjects and successfully approximating the result of the experiment, we use the error of mean square which is represented by

$$E(\alpha_1,\beta_1,\alpha_2,\beta_2) = \sum_{x_1=9}^{0} (p_{x_1}^{\text{sim}} - p_{x_1}^{\text{sub}})^2 + \sum_{x_1=9}^{0} (q_{x_1}^{\text{sim}} - q_{x_1}^{\text{sub}})^2, \tag{3}$$

where $p_{x_1}^{\text{sub}}$ and $p_{x_1}^{\text{sim}}$ are the fraction of the human subjects and the artificial agents making an offer $x_1 \in \{9,8,\ldots,0\}$ in the experiment and in the simulation, respectively; $q_{x_1}^{\text{sub}}$ and $q_{x_1}^{\text{sim}}$ are the fraction of the human subjects and the artificial agents accepting the offer x_1 in the experiment and in the simulation, respectively.
By executing 100 runs for all the 2541 cases of parameter variations, it is found that the standard set of the parameters is $(\alpha_1,\beta_1,\alpha_2,\beta_2) = (0.4,0,1.1,0)$ minimizing the error of mean square Eq. (3) and the minimum is $E(\alpha_1,\beta_1,\alpha_2,\beta_2) = 0.1263$; at the standard set of the parameters $(\alpha_1,\beta_1,\alpha_2,\beta_2) = (0.4,0,1.1,0)$, the distribution of offers by agent *1* and the rate of acceptance for any offer are given in Fig. 5 with the behavior of human subjects in the experiment. The values of the parameters in the utility function of agent *1* are $\alpha_1 = 0.4$ and $\beta_1 = 0$, and the penalty is not larger than 40% of the excess of the payoff of an agent over that of the other. In contrast, the value of the coefficient $\beta_2 = 1.1$ in the utility function of agent *2* are considerably large, and therefore it appears that agent *2* strongly ask the opponent for a fair offer compared with agent *1*.

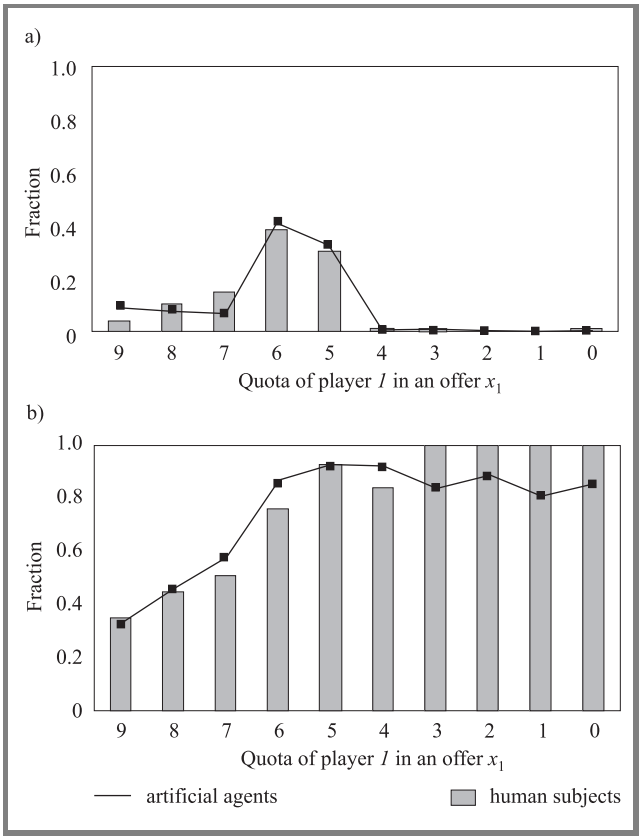

Fig. 5. Behavior of artificial agents and human subjects at the standard set of the parameters: (a) distribution of offers; (b) rate of acceptance.

The behavior of agents *1* and *2* can be characterized by the distribution of offers and the rate of acceptance, respectively. As can be seen in Fig. 5, all in all, the behavior of artificial agents in the simulation successfully approximates that of human subjects in the experiment. We will begin by examining the offers by agent *1*. The frequencies of the offers in which the quota of agent *1* is larger than 4, $x_1 > 4$, by the artificial agents in the simulation are similar to those by the human subjects in the experiments. For the offers such that the quota of agent *1* is smaller than or equal to 4, $x_1 \leq 4$, the behavior of the artificial agents in the simulation is almost the same as that of the human subjects in the experiment. Next, we look into the rate of acceptance. For the offers in which the quota of agent *1* is larger than or equal to 4, $x_1 \geq 4$, both of the rates of the simulation and the experiment denote a similar tendency; for the other offers, $x_1 \leq 3$, however, the rate of the simulation is slightly smaller than that of the experiment. This is attributed to the fact that as seen in the graph of Fig. 5a, the offers in which the quota of agent *1* is smaller than or equal to 4 are hardly proposed in the simulation and therefore the ar-

tificial agents cannot sufficiently learn how they respond such offers.

In Fig. 6, we show transitions of the average offer by agent *1* and the average rate of acceptance by agent *2* in the early

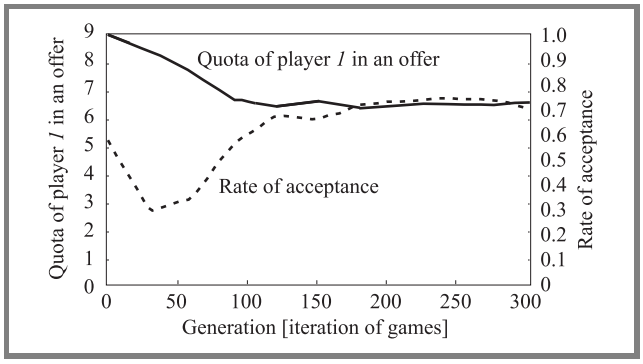

Fig. 6. Transitions of the average offer and acceptance rate.

generations of the simulation. As seen in the figure, at the beginning of the simulation, agent *1* makes the offer $(9,1)$ and agent *2* accepts it with the probability of about 0.55; it is conceivable that the couple of these actions is due to the preliminary learning of the neural network. Just after the start of the learning by the genetic algorithm, agent *2* begins to reject extremely unfair offers such as the offer $(9,1)$. However, as a quota x_1 of agent *1* in an offer (x_1, x_2) decreases by a high incidence of rejection of unfair offers by agent *2*, the rate of acceptance of the offer increases; after 150 generations, the average offer by agent *1* converges to an appreciably fair offer $(6.15, 3.85)$ and the average rate of acceptance by agent *2* also converges to about 0.68.

Table 1
Utilities of agents *1* and *2* at the standard set of the parameters

x_1	9	8	7	6	5	4	3	2	1	0
u_1	9	8	7	6	5	3.2	1.4	−0.4	−2.2	−4.0
u_2	−7.8	−4.6	−1.4	1.8	5	6	7	8	9	10

In Table 1, the utilities of agents *1* and *2* are shown at the standard set of the parameters $(\alpha_1, \beta_1, \alpha_2, \beta_2) = (0.4, 0, 1.1, 0)$. As seen in the table, the utility of agent *1* is an increasing function with the quota x_1 of agent *1*; the utility of agent *2* is a decreasing function with x_1. Especially, because the value of α_2, which is the penalty coefficient for the excess of the payoff of agent *1* over the payoff of agent *2*'s self in the utility of agent *2*, is relatively large, the utilities of agent *2* become negative when the quota x_1 of agent *1* is larger than or equal to 7, $x_1 \geq 7$. From the fact that the utility of agent *2* is zero when agent *2* rejects an offer, it is preferable for agent *2* to reject such offers. Such behavior of agent *2* can be interpreted as the punishment for unfair proposals by agent *1*. As can be seen in Fig. 6, through the repeated rejections by agent *2*, agent *1* gradually lowers a quota of agent *1*'s self in offers. This process can be explained by the learning of agent *1*. For the offer $(6,4)$, conversely it is advantageous for agent *2* to accept it. It seems to be for this reason that the frequency of the offer $(6,4)$ is the largest.

From the result of the simulation, it is conceivable that the developed agent-based simulation system successfully approximates the behavior of human subjects in the experiment by incorporating the fairness in the learning mechanism of the artificial agents. Moreover, while Abbink *et al.* [1] conclude that a fairness motive is a better explanation for why player *2* rejects unfair offers compared with learning, our result is consistent with their argument.

While we have found the standard set of the parameters imitating the behavior of human subjects by varying values of the parameters, we should examine effects of individual parameters on the behavior of the artificial agents. To verify that the behavior of agent *1* is mainly revised through the learning, by varying values of the parameters α_1 and β_1 in the utility function of agent *1*, we examine change of the behavior of the artificial agents. Moreover, while we suppose that fairness and the corresponding punishment largely explain the behavior of agent *2*, to confirm this argument, we also investigate change of the behavior of the artificial agents by varying value of the parameter α_2 in the utility function of agent *2*.

4.2. Effect of learning on the behavior of agent 1

Fixing the values of α_1, α_2 and β_2 at the standard setting $\alpha_1 = 0.4$, $\alpha_2 = 1.1$ and $\beta_2 = 0$, we vary the value of β_1 from 0 to 0.5 at intervals of 0.1. The result of this treatment is given in Fig. 7 showing the average offer and the average rate of acceptance.

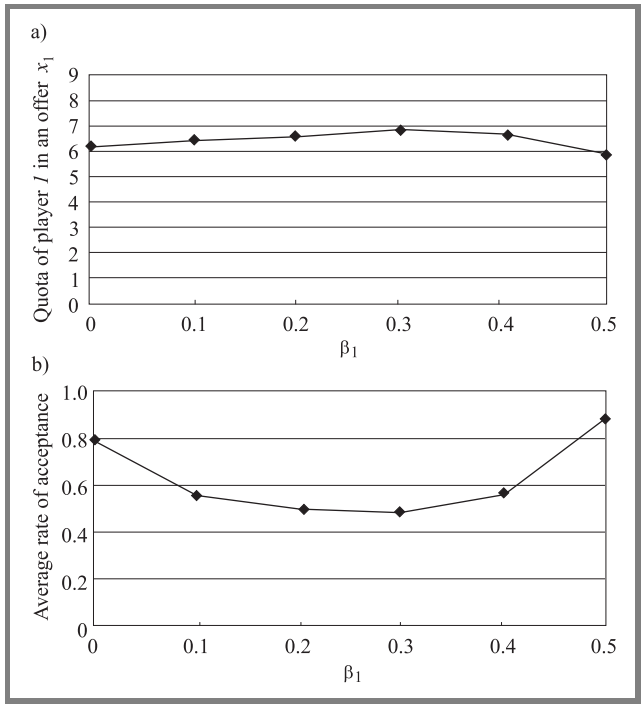

Fig. 7. Change of the behavior with respect to the parameter β_1: (a) average offer; (b) rate of acceptance.

As can be seen in Fig. 7, the average quota x_1 of agent *1* in offers remains almost the same in the range $0.0 \leq \beta_1 \leq 0.4$; when $\beta_1 = 0.5$, because the number of agent *1* making fairer offers increases, the average quota x_1 decreases below 6. Although the average rate of acceptance is relatively high when $\beta_1 = 0.0$ compared with the cases of $\beta_1 = 0.1, 0.2, 0.3, 0.4$, the average rates of acceptance are almost the same when $\beta_1 = 0.1, 0.2, 0.3, 0.4$. On the other hand, when $\beta_1 = 0.5$, because the average quota x_1 decreases and offers become fair, the average rate of acceptance obviously rises.

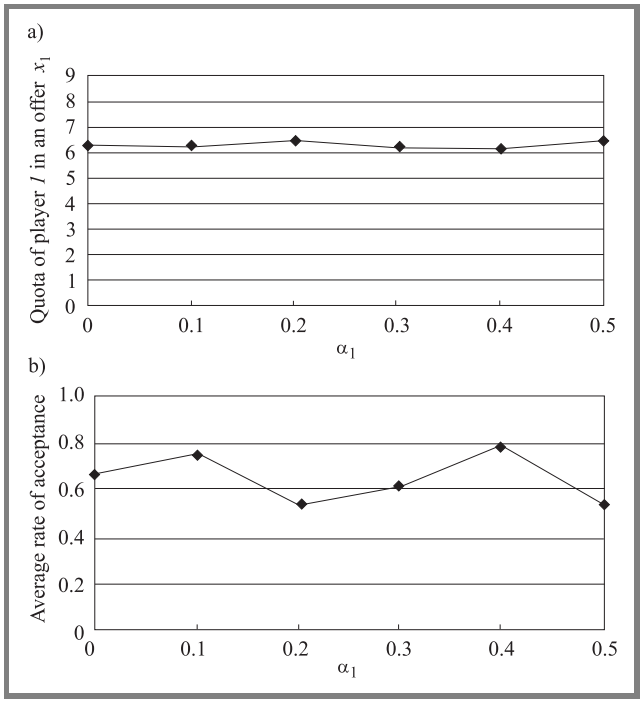

Fig. 8. Change of the behavior with respect to the parameter α_1: (a) average offer; (b) rate of acceptance.

For sensitivity with respect to the parameter α_1, the average offer and the average rate of acceptance are similarly given in Fig. 8. As can be seen in Fig. 8, the average quota x_1 of agent *1* in offers remains almost same in the range $0.0 \leq \alpha_1 \leq 0.5$. Moreover, from the graph of Fig. 8a, it is found that there is little linkage between the average rate of acceptance of agent *2* and the change of the value of α_1.

From the above observation, the sensitivity of the behavior of the artificial agents to the change of parameter β_1 or α_1 from zero is not so high, and it would be said that introduction of the parameter β_1 or α_1 does not have a major function in explanation of the behavior of the artificial agents. Thus, the effect of the parameter of fairness is relatively small, and it appears that the behavior of agent *1* is mainly revised through the learning.

When $\pi_1 > \pi_2$, the utility function of agent *1* is represented as $u_1(\pi_1, \pi_2) = (1 - 2\beta_1)\pi_1 + 10\beta_1$. If $\beta_1 < 0.5$, because the coefficient of π_1 is smaller than one, the influence of agent *2*'s decision of acceptance or rejection on the utility of agent *1* is evidently larger than that of the offer by agent *1*'s self. For the parameter α_1, because agent *1* rarely makes offers such that the quota of agent *1* is smaller than or equal to 4, $x_1 \leq 4$, and α_1 is valid when $\pi_1 < \pi_2$, the parameter α_1 has little influence on the behavior of agent *1*. From this viewpoint, it is also found that the behavior of agent *1* be strongly affected by learning through a series of actions of agent *2*.

4.3. Effect of punishment on the behavior of agent 2

To observe effect of the punishment on the behavior of agent *2*, we conduct an additional treatment by varying the value of α_2 from 0 to 2 at intervals of 0.1, fixing the values of α_1, β_1 and β_2 at $\alpha_1 = 0$, $\beta_1 = 0$ and $\beta_2 = 0$. The result of this treatment is given in Fig. 9.

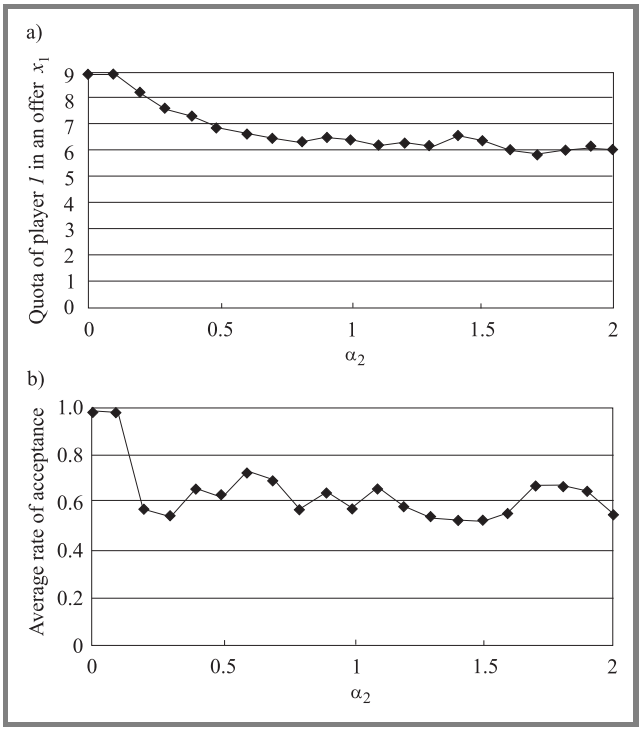

Fig. 9. Change of the behavior with respect to the parameter α_2: (a) average offer; (b) rate of acceptance.

As can be seen in Fig. 9, the average quota x_1 of agent *1* in offers specifically decreases in the range $0.1 \leq \alpha_2 \leq 0.8$, and the average rate of acceptance steeply drops from $\alpha_2 = 0.1$ to 0.2. It is just conceivable that the behavior of the artificial agents is very sensitive to the change of parameter α_2 from zero, and the behavior of agent *1* is mainly explained by introduction of the parameter α_2 of the fairness and punishment.

5. Conclusions

We have developed agent-based simulation system for analyzing the behavior of human subjects in the experiment. The learning mechanism incorporating the concept

of fairness in the system efficiently works, and it is shown that our artificial adaptive agents successfully approximates the behavior of human subjects in the laboratory experiment by Roth *et al*. [20]. Through the simulation analysis, we have verified that the behavior of agent *1* is mainly revised through the learning, and fairness and corresponding punishment largely explain the behavior of agent *2*.

References

[1] K. Abbink, G. E. Bolton, A. Sadrieh, and F.-F. Tang, "Adaptive learning versus punishment in ultimatum bargaining", *Games Econom. Behav.*, vol. 37, pp. 1–25, 2001.

[2] G. E. Bolton, "A comparative model of bargaining: theory and evidence", *Amer. Econom. Rev.*, vol. 81, pp. 1096–1136, 1991.

[3] G. E. Bolton and A. Ockenfels, "ERC: a theory of equity, reciprocity, and competition", *Amer. Econom. Rev.*, vol. 90, pp. 166–193, 2000.

[4] G. E. Bolton and R. Zwick, "Anonymity versus punishment in ultimatum bargaining", *Game Econom. Behav.*, vol. 10, pp. 95–121, 1995.

[5] M. Costa-Gomes and K. G. Zauner, "Ultimatum bargaining behavior in Israel, Japan, Slovenia, and the United States: a social utility analysis", *Game Econom. Behav.*, vol. 34, pp. 238–269, 2001.

[6] J. Duffy and N. Feltovich, "Does observation of others affect learning in strategic envirnments? An experimental study", *Int. J. Game Theory*, vol. 28, pp. 131–140, 1999.

[7] E. Fehr and K. M. Schmidt, "A theory of fairness, competition and cooperation", *Q. J. Econom.*, vol. 114, pp. 817–868, 1999.

[8] R. Forsythe, J. L. Horowitz, N. E. Savin, and M. Sefton, "Fairness in simple bargaining experiments", *Games Econom. Behav.*, vol. 6, pp. 347–369, 1994.

[9] J. Gale, K. G. Binmore, and L. Samuelson, "Learning to be imperfect: the ultimatum game", *Games Econom. Behav.*, vol. 8, pp. 56–90, 1995.

[10] D. E. Goldberg, *Genetic Algorithms in Search, Optimization, and Machine Learning.* Reading: Addison Wesley, 1989.

[11] W. Güth, R. Schmittberger, and B. Schwarze, "An experimental analysis of ultimatum bargaining", *J. Econom. Behav. Organ.*, vol. 3, pp. 367–388, 1982.

[12] M. H. Hassoun, *Fundamentals of Artificial Neural Networks*. Cambridge: The MIT Press, 1995.

[13] E. Hoffman, K. A. McCabe, K. Shachat, and V. L. Smith, "Preferences, property rights, and anonymity in bargaining games", *Games Econom. Behav.*, vol. 7, pp. 346–380, 1994.

[14] E. Hoffman, K. A. McCabe, and V. L. Smith, "On expectations and the monetary stakes in ultimatum games", *Int. J. Game Theory*, vol. 25, pp. 289–301, 1996.

[15] D. Kahneman, J. L. Knetsch, and R. H. Thaler, "Fairness and the assumptions of economics", *J. Bus.*, vol. 59, pp. S285–S300, 1986.

[16] R. D. McKelvey and T. R. Palfrey, "Quantal response equilibria for normal form games", *Games Econom. Behav.*, vol. 10, pp. 6–38, 1995.

[17] J. Neelin, H. Sonnenschein, and M. Spiegel, "A further test of noncooperative bargaining theory: comment", *Amer. Econom. Rev.*, vol. 78, pp. 824–836, 1988.

[18] M. Rabin, "Incorporating fairness into game theory and economics", *Amer. Econom. Rev.*, vol. 83, pp. 1281–1302, 1993.

[19] A. E. Roth and I. Erev, "Learning in extensive form games: experimental data and simple dynamic models in the intermediate term", *Games Econom. Behav.*, vol. 8, pp. 163–212, 1995.

[20] A. Roth, V. Prasnikar, M. Okuno-Fujiwara, and S. Zamir, "Bargaining and market behavior in Jerusalem, Ljubljana, Pittsburgh, and Tokyo: an experimental study", *Amer. Econom. Rev.*, vol. 81, pp. 1068–1095, 1991.

[21] E. Weg and V. Smith, "On the failure to induce meager offers in ultimatum game", *J. Econom. Psychol.*, vol. 14, pp. 17–32, 1993.

[22] K.-O. Yi, "Quantal-response equilibrium models of the ultimatum bargaining game", *Games Econom. Behav.*, vol. 51, pp. 324–348, 2005.

Tomohiro Hayashida is currently Assistant Professor at Department of Artificial Complex Systems Engineering, Graduate School of Engineering of the Hiroshima University, Japan. His current research interests are agent-based simulation analysis, game theory, and decision making theory.

e-mail: hayashida@hiroshima-u.ac.jp
Department of Artificial Complex Systems Engineering
Graduate School of Engineering, Hiroshima University
1-4-1 Kagamayama, Higashi-Hiroshima, 739-8527, Japan

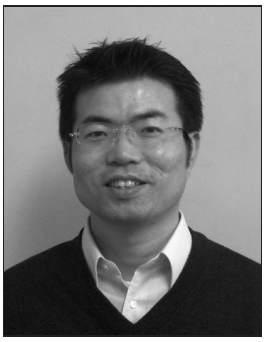

Hideki Katagiri is currently Associate Professor at Department of Artificial Complex Systems Engineering, Graduate School of Engineering of the Hiroshima University, Japan. His current research interests are fuzzy stochastic programming, soft computing and marketing science.

e-mail: katagiri-h@hiroshima-u.ac.jp
Department of Artificial Complex Systems Engineering
Graduate School of Engineering, Hiroshima University
1-4-1 Kagamayama, Higashi-Hiroshima, 739-8527, Japan

Ichiro Nishizaki – for biography, see this issue, p. 35.

Paper

Application of open multi-commodity market data model on the communication bandwidth market

Przemysław Kacprzak, Mariusz Kaleta, Piotr Pałka, Kamil Smolira, Eugeniusz Toczyłowski, and Tomasz Traczyk

Abstract— In the paper the market model for balancing communication bandwidth trade (BCBT) is analyzed in the form of multi-commodity market data model (M^3). The distinguishing feature of BCBT model is that it assumes that market players can place buy offers not only for isolated network resources – inter-node links, but also for end-to-end network paths of predefined capacity, that is, every offer concerns a point-to-point bandwidth connection between a pair of specified locations in a communication network. The model enables effective balancing of sell and buy offers for network resources in a way which maximizes global economic welfare. The open multi-commodity market data model provides efficient and clear mechanisms, which support the environment of auctions and multi-commodity exchanges, especially when the trade is constrained by the infrastructure resources. Thus the model may be used in designing open information systems for market balancing and clearing in the context of multi-commodity trade in various network infrastructure sectors.

Keywords— communication bandwidth trade, market clearing, multi-commodity trade.

1. Introduction

Communication bandwidth trading is typically accomplished by bilateral agreements between telecom companies. The agreements are usually settled using complex and nontransparent negotiations, which cause the whole process difficult to automate. Still increasing number of traders and complexity of network resources and services also have big impact on difficulties in elaborating complex information system serving exchange processes. Thus, the need for fair, efficient and clear market rules, in the form of, e.g., auctions, markets or exchange, becomes quite evident.

The primary requirement of the multi-commodity market data model (M^3) is an easy exchange of all data between various market entities and market balancing processes. The M^3 model consists of several layers, which are the formal mathematical model (see [7]), conceptual data model, expressed in form of UML class diagrams (see [6, 7, 11]), exemplary relational database structure, XML schemas for static data (see [11]), communication models, XML schemas for messages, and Web services definitions.

Main purpose of the paper is to present the application of M^3 for the balancing communication bandwidth trade (BCBT) problem and to demonstrate that M^3 is a suitable tool for designing the communication bandwidth markets. We analyze the case study from [14]. In the example, data exchange process is presented, including offer submission, status of the auction broadcasting, resending statuses of particular offers, etc. The snippets of XML files, containing pieces of static data, are presented.

2. Data model standard for multi-commodity markets

At present, in many network industries, functionality and efficiency of the existing control and management designs are not completely satisfactory. The world-wide market liberalization and deregulation processes are being implemented in many network infrastructure sectors, including telecommunication, power systems, computer, rail and transport networks, water, urban systems and others.

Many researchers and professionals around the world participate in development, investigation and implementation of a variety of new ideas related to auction and market clearing systems under various market conditions. In the network systems, an efficient market balance may be obtained in a single balancing process by joint optimization of trade of many elementary commodities and services related to buy and sell offers of the network resources. For this purpose the multi-commodity exchanges can be used, in addition to single-commodity exchanges and bilateral trading. The basic multi-commodity market clearing models are in the LP or MILP forms (see [15]).

Apart from traditional auctions, long-term and medium-term single-commodity market segments, or day-ahead and intra-day-markets, there is a need for designing specific problem-oriented multi-commodity auctions and balancing market mechanisms, which must provide feasible execution of sales contracts and assure timely delivery of many goods and services.

In our previous research [11] we have initiated the design of the open multi-commodity market data model that may

be used in designing information systems for market balancing and clearing in the context of multi-commodity trade in various network infrastructure sectors. In this paper we address the generic telecommunication design issues of M^3. One purpose of the open M^3 model is that it creates a flexible framework for development of new market models and algorithms, benchmark data repository, and gives possibility for integration of software components which implement balancing mechanisms. Finally, it will help the community to determine the best industrial standards of data interchange and enable for an easy public access and exchange of various market data.

3. M^3 and the BCBT market

In Fig. 1, we can see four nodes (A, B, C and D), five inter node links (solid lines), which are simultaneously the sell offers and two buy offers, concerning end-to-end network paths (dashed lines). Sell offer notation: "x/y" means willingness to sell up to y units of bandwidth at price at least x. Buy offer notation: "$d : x/y$" means that buyer d has willingness to buy up to y units of bandwidth at price x or lower.

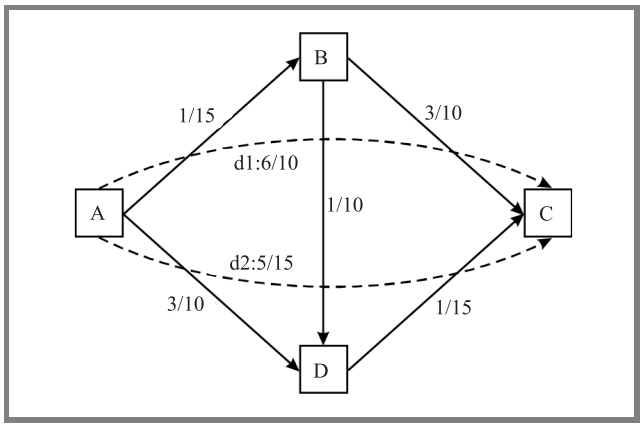

Fig. 1. Physical telecommunication network.

3.1. Infrastructure

To set a correct infrastructure model, we need to define physical network (Fig. 1). On the BCBT market commodities and offers are defined in context of network, so the description of network is in the core of M^3 data model. Network is modeled as acyclic graph, for the sake of generality let us assume N graphs, where nth graph is defined by $\langle V^n, E^n, P^{V^n}, P^{E^n} \rangle$, $n \in N$ is an index of network model, V^n is a set of nodes, E^n is a set of edges, P^{V^n} and P^{E^n} are parameters of vertices and arcs, respectively.
In M^3 model the commodities which are in our example, i.e., physical links and end-to-end network paths, have to be associated to one of network nodes, or edges. As the end-to-end network path should be associated to the network edge, but the edge could not exist (e.g., there is not edge for path A-C, see Fig. 1). The M^3 model allows for defining a virtual networks, which are an aggregation of a lower level network. Thus the need to define network with all connection between every pair of nodes, that is the complete network (Fig. 2), is obvious.

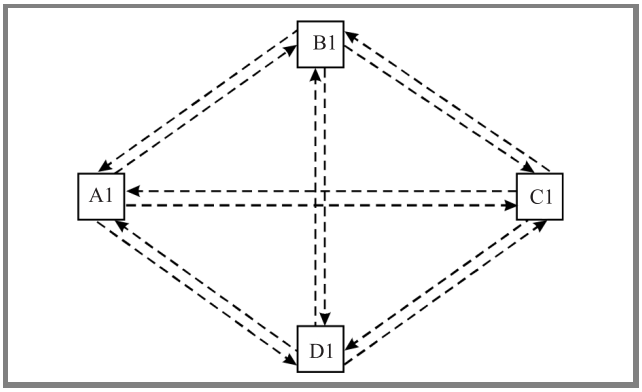

Fig. 2. Complete, virtual network.

Every graph consists of set of edges and nodes. Definition of a single node in one of the networks is the following (node A):

```
<m3:node id="ex:nodeA"
  dref="ex:CommunicationNode">
 <m3:name>Node A</m3:name>
</m3:node>
```

The `dref="ex:CommunicationNode"` attribute means that this node is an instance of a `CommunicationNode` which is a `NetworkNodeKind` and is defined as

```
<m3:NetworkNodeKind
   id="ex:CommunicationNode">
  <m3:name>Node</m3:name>
  <m3:description>
    Definition of node in communication
    network
  </m3:description>
</m3:NetworkNodeKind>
```

The `CommunicationNode` is a simple meta-class. It contains only required set of elements and attributes, like unique *identifier*, *name* of the class and the human readable *description* of the class.
Definition of a particular arc, for example arc A-B, is the following:

```
<m3:arc id="ex:arcA-B"
   dref="ex:BandwidthPath">
  <m3:parameter
    dref="ex:Capacity">15</m3:parameter>
  <m3:predecessor ref="ex:node1"/>
  <m3:successor ref="ex:node2"/>
</m3:arc>
```

The m3:predecessor element references to a predecessor of this arc, similarly the m3:successor element references to a successor of this arc. The dref="ex:BandwidthPath" attribute means that this arc is an instance of a BandwidthPath which is defined:

```
<m3:NetworkArcKind id="ex:BandwidthPath">
  <m3:name>Physical link</m3:name>
  <m3:description>
    Definition of link in
    a physical communication network
  </m3:description>
  <m3:ParameterDefinition id="ex:Capacity"
    dataType="xsd:double" required="true"
    unitOfMeasure="Tb/month">
    <m3:name>Capacity of the link</m3:name>
  </m3:ParameterDefinition>
</m3:NetworkArcKind>
```

In addition to required elements, this meta-class contains a parameter element m3:parameter. It references to parameter definition dref="ex:Capacity", which contains short *name* of the parameter, human-readable *description* of it, *data type*, attribute which defines if the generic parameter is *required* in all instances and the optional *unit of measure*. Thanks to parameter elements, we can model complex components like, e.g., network links, generating units, etc.

3.2. Time structure

Each balancing process is related to a time structure. Commodities are to be delivered in determined time slots. Thus the time horizon must be divided into time segments and every commodity is related to the specific time slot. The time structure is modeled as a directed acyclic graph $C = \langle V^C, E^C \rangle$, where vertices V^C define time slots, and edges describe aggregation between time slots. Time structure includes basic time slots, e.g., hours. By aggregations of time slots one may form more sophisticated slots, e.g., load peak hours or days of week.

The time structure for the BCBT is very simple – it contains time periods which are particular months:

```
<m3:calendar>
  <!-- ... -->
  <m3:CalendarPeriod id="ex:M0704"
    periodType="ex:one-month"
    startTime="2007-04-01T00:00:00"
    endTime="2007-05-01T00:00:00"/>
  <m3:CalendarPeriod id="ex:M0705"
    periodType="ex:one-month"
    startTime="2007-05-01T00:00:00"
    endTime="2007-06-01T00:00:00"/>
  <m3:CalendarPeriod id="ex:M0706"
    periodType="ex:one-month"
    startTime="2007-06-01T00:00:00"
    endTime="2007-07-01T00:00:00"/>
  <!-- ... -->
</m3:calendar>
```

Nevertheless the time structure could have more complex structure in case of commodities defined for different time slots simultaneously, e.g., days and months.

3.3. Market entities

Market entities structure describes market players and relations between them. Again, it is modeled as a directed acyclic graph. Market entities form a hierarchy, where a given market entity may be composed of some other market entities. Market entities are related to infrastructure vertices. This relation has different semantic, depending on relation type, e.g., is located, can deliver commodities, etc.:

```
<!-- buyer -->
<m3:MarketEntity id="ex:buyer-d1"
  dref="m3:bandwidth-buyer">
  <m3:name>buyer-d1</m3:name>
  <m3:uri>
    http://www.bandwidth.buyer.pl/d1
  </m3:uri>
</m3:MarketEntity>
<!-- remaining buyers ... -->
<!-- seller -->
<m3:MarketEntity id="ex:brokerA-B"
  dref="m3:link-broker">
  <m3:name>brokerA-B</m3:name>
  <m3:uri>
    http://www.link.broker.pl/A-B
  </m3:uri>
</m3:MarketEntity>
<!-- remaining sellers ... -->
```

3.4. Commodities

In M^3 the commodity have to be associated to some node or edge from infrastructure model. Such association can have different meanings, e.g., some commodity could be put on the market in particular network node. The commodity have to be also related to some time slot from time structure. Finally, the definition of commodity kind has to be included. In our example we have two kinds of commodities, i.e., physical links and end-to-end network paths. Because we have five edges in physical network, we could define up to five different commodities of kind physical link in single time slot (with assumption, that physical link commodity could be associated only to edge of base network). Similarly, as we have twelve different edges in the complete network, we can define up to twelve different commodities of kind network path in single time slot (with assumption,

that network paths commodity could be associated only to edge of complete, virtual network):

```
<!-- one of links -->
<m3:Commodity id="ex:btH0705-D-C"
  dref="ex:bandwidth-trade-link">
  <m3:description>
    Bandwidth trade link D-C on May 2007
  </m3:description>
  <m3:availableAt ref="ex:arcD-C"/>
  <m3:CalendarScheduledCommodity
    ref="ex:M0705"/>
</m3:Commodity>
<!-- path -->
<m3:Commodity id="ex:vpA1-C1M0705"
    dref="ex:bandwidth-trade-path">
  <m3:description>
    Bandwidth end-to-end network path
    A1-C1 on May 2007
  </m3:description>
  <m3:availableAt ref="ex:arcA1-C1"/>
  <m3:CalendarScheduledCommodity
    ref="ex:M0705"/>
</m3:Commodity>
```

3.5. Offers

Data model M^3 provides three types of offers: simple, integrated and grouping offers. Simple offer is described by admissible range of commodity volumes and a unit price. Integrated offer is a typical type of offer for multi-commodity turnover, where players trade with packages (or bundles) of commodities with fixed proportions of commodities in the offer. The most complex type of offers are grouping offers. Grouping offers aggregate a subset of other simple or integrated offers and describes relation between these offers. Grouping offers allow the market entities to define individual constraints.
The input offers are the elementary offers:

```
<!-- sell offer -->
<m3:Offer id="ex:o20421-89"
    offeredPrice="1.00">
  <m3:description>
    Bandwidth sell offer on the edge A-B
  </m3:description>
  <m3:offeredBy ref="ex:brokerA-B"/>
  <m3:offerStatus status="m3:offer-open">
    <m3:durationPeriod startTime="2007-05"
      endTime="2007-06"/>
  </m3:offerStatus>
  <m3:volumeRange minValue="0"
    maxValue="15"/>
  <m3:ElementaryOffer>
    <m3:offeredCommodity shareFactor="1"
      ref="ex:btH0705-A-B"/>
  </m3:ElementaryOffer>
</m3:Offer>
<!-- buy offer -->
<m3:Offer id="ex:o20421-94"
   offeredPrice="6.00">
  <m3:description>
    Point-to-point bandwidth buy offer,
    from point A to C
  </m3:description>
  <m3:offeredBy ref="ex:buyer-d1"/>
  <m3:volumeRange minValue="0"
    maxValue="10"/>
  <m3:ElementaryOffer>
    <m3:offeredCommodity shareFactor="-1"
      ref="ex:vpA1-C1M0705"/>
  </m3:ElementaryOffer>
</m3:Offer>
```

To provide properly defined output flows in the network, a detailed flow must be provided for each end-to-end buy offer, so the output offers are represented as the bundled offers, where each elementary offer represents flow on particular arc. Let us focus on the d1 buy offer, and assume

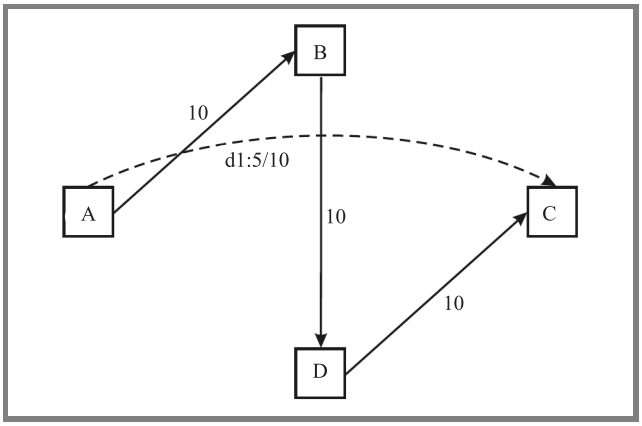

Fig. 3. Output offer for buyer d1.

that it is accepted with volume 10, on the path A-B-D-C (Fig. 3). The output offer is as follows:

```
<!-- output buy offer -->
<m3:Offer id="ex:o20421-94"
    offeredPrice="6.00"
    buyPrice="5.0" acceptedVolume="10">
  <m3:description>
    End-to-end bandwidth buy offer
    from point A to C
  </m3:description>
  <m3:offeredBy ref="ex:buyer-d1"/>
  <m3:volumeRange minValue="0"
    maxValue="10"/>
  <m3:BundledOffer>
    <m3:offeredCommodity shareFactor="1"
      ref="ex:A-BM0705"/>
    <m3:offeredCommodity shareFactor="1"
      ref="ex:B-DM0705"/>
    <m3:offeredCommodity shareFactor="1"
      ref="ex:D-CM0705"/>
  </m3:BundledOffer>
</m3:Offer>
```

4. Summary

Present trade can be greatly improved by introducing multi-commodity turnover rules. M^3 is not limited to telecommunication markets, it may be used on other infrastructure markets, for example on energy and transmission rights market, many different commodities/services can exist, e.g., energy, flowgate rights, point-to-point optional transmission rights, point-to-point obligatory transmission rights, put and call options for energy, and various reserves. As the specified commodities are strictly tied, there is no possibility to form seven different markets. Elaborated mechanisms of multi-commodity trade are sufficient also to design others markets. Designed and planned applications of M^3 exists, e.g., different energy turnover platforms, power balancing markets, multi-stage markets [7], etc. In context of the distributed environment of multilateral, multi-commodity turnover, this paper forms a basis for future work on a M^3 model. Further work is to evolve syntax of simple object access protocol (SOAP) messages, elaborate other classes of offers.

The paper presents the overall design of the open multi-commodity market data model. The proposed model has many potential practical applications. As it was shown, M^3 may be used in a wide range of market-oriented network systems and may significantly facilitate communication, coordination and modeling procedures. Especially the classes of balancing processes for which M^3 adequately describes required data include multi-stage markets – where the whole market balance is obtained as a result of number of consecutive balancing processes, multilateral distributed multi-agent market systems – where clearing is performed in distributed environment of different points of service. M^3 may be used in designing information systems for market balancing and clearing in the context of multi-commodity trade in various network infrastructure sectors. M^3 provides a set of formal data models, which results in XML-derived information interchange specification. The unified data model may enable cooperation and easy data exchange between different research teams, as well as the market entities.

Acknowledgments

The authors acknowledge the Ministry of Science and Higher Education of Poland for partially supporting the research through Project 3T11C00527.

References

[1] G. Cheliotis, "A market-based model of bandwidth and a new approach to end-to-end path computation with quality guarantees", Technical Report, IBM Research, Zurich, 2000.

[2] S. S. Chiu and J. P. Crametz, "Taking advantage of the emerging bandwidth exchange market", White paper, RateXchange Ltd., 1999.

[3] C. Courcoubetis, M. P. Dramitinos, and G. D. Stamoulis, "An auction mechanism for bandwidth allocation over paths", in *17th Int. Teletraf. Congr. ITC-17*, Salvador da Bahia, Brazil, 2001, pp. 1163–1173.

[4] C. Courcoubetis, R. Weber, and M. Coe, *Pricing Communication Networks: Economics, Technology and Modeling*. New York: Wiley, 2003.

[5] L. A. DaSilva, "Pricing for QoS-enabled networks: a survey", *IEEE Commun. Surv. Tutor.*, vol. 3, no. 2, pp. 14–20, 2000.

[6] P. Kacprzak, M. Kaleta, P. Pałka, K. Smolira, E. Toczyłowski, and T. Traczyk, "M^3: open multi-commodity market data model for network systems", in *Proc. XVI Int. Conf. Syst. Sci.*, Wrocław, Poland, 2007.

[7] P. Kacprzak, M. Kaleta, P. Pałka, K. Smolira, E. Toczyłowski, and T. Traczyk, "Open multi-commodity market data model for network systems", Technical Report, Warsaw University of Technology, Institute of Control and Computation Engineering, 2006.

[8] *The Economic Theory of Auctions*, P. Klemperer, Ed. Cheltenham: Elgar, 2000.

[9] A. A. Lazar and N. Semret, "Design and analysis of progressive second price auction for network bandwidth sharing", *Telecommun. Syst.* (Special Issue on Network Economics), 2000.

[10] J. K. MacKie-Mason and H. R. Varian, "Pricing the Internet", in *Public Access to the Internet*, B. Kahin and J. Keller, Eds. Cambridge: MIT Press, 1995, pp. 269–314.

[11] "Multi-commodity market model (M^3)", http://www.openM3.org

[12] M. Pióro and D. Medhi, *Routing, Flow, and Capacity Design in Communication and Computer Network*. San Francisco: Morgan Kaufman, 2004.

[13] W. Stańczuk and K. Goworek, "Metody ustalania cen usług w sieciach pakietowych", *Przegląd Telekomunikacyjny i Wiadomości Telekomunikacyjne*, nr 11–12, 2002 (in Polish).

[14] W. Stańczuk, J. Lubacz, and E. Toczyłowski, "Trading links and paths on a communication bandwidth market", Technical Report, Warsaw University of Technology, Institute of Telecommunication, 2007.

[15] E. Toczyłowski, *Optymalizacja procesów rynkowych przy ograniczeniach*. Warsaw: EXIT, 2002 (in Polish).

Przemysław Kacprzak received the M.Sc. degree in 2004 from the Warsaw University of Technology, Poland. Currently he is a Ph.D. candidate in computer science at the Institute of Control and Computation Engineering at the Warsaw University of Technology. His research interests include operational research, optimization and electricity markets. His current research is focused on application of multi-commodity turnover models.
e-mail: P.Kacprzak@elka.pw.edu.pl
Institute of Control and Computation Engineering
Warsaw University of Technology
Nowowiejska st 15/19
00-665 Warsaw, Poland

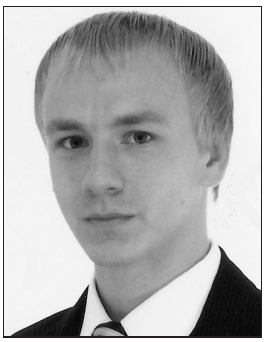

Mariusz Kaleta received the M.Sc. degree in 2000 and the Ph.D. degree in 2005 from the Warsaw University of Technology, Poland. Currently he is an Assistant Professor at the Institute of Control and Computation Engineering at the Warsaw University of Technology. His research interests include operations research, management in-

formation systems, discrete optimization, decision support. His current research is focused on infrastructure market designing, cost allocation problems and packing problems.
e-mail: M.Kaleta@ia.pw.edu.pl
Institute of Control and Computation Engineering
Warsaw University of Technology
Nowowiejska st 15/19
00-665 Warsaw, Poland

Piotr Pałka received the M.Sc. degree in 2005 from the Warsaw University of Technology, Poland. Currently he is a Ph.D. candidate in computer science at the Institute of Control and Computation Engineering at the Warsaw University of Technology. His research interest is incentive compatibility on the infrastructure markets. His current research is focused on application of multi-commodity turnover models.
e-mail: P.Palka@ia.pw.edu.pl
Institute of Control and Computation Engineering
Warsaw University of Technology
Nowowiejska st 15/19
00-665 Warsaw, Poland

Kamil Smolira received the M.Sc. degree in 2003 from the Warsaw University of Technology, Poland. Currently he is a Ph.D. candidate in computer science at the Institute of Control and Computation Engineering at the Warsaw University of Technology. His research interests are real-time infrastructure markets. His current research is focused on infrastructure market pricing algorithms.
e-mail: ksmolira@elka.pw.edu.pl
Institute of Control and Computation Engineering
Warsaw University of Technology
Nowowiejska st 15/19
00-665 Warsaw, Poland

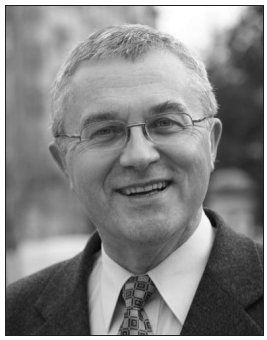

Eugeniusz Toczyłowski is Professor, the Head of Operations Research and Management Systems Division at the Institute of Control and Computation Engineering at the Warsaw University of Technology, Poland. He received the M.Sc. degree in 1973, Ph.D. in 1976, D.Sc. in 1989, and the title of full Professor in 2004. His main research interests are centered around the operations research models and methods, including structural approaches to large scale and discrete optimization, auction theory and competitive market design under constraints, multi-commodity trading models, and design of management information systems.
e-mail: E.Toczylowski@ia.pw.edu.pl
Institute of Control and Computation Engineering
Warsaw University of Technology
Nowowiejska st 15/19
00-665 Warsaw, Poland

Tomasz Traczyk received the M.Sc. degree in 1984 and the Ph.D. degree in 1992 from the Warsaw University of Technology, Poland. Currently he is a Associate Professor (Docent) at the Institute of Control and Computation Engineering at the Warsaw University of Technology. His research interests include applications of databases and XML. His current researches are focused on information and communication models for multi-commodity turnover and applications of generative programming for version management of information systems.
e-mail: T.Traczyk@ia.pw.edu.pl
Institute of Control and Computation Engineering
Warsaw University of Technology
Nowowiejska st 15/19
00-665 Warsaw, Poland

Paper

Economic disparities among regions in Japan and the problem of the spread of information and communication equipment in the countryside

Hidetomo Oyaizu

Abstract—Japan's government believed that the development of ICT networks and penetration of information and communications equipment in the countryside reduce the economic and population disparities among regions. Since the latter half of the 90s, some local governments built "intelligent facilities" equipped with ICT network so as to foster the information and communications industry in their area as part of regional "informatization policy". However, "intelligent buildings" failed to attract information and communication companies, economic disparities among regions are in fact widening, while the macro economy is recovering and expanding. Main points are the contents of the regional informatization policy and the effect on the development of ICT networks and the information and communication industry. As "economy of concentration" works more in the information and communications economy, the development of ICT networks and related industries would concentrate economic power in urban areas. At present, it is essential for the regional informatization policy to develop information and telecommunications infrastructure that addresses the needs of residents who lack access to information, and to implement careful information literacy education for residents.

Keywords—economic disparities among regions, regional informatization policy, digital divide, economy of concentration.

1. The relation of economic disparities among regions and the spread of information and communication equipment

1.1. "The lost decade" and regional income disparities

During the 90s, the Japanese economy fell into a recession of unprecedented length. Therefore, the 90s have been dubbed "the lost decade". The development of information and communication networks came to be seen as a necessary stimulus for improving efficiency of the macro economy, and the government adopted the belief that its development was particularly important in the countryside, where social infrastructure lagged behind that of large cities. In fact, in terms of macro economy, government investment in the IT field and corporate information investment had a good effect on economic growth. Japan's information and communications industry has been expanding and is a leading industry today (Table 1).

The information and communications industry consists of eight sectors:

- communications;
- broadcasting;
- information services;
- video picture, sound information, character information production and distribution;
- manufacture of information and communication electronics equipment and related products;
- information and communications related services;
- information and communications related construction work;
- research.

Types of business that comprise four sectors with largest number of employees, based on 2004 data [1] are:

- information services (employees, 1,004,204) consist of two businesses: computer programming and other software services and data processing and information services;
- research (771,715), which cannot be further subdivided;
- information and communications related services (662,383) consist of four businesses: rental services of information and communications equipment, advertising, printing and bookbinding businesses, cinemas, and legitimate theatres;
- communications (634,118) consists of four businesses: postal service, fixed telecommunications, mobile telecommunications and services incidental to telecommunications.

Table 1
Growth of Japanese information and communications industry [1]

Year	1995	1996	1997	1998	1999	2000	2001	2002	2003	2004
Gross domestic product (GDP) generated by information and communications industry [billion yen]	32 905	37 519	40 596	42 415	43 939	46 355	50 807	52 927	56 686	61 909
Growth rate [%]		14.0	8.2	4.5	3.6	5.5	9.6	4.2	7.1	9.2
Information and communications industry share of total GDP [%]	6.8	7.6	8.1	8.6	9.0	9.3	10.2	10.5	11.0	11.7

Consequently, since the latter half of the 90s the ownership of information communication equipment and use of Internet among households have dramatically increased in Japan (Fig. 1).

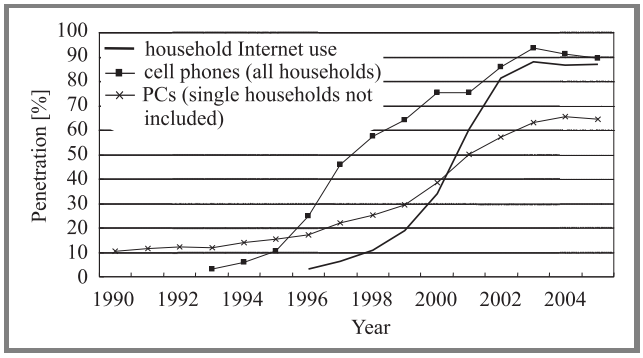

Fig. 1. Changes of penetration of information and communications equipment and Internet access [2].

Figure 2 shows trends in regional economic disparities in terms of the coefficient of variation for per capita prefectural income and per capita compensation of employees in the 47 prefectures of Japan. Between 1990 and 2001, the coefficients of variation for the two indicators declined, while in subsequent years they have risen. In other words, throughout "the lost decade", regional disparities narrowed, and they have been widening in subsequent years due to the business recovery since 2001.

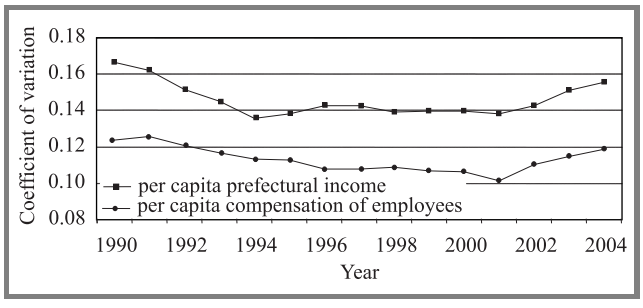

Fig. 2. Changes of coefficient of variation on per capita regional income [3].

That is to say, nowadays, information and communication network investment in the countryside has not boosted economic activity. Why has this happened? Tables 2 and 3 show the top and bottom five prefectures in terms of per capita prefectural income in 1990 and 2003. As you can see on the map (Fig. 3), all the top five are located in the center of Honshu island. On the other hand, the bottom five are mostly thinly populated prefectures located in the areas far from central Japan, or in isolated or mountainous areas.

Table 2
Top five and bottom five prefectures – fiscal year 1990 [3]

Top prefecture	Per capita prefectural income [thousand yen]	Bottom prefecture	Per capita prefectural income [thousand yen]
Tokyo	4139	Okinawa	1892
Osaka	3596	Nagasaki	2001
Aichi	3318	Kagoshima	2066
Kanagawa	3219	Miyazaki	2068
Saitama	3135	Kouchi	2116

Table 3
Top five and bottom five prefectures – fiscal year 2003 [3]

Top prefecture	Per capita prefectural income [thousand yen]	Bottom prefecture	Per capita prefectural income [thousand yen]
Tokyo	4267	Okinawa	2042
Aichi	3403	Aomori	2160
Shizuoka	3226	Nagasaki	2187
Siga	3205	Kouchi	2238
Kanagawa	3184	Kagoshima	2239

As for the information and communications industry, they can easily get profit in urban areas due to economy of concentration. Conversely, in isolated or mountainous areas, information and communications companies, especially telephone operators, are not willing to invest because of comparatively high investment costs.

After 2000, most successful and expanding businesses in Japan have been related to the information and communications industry; almost all these companies have been concentrated in big cities.

Therefore, the development of information and communication networks in the countryside by the government during

Fig. 3. Regions and prefectures of Japan.

"the lost decade" has not caused enough effective demand in those areas. That explains why the economies of rural prefectures have been stagnant in recent years.

1.2. Correlation between penetration of information and communications equipment and regional economy

Standard (fixed-line) telephones and TV sets are classified as information and communications equipment, but they are owned by almost every household, and therefore cannot be used as indicators for regional informatization disparities. Accordingly, we should use ownership of mobile phones, PCs and satellite receivers (satellite TV subscription) as indicators for regional informatization disparities, and examine their correlations with the regional economy. In fact, looking at the top five and bottom five prefectures by ownership of mobile phones and PCs (Tables 4 and 5) we find a resemblance in terms of per capita prefectural income.

Table 4
Top five and bottom five prefectures by penetration of mobile phones (1999) [2]

Top prefecture	Penetration among households [%]	Bottom prefecture	Penetration among households [%]
Fukui	73.1	Hokkaido	53.2
Ishikawa	71.7	Yamaguchi	54.4
Shiga	71.2	Miyazaki	54.5
Tokushima	71.0	Kagoshima	55.8
Saitama	70.8	Aomori/Akita	57.3

Table 5
Top five and bottom five prefectures by PC penetration (2004) [2]

Top prefecture	Penetration among households [%]	Bottom prefecture	Penetration among households [%]
Kanagawa	77.4	Okinawa	43.4
Aichi	76.1	Nagasaki	53.8
Siga	76.0	Aomori	56.2
Fukui	76.0	Kouchi	56.4
Nara	75.6	Kagoshima	57.7

Considering this fact, we will look at the relationship between ownership of information and communications equipment and per capita prefectural income using regression analysis.

Correlation between per capita prefectural income and ownership of information and communications equipment is shown in Fig. 4. Since Tokyo prefecture is an exceptional case, analysis excludes the Tokyo data, and the total num-

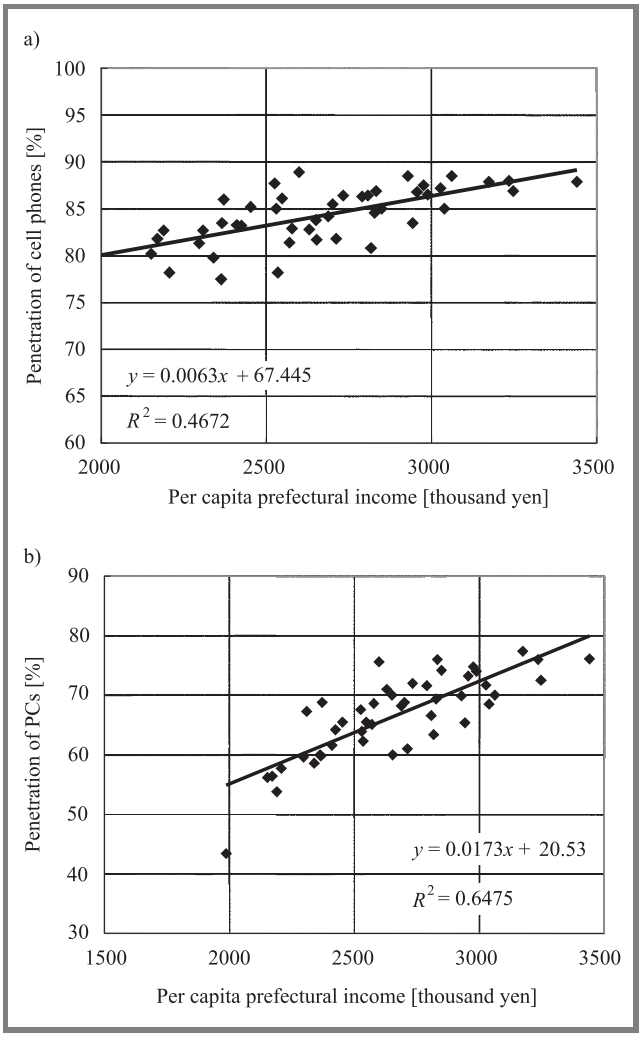

Fig. 4. Correlation between per capita income and penetration of information equipment: mobile phones (a) and PCs (b).

ber of data points is 46. Correlations are strong: the more developed regional economy is, the greater the availability of information equipment.

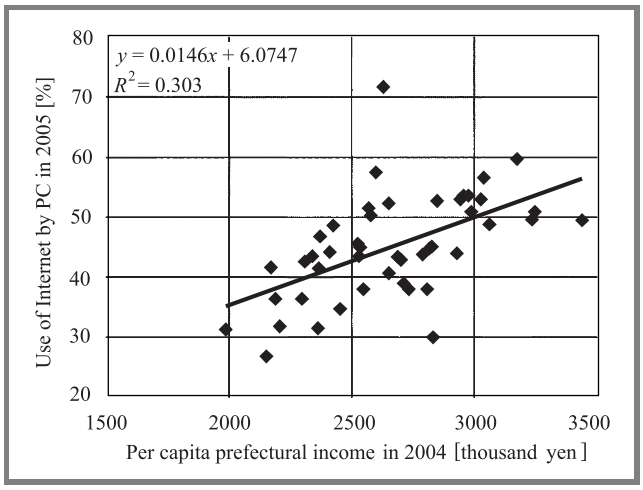

Fig. 5. Correlation between per capita income and use of information technology (2004).

However, the correlation between per capita income and use of information technology, meaning connecting the PCs to Internet, is not strong (Fig. 5). This is an astonishing fact and the problem is thought to lie in the use of PCs.

2. Features of Japan's regional informatization policy

2.1. Definition of regional informatization and regional informatization policy

Presently, there is no unified definition in Japan of *regional informatization* or any consensus on what the term means. In practice, it is interpreted differently by different researchers [4]. By the same token, *regional information* (*informatization*) *policy* and *regional information system* are used with a variety of different meanings by researchers. In this paper, I will consider regional informatization in the following broad framework (Table 6).

Table 6
Classification of *regional informatization*

A	Informatization for regional residents	1	Development of regional telecommunication infrastructure
		2	Penetration of information and telecommunications equipment among regional residents
		3	Use of information and telecommunication equipment by regional residents
B	Informatization of local governments (municipalities)	e-public administration (e-municipality)	

Based on the above, *regional informatization policy* is defined in this paper as a policy to promote regional informatization by governments, at both the national and local levels [5].

2.2. Japan's 90's regional informatization policy

During late 90s, Japan's regional informatization was focused on items A-1, A-2 in Table 6, which meant development of information and communications networks around Japan. The government thought this would stop the concentration of population and economic power in big cities and consequently to narrow economic disparity between urban and rural areas [6]. Some local governments built "intelligent facilities" to foster development of information and communications industry in their area. Those policies had succeeded in recovering macroeconomy, but the information and communications companies have rather centered in big cities. "Intelligent buildings" failed to attract the information and communication companies.

2.3. Japan's recent regional informatization policy

Now Japan's government is eager to carry out IT policy including regional informatization policy. The strategic objective of the *e-Japan Strategy II*, announced in July 2003, emphasized the usage and application of IT, and based on that strategic objective, the government announced *New IT Reform Strategy* in January 2006. The strategic objective of the *e-Japan Strategy II* was to emphasize the usage and application of IT, and based on that strategic objective. *New IT Reform Strategy* aims to create a society where everyone can enjoy the benefits of IT at any time and any place. Under the new strategy [1] both national and local governments and municipalities are called upon to implement measures to reach the following targets of the strategy by 2010, and:

– resolve problems faced by Japanese society by means of IT (structural reform of medical care, environmental-friendly society, the world's most effective e-public administration, and realization of an affluent society throughout people's life cycles by means of telework and e-learning);

– develop IT infrastructure (development of an IT infrastructure that eliminates the digital divide, and nurturing of world-class human resources specializing in sophisticated and advanced IT);

– send a message to the rest of the world showing Japan's determination to seek structural reform and make international contributions.

Japan's government has been focusing on expanding broadband service and e-public administration – see items A-1 and B in Table 6. Japan's broadband usage fees are, as has

been frequently mentioned in recent years by the government, among the lowest in the world (Fig. 6). The white paper [1] emphasizes that this is a result of government policy which prompted price competition.

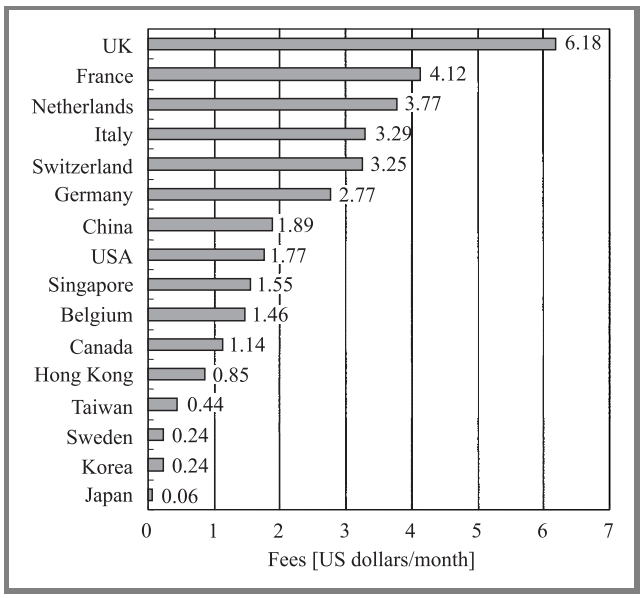

Fig. 6. Broadband access fees in selected countries (in descending order) [1]. (Note: Based on the offered speed and usage fees of DSL and cable Internet access in each country (*The Portable Internet*, ITU, Sept. 2004), the usage fee for 100 kbps access is calculated.).

Japan's broadband penetration is low by international standards, and broadband service is not yet universally available. Penetration is much higher in South Korea, Belgium, Hong Kong and Canada, where usage fees are far higher than in Japan (Fig. 7). Looking at the broadband penetration by prefecture, the top three prefectures are Tokyo, Kanagawa and Shizuoka, with 37.7%, 36.7% and 33.5%, respectively. The lowest two are Kagoshima and Kouchi with 10.4% and 14.3%, respectively – much lower than the top three, or even the national average of 27.6% (Table 7).

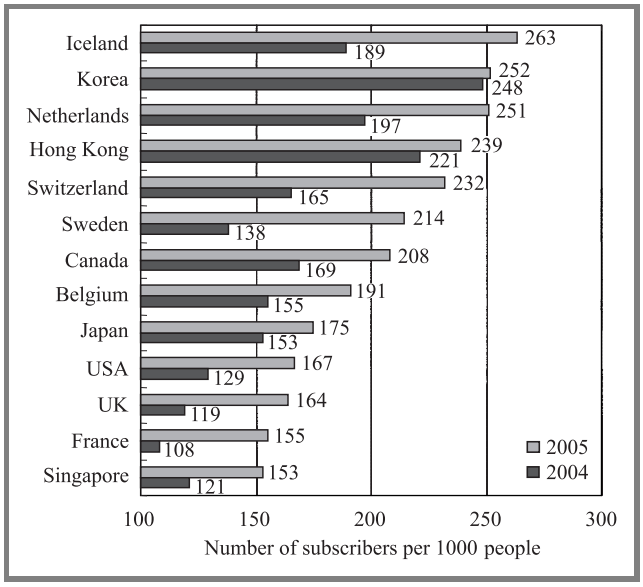

Fig. 7. Countries with high broadband penetration [1].

Table 7
Top five and bottom five prefectures by broadband penetration in 2006 [1]

Top prefecture	Penetration among households [%]	Bottom prefecture	Penetration among households [%]
Tokyo	37.7	Kagoshima	10.4
Kanagawa	36.7	Kouchi	14.3
Shizuoka	33.5	Kumamoto	15.5
Fukui	33.3	Aomori	16.8
Mie	33.3	Miyazaki	16.9

This regional digital divide still prevails, and because of the lagging prefectures, Japan's broadband dissemination rate is lower than that of other countries. In Japan, there were estimated to be 87.54 million Internet users at the end of 2006, making up 68.5% of the total population. The number of users has continued to decline from 2003, the peak year, though the usage rate is rising, albeit at a decreasing rate.

Table 8 indicates that nearly 90% of people from their late teens through their 40s use the Internet, while among those in their late 60s the proportion falls to 48.0% and for those in their 70s and over to around 30%. Comparing by size of municipality, the usage rate was 81.3% for the central Tokyo wards, ordinance-designated large cities and prefectural seats, but was significantly lower in other cities and in towns and villages, where the rate was 74.1% and 63.4%, respectively. Mr. Honkawa, an information science analyst, pointed out that the digital divide reduces use of the Internet and broadband access in Japan [7].

Table 8
Popularity of Internet usage by age groups [%] [1]

Age group	2004	2005	2006
6–12	62.8	65.9	67.9
13–19	90.7	93.9	93.0
20s	92.3	95.0	94.4
30s	90.5	92.8	92.5
40s	84.8	90.6	89.3
50s	65.8	75.3	75.2
60–64	49.0	55.2	59.7
65–69	27.3	42.0	48.0
70s	15.4	19.3	32.3
80s	6.9	7.2	16.0
Area	2004	2005	2006
Central Tokyo wards, ordinance-designated big cities and prefectural seats	78.2	79.3	81.3
Other cities	68.0	73.5	74.1
Towns and villages	56.9	68.4	63.4

3. Problems with regional informatization policy and example of successful case by local government

3.1. Problems of regional informatization policy by local governments

Municipality expenditures on informatization have increased in line with the central government's call for a regional informatization policy, as stated earlier. Municipalities have focused, in particular, on their own informatization, with the aim to become e-municipalities [8]. However, there are a number of regional informatization policies that were induced by a "demonstration effect", based on the view, for example, that as the neighboring prefecture (or neighboring city) has deployed a CATV network or constructed facilities related to informatization, one's own prefecture (or our city) should follow suit [4].

Most of these regional informatization projects induced by a "demonstration effect" are not created to fulfill the needs of residents of rural areas, in particular in sparsely populated areas with many elderly people, and thus it seems unlikely that they will help improve the productivity of the affected region as a whole in the long run.

3.2. Successful case of regional informatization: Yamada village

The term IT literacy is sometimes used in a way that includes the ability of people to make full use of information and telecommunications equipment, and we use the term in that sense in this report. Even if the regional telecommunication infrastructure is well developed, information and telecommunications equipment has widely penetrated among regional residents, the Internet is accessible from anywhere in the region, a lack of IT literacy among residents can lead to a digital divide, for example, between those who can operate PCs and those who cannot. The successful case of regional informatization can be found in Yamada village in the Toyama prefecture [9]. Yamada is a mountain village with a population of approximately 2100, located in a isolated rural area. The majority of residents in Yamada were not familiar with "keyboards" and had never used PCs before. The village succeeded in solving a lack of IT literacy among residents in the end of the 90s, by using the following policies: since 1996, PCs have been lent to all villagers who wanted them, and simple information network facilities were constructed. In particular, a university located in Takaoka (the second largest city in Toyama prefecture) has sent students to the village every year as a part of their collage (Takaoka National Collage) education course, to teach villagers how to operate PCs. Most villagers have been trained basic IT skills regularly at simple building called Information Center in one to one classes. As a result, in 1998 the Internet usage rate of the whole village rose above that of the central Tokyo wards. This successful project cost about 350 million yen a year. The village did not build expensive "intelligent facilities" but majority of villagers have been satisfied with this informatization policy.

It could be said that the main priority of regional informatization policy should not be the computerization of various operations run by municipalities including e-public administration (e-municipality) or the construction of informatization-related facilities. There is a clear digital divide between the metropolitan region and rural areas. However, though there is no detailed data available to support this supposition, it appears that the disparities between cities and towns and villages within the same rural areas are even more significant [10].

4. Concluding remarks: desirable direction for regional informatization

4.1. Risk of "government failures"

More developed information and telecommunications infrastructure in rural areas and increased ownership and usage of information and telecommunications equipment could enhance the economy of rural areas, but is unlikely to help narrow regional economic disparities.

The correlation between average prefectural land prices (expected earnings for broadband supplier) and the penetration of broadband (investment in broadband facilities) is strong (Fig. 8).

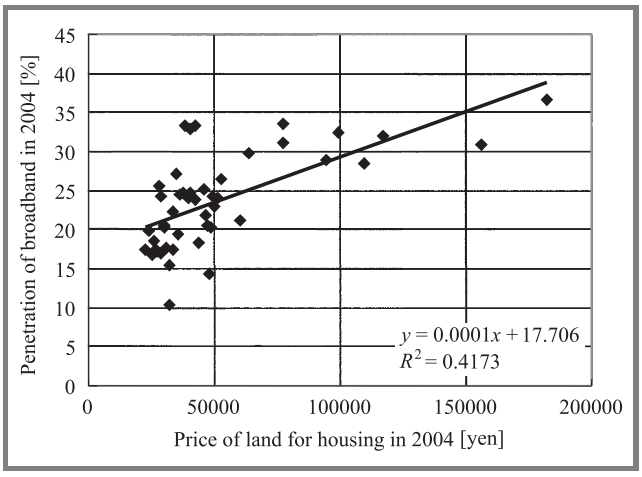

Fig. 8. Correlation between land price and broadband penetration.

It is interpreted that the information and telecommunication business has little that prospect of breaking into rural areas, so it is difficult for businesses in those areas to attract private sector investment. Leaving everything to market principles can lead to adverse effects of excessive concentration of economic power and population, or what is known as "market failure" [11].

On the other hand, it is difficult to say that it was effective for rural municipalities to invest independently into

Table 9
Share of home employed persons in large areas [%] [3]

Year	Hokkaido-Tohoku	Kantou	Chubu	Kinki	Chugoku	Shikoku	Kyushu	Total
1990	14.5	34.3	15.0	15.7	6.3	3.4	10.8	100
1993	14.3	34.6	15.0	15.8	6.2	3.3	10.8	100
1994	14.3	34.5	15.1	15.7	6.2	3.3	10.8	100
1995	14.3	34.5	15.1	15.7	6.2	3.3	10.9	100
1996	14.4	34.4	15.2	15.7	6.2	3.3	10.8	100
1997	14.4	34.5	15.2	15.6	6.2	3.3	10.9	100
1998	14.3	34.7	15.2	15.5	6.1	3.3	10.9	100
1999	14.3	34.8	15.1	15.5	6.1	3.2	10.9	100
2000	14.3	34.8	15.1	15.5	6.1	3.2	10.9	100
2001	14.2	35.0	15.1	15.4	6.1	3.2	10.9	100
2002	14.2	35.1	15.2	15.3	6.1	3.2	10.9	100
2003	14.1	35.2	15.3	15.2	6.1	3.2	10.9	100
2004	13.8	35.4	15.3	15.3	6.1	3.2	10.9	100

informatization and the construction of informatization-related facilities in an attempt to close the regional economic disparities. Rather, it appears that such endeavors by rural municipalities caused "government failures", which refers to public spending that does not meet true needs of residents.

Regional informatization often does not go beyond mere computerization of public administration, meaning the promotion of the efficiency of civil services provided by municipalities [12].

4.2. Growth of information and communications industry and "economy of concentration"

Following the end of World War II, the Japanese government formulated the Comprehensive National Development Plan, a long-term plan that served as essential guidance for national land development at the time. Five such national development plans have been formulated up to the present, each aiming primarily to achieve balanced development in the whole of Japan [13].

The latest national development plan, the *Grand Design for the 21st Century*, was adopted by the cabinet in March 1998. It aims to promote the development of information and telecommunications networks in rural areas, and in particular fiber-optic networks, which are expected to attract businesses that have a relatively large degree of freedom to locate their operations in rural areas. However, the latest development plan does not clarify which type of business has significant flexibility regarding the location of operations.

Looking at per capita home employed person's productivity in 7 areas, the highest has been in the Kantou area where Tokyo is located. Considering the share of home employed persons, the number in the Kantou area has been the highest, too (Fig. 9). Furthermore, this share has been expanding somewhat since 2000 (Table 9). New information and communications companies have been established in urban areas recently.

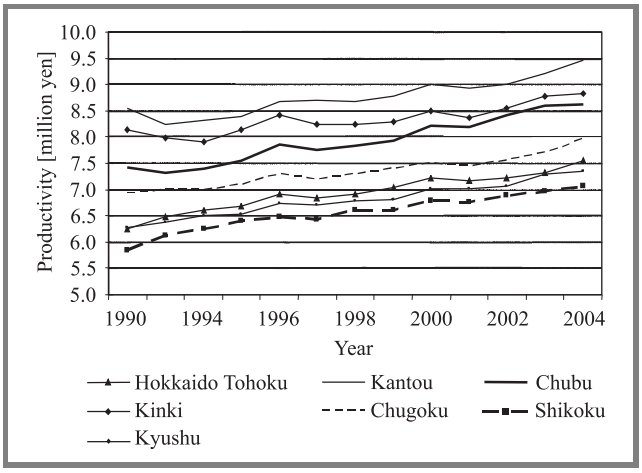

Fig. 9. Changes of per capita productivity of home working persons in large areas [3].

Businesses operating in the information service sector, the largest source of employment in the information and communications industry, are largely engaged in services for other businesses rather than to individuals and they tend to prefer to locate their operations in areas where business establishments are concentrated (Table 10).

Therefore, it would be incorrect to conclude that if the telecommunication infrastructure becomes better developed in rural areas, information service businesses will be encouraged to locate their operations there. So it is interpreted that "economy of concentration" has been working more in the information economy.

Table 10
Annual revenues of IT industry in Japan [million yen] and Tokyo's share [14]

Year	Japan	Tokyo prefecture	Growth rate [%]	Tokyo's share [%]
1991	6 825 247	3 637 919		52.9
1992	7 127 618	3 803 327	4.5	53.4
1993	6 514 358	3 371 034	–11.4	51.7
1994	6 177 007	3 152 205	–6.5	51.0
1995	6 362 183	3 169 921	0.6	49.8
1996	7 143 543	3 655 082	15.3	51.2
1997	7 587 959	3 982 493	9.0	52.5
1998	9 800 606	5 098 666	28.0	52.0
1999	10 151 890	5 383 935	5.6	53.0
2000	10 722 864	5 783 936	7.4	53.9
2001	13 703 868	5 837 592	35.5	57.2
2002	13 973 141	8 002 468	2.1	57.3
2003	14 170 633	8 145 871	1.8	57.5
2004	14 527 056	8 858 191	8.7	61.0

4.3. Priority should be on providing information literacy education to those who lack access to information

A more developed ICT in rural areas and increased ownership and usage of information and telecommunication equipment could enhance the economic power of rural areas, but would be unlikely to help narrow regional economic disparities. It is difficult to say that it was effective for rural municipalities to construct informatization-related facilities in an attempt to attract information and communications companies and to close the regional economic disparities. If local governments supply their services using IT (e-municipality), majority of their residents separated by the digital divide will not benefit from these public goods.

At present, it is essential for the regional informatization policy to develop information and telecommunications infrastructure that addresses needs of residents who lack access to information, and to implement careful information literacy education for residents, listed as item A-3 in Table 6.

The majority of people in isolated or mountainous areas in Japan are aged. In the future, they will have to operate information and communications equipment to get critical information or services such as medical, financial and legal [15]. Reducing the digital divide would foster the information and communications industry in the end.

References

[1] "White Paper on Information and Telecommunications", 2005–2007 Edition, The Ministry of Internal Affairs and Communications.

[2] "Trend Report on Use of Communications", 2000 and 2005 Edition, Ministry of Internal Affairs and Communications, Information and Communications Policy Bureau.

[3] "Annual Report on Prefectural Accounts", 2004–2006 Edition, Government of Japan, Economic and Social Research Institute Cabinet Office.

[4] Y. Horigome, "Study on requirement of regional information telecommunications policy in rural areas – viewpoint from human element in region", *Gakuironbun Kougaishu*, no. 36, 2005 (in Japanese), http://www.soc.titech.ac.jp/publication/Theses2005/doctor/horigome.pdf

[5] H. Oishi, *Regional Informatization: Theory And Policy*. Kyoto: Sekaishiso Sha, 1992 (in Japanese).

[6] S. Tsuda, "Progress of regional informatization and changes in people's awareness as citizens", *Media Commun.*, no. 55, pp. 33–48, 2005 (in Japanese).

[7] Y. Honkawa, http://www2.biglobe.ne.jp/∼machi-IT/021-1.pdf

[8] H. Kobayashi, "What must e-local governments do? Looking back at the last 20 years of regional informatization", *Kaigai denki tsushin*, pp. 37–40, May 2004 (in Japanese).

[9] Y. Komatsu Naokoto Kogou, "The Internet and its impact on small, rural Japanese village", in *Feminist Definitions of Caring Communities and Healthy Lifestyles*. Ontario: Your Scrivener Press, 2001, pp. 299–303.

[10] M. Yamanaka, "Analysis of factors behind the digital divide in local communities and research on IT education", *Denkitsushin fukyu*, no. 18, pp. 114–120, 2002 (in Japanese), http://www.taf.or.jp/publication/kjosei_18/pdf/016.pdf

[11] M. Mima, "Future of regional informatization policies utilizing the Internet: observations on the "externality approach", 2002 (in Japanese), http://www2u.biglobe.ne.jp/ machi-IT/021-1.pdf

[12] Y. Yuasa, S. Sakamoto, and H. Sai, *Regional Informatization: Potential of Informatization Rooted in Local Communities*. Kyoto: Koyo Shobo, 2004 (in Japanese).

[13] A. Yamazaki, *Japan's National Land Planning and Regional Development: Economic Development and Spatial Structure for High Mobility*. Tokyo: Toyo Keizai Shinpo Sha, 1998 (in Japanese).

[14] "White Paper on Information Business Industry", 1991–2006 Edition, The Ministry of Economics and Industry.

[15] T. Ida, "Nation-wide introduction of optic fiber networks for homes based on user fees", Keizai Kyoushitsu *Nihon Keizai Shimbun*, June 2005 (in Japanese).

Hidetomo Oyaizu was born in Yamaguchi, Japan, in 1962. He received the Master of degree in economics from Waseda University, Japan, in 1988. From 1988 to 2000, he worked as an economic researcher at Think Tank, Mitsubishi Research Institute, where he has been involved in research on the regional econometric model and petrochemical industry. He has co-authored over 10 books on industries in Japan. At present, he teaches regional economics as an Associate Professor at Faculty of Economics in University of Toyama. His interests are regional economics and the theory of industrial organization.

e-mail: oyaizu@eco.u-toyama.ac.jp
Faculty of Economics
University of Toyama
3190 Gofuku, Toyama-shi, Toyamaken 930-8555, Japan

Paper

Possibility for the application of publications analysis to evaluation of research institutes

Toshiya Kobayashi and Saburo Ogata

Abstract—This study looks at the possibility of using publications analysis, which has been used by companies as a basic survey method for formulating publications strategies, as a quantitative index for evaluating researches conducted by national universities. The study also describes the reality of public outreach toward Japanese society, being carried out by research institutes such as universities, through publications analysis.

Keywords—public outreach, publications analysis, science policy evaluations, technology blanding, Third Basic Program for Science and Technology.

1. Introduction

In August 1997, an "Outline index for evaluation common to all research and development activities in Japan" was formulated with the aim to evaluate R&D based on the First Basic Program for Science and Technology, launched in 1996. Research conducted in universities at national expense have been targeted for evaluation.

How is quantitative analysis conducted on the results of research? Two common methods are to look at the number of papers published and the number of citations in other publications. However, there are few indices on items such as the number of theses written or quoted, for which evaluators and evaluees can unanimously agree. In this research, we will examine, through empirical research, the potential to expand the use of the quantitative index.

2. The position of this research

First, it is important to gain a quantitative grasp of how the media report on research institutes and researchers. Public outreach is used as an index for evaluating how institutes and research activities are publicized. Consequently, gaining a grasp of public outreach can be one method for evaluating research work.

We decided that it would be important to conduct an initial empirical examination to quantitatively and qualitatively grasp how research institutes and researchers in Japan have been portrayed in the media, based on the view that this could lead to the establishment of an index for research institutes and researchers to dispatch information proactively, appropriately and efficiently. To do this, we decided to use "publications analysis", which has been used as part of activities to survey a corporate image leading to brand-building [1].

3. Degree of public outreach is utilized for evaluation of research institutes

Under the Third Basic Program for Science and Technology approved by the Japanese government on March 28, 2006, public outreach activities are defined as "education activities for the general public carried out by research and development organizations and institutes", and clearly positioned such activities as a basic responsibility of such organizations and institutions [2]. Therefore, it is projected that the degree of public outreach will become an important indicator for evaluating research institutes and research in the future. In positioning public outreach as such an indicator, first of all, it is important to quantitatively and qualitatively grasp how research institutes and researchers in Japan have been portrayed by the media to date [3].

We note, however, that there is a perception gap between those who dispatch information and those who receive it. The Japanese government's "White Paper on Science and Technology 2003" found that many scientists obtained information on social needs and trends relating to science from trends in academia and organizations, through their

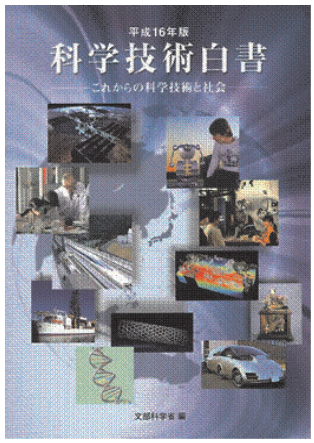

Fig. 1. "White Paper on Science and Technology 2003" by Japanese government.

work and from science magazines, rather than from the media such as newspapers and TV. By contrast, members of the public mainly get information on science and technology and universities through TV and newspapers. In addition, very few scientists said that they wanted to use newspapers and TV as a place to report their research. Consequently, we believe there is a need to conduct publications analysis on the degree of information actually dispatched by researchers through the media (Fig. 1).

4. What is publications analysis?

We would like to briefly discuss the nature of publications analysis. It is a method for analyzing corporate brand image spread through the mass media on a practical level. Basically, it looks at all publications including TV and radio, newspapers and the Internet. The method involves observing the volume and quality of articles carried in newspapers on specific target companies and organizations.

What is the significance of using newspapers, as we did in our research, as a target of publications analysis? Newspapers are a source of TV and web news, and the four major national papers cover nearly all of Japan. According to the Japan Newspaper Publishers and Editors Association, 52,568,032 copies of daily papers are published nationwide. This means that 1.04 newspapers are read per household every morning. In addition, since newspapers are read by multiple persons in each household or office, the actual number of readers far exceeds the number of copies sold. According to the Association, 2.8 people read each newspaper in turns. In other words, the number of readers exceeds the entire population of Japan. Therefore, these data indicate that newspapers are the most deep-rooted and trusted media among people in Japan.

5. Evaluating contents of public outreach through publications analysis

Consequently, we decided to base our research on articles in newspapers. We began by collecting news articles using Nikkei News Telecom 21, a large-scale database that permits searches of articles from commercial newspapers, to observe how universities' public outreach activities were reported.

The targets for research were seven national universities – Hokkaido, Tohoku, Tokyo, Nagoya, Kyoto, Osaka and Kyushu Universities – whose histories go back further than other national universities. The period of research was 15 years, from 1991 to 2005. The media targeted for the research were four national newspapers – Nikkei (Nihon Keizai Shimbun), Mainichi, Asahi and Yomiuri, including both morning and evening editions.

The total number of articles covering universities in general was found to be about 600,000, and among them, we found about 66,000 articles covering the seven universities. From those 66,000, we selected 100 articles for each of the years 1991, 1996, 2001 and 2005, adding up to four hundred articles, for each university, and used them for the analysis.

Table 1
Items directly related to university and research are taken to be activities, research, evaluations of activities, and prizes

Quotations	Quotations regarding research carried out by researchers belonging to university
	Quotations or comments by professors belonging to university
	Joint research with external research organization
	As partner or business partner of company
Biography	Affiliation or biography of person in newspaper article
	Biography of participant in roundtable discussion
	Biography (obituary) of deceased person
Activities	Introduction to activities of university
	University program or holding of symposium, etc.
	Introduction to links with external organizations
Research activities	University research activities
Evaluation of activities	Evaluation of university, internal venture, etc.
Personnel	Article on personnel change at university
Receipt of award	Receipt of award
Affiliation	Article on book published by publishing company affiliated with university
Setting	Setting for historical background
	Setting for article

Please look at Table 1 and Fig. 2. You will note that there were many more articles covering Tokyo University than covering the other six universities. You will also note that from 1996 to 2000, the number of articles dealing with Tokyo University and Kyoto University rose.

Next, we analyzed the contents of the articles. It would have proven impossible to read all 65,000 articles in

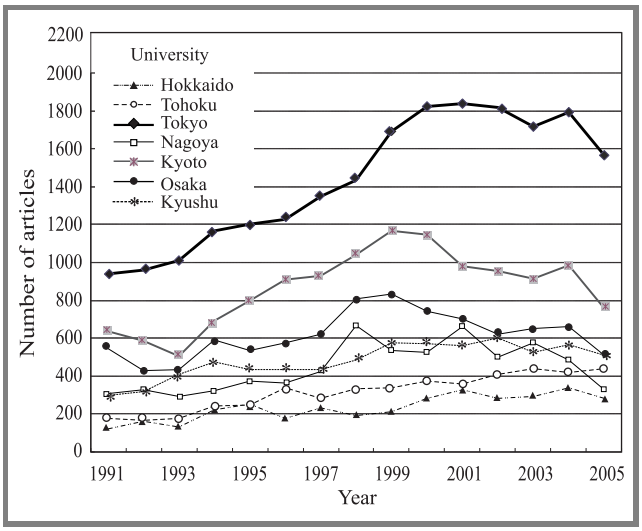

Fig. 2. Changes in number of articles by university and year.

Table 2
Report number-of-cases transition of the famous national universities in Japan

Year	Name of university							
	Hokkaido	Tohoku	Tokyo	Nagoya	Kyoto	Osaka	Kyushu	Total
1991	122	175	939	310	635	544	298	3.023
1992	164	169	960	330	587	428	316	2,954
1993	131	179	1,008	295	505	436	407	2,961
1994	222	240	1,169	325	693	589	473	3,711
1995	254	246	1,203	376	798	535	432	3,844
1996	179	340	1,228	366	911	574	432	4.030
1997	230	285	1,350	423	930	623	434	4,275
1998	194	331	1,432	669	1,039	806	486	4,957
1999	211	338	1,690	535	1,168	833	577	5,352
2000	281	376	1,824	525	1,148	740	571	5,467
2001	326	360	1,840	663	982	700	560	5,431
2002	284	407	1,819	499	953	619	600	5,181
2003	293	437	1,717	575	915	649	523	5,109
2004	339	421	1,791	486	986	662	564	5,249
2005	285	441	1,564	330	756	509	510	4,395
Total	3,515	4,747	21,534	6,707	13,006	9,247	7,183	65,939
Source: Nikkei News Telecom 21.								

Table 3
Components of negative image

Students	Teachers and university administration				Both students and teachers		
Cheating	Falseness	Go to a hooker	Punitive dismissal	Sexual molester	Distrust	Lynch	WINNY
Use of stand-ins	Bribe-giving	Academic harassment	Fallacy	Misappropriation of money	Retribution	Asault and battery	Information leaks
Declining academic achievement	Embezzlement	Sexual harassment	Plagiarism	Misplay	Listen-in	Awakening drug	Plagiarism
	Concealment	Acceptance of a bribe	Washout	Suspension of employment	Reprimand	Drug	Burglary
	Concoction	Downfall	Medical error	Breach	Judicial action	Hashish	Apprehension
	Plagiarise	Failure	Illegal waste disposal	Apology	Go to court	Violence	Indictment

the database dealing with the seven universities, so we selected 400 news articles for analysis. We found that positive articles could be classified into nine groups listed in Table 2. They dealt mainly with the universities' activities, research, evaluations of activities, and prizes.

6. Components of negative image

We also found from the survey that the following negative articles reported on scandals involving them, leading to the deterioration of the universities' images. There were three main subjects of negative articles: scandals caused by students, scandals caused by teachers and/or university administrations, and scandals caused by both students and teachers. Typical scandals caused by students involved cheating, use of stand-ins for entrance examinations, and other articles related to declining academic achievement. Scandals caused by teachers included academic harassment, forgery and other acts relevant to research. Finally, scandals caused by both of students and teachers were classified as being related to crimes in general. Specific items are shown in Table 3.

7. Conclusion

We obtained the following results. First, our publications analysis succeeded in finding clues regarding how universities in Japan have carried out public outreach toward society using the media, including newspapers.
We also found that articles on public outreach included both positive and negative ones about universities. We also found the specific components of this.
We believe, however, that the following concerns can be raised concerning the actual use of public outreach to evaluate research institutes through publications analysis in the future. Research institutes will tend to skip basic research while focusing on research themes that are easily accepted by the media. This, in turn, may lead to a deterioration of basic research in universities in Japan.
Finally, with regard to future tasks related to the creation of a news article classification tool, we must note that it would have been extremely difficult for humans to manually classify the 65,000 articles on the seven national universities obtained in our preliminary survey, so it should be done automatically. Specific keywords could be checked from the headlines and bodies of stories for classification, and a tool for aggregating the classified keywords should be considered.

Acknowledgments

We are thankful to the Ministry of Education, Culture, Sports, Science and Technology (MEXT) and Japan Society for the Promotion of Science (JSPS) for supporting this research.

References

[1] T. Kobayashi and S. Ogata, "Efforts to evaluate national universities quantitatively through the application of publications analysis", in *21st Ann. Conf. Japan Society for Science Policy and Research Management*, Tokyo, Japan, 2006.

[2] T. Shinozaki, "Toward the effective promotion of public outreach activities by researchers", Safety Policy Research Division, Mitsubishi Research Institute, MRI TODAY, October 4, 2005, http://www.mri.co.jp/COLUMN/TODAY/SHINOZAKI/2005/1004ST.html

[3] H. Kamata, "Public outreach as a basic science frontier", University of Tokyo Press, Dec. 2004, no. 386, pp. 22–28.

Toshiya Kobayashi was born in 1960. He received B.S. in social science in 1984, and Master of art and science in 1997. His professional career in public affairs and advertising business started in advertising industry (1984–1992). His interests focused on studying science and technology policy in think tank (1992–2002). Mr Kobayashi was the Head of environment and human science research group in its think tank. He become an Associate Professor of University of Tokyo in 2002, and an Associate Professor of Japan Advanced Institute of Science and Technology (JAIST) in 2004. Author of 32 published papers, co-author of 7 papers and co-author of 8 books.
e-mail: t-kobaya@jaist.ac.jp
Japan Advanced Institute of Science
and Technology (JAIST)
Asahidai, Nomi, Ishikawa Pref. 923-1292, Japan

Saburo Ogata was born in 1963. He received B.S. in economics in 1987 and M.Sc. in 1998. Mr Ogata started his professional career as a researcher in a banking company in 1987. He was a senior researcher (1997–1998, 2001–2007) and a Director of research group on knowledge-based society (2005–2007) of the Institute for Future Technology. He was also a visiting researcher of Research Center of Advanced Science and Technology, The University of Tokyo (2002–2005), a lecturer (non-permanent post) of Tokai University (2004–2007), and a visiting Associate Professor of Japan Advanced Institute of Science and Technology (2005–2006). He became a research Associate Professor of Japan Advanced Institute of Science and Technology in 2007. He is a co-author of 3 books (in Japanese).
e-mail: s-ogata@jaist.ac.jp
Japan Advanced Institute of Science
and Technology (JAIST)
Asahidai, Nomi, Ishikawa Pref. 923-1292, Japan

Invited paper

Analysis of propagation of orthogonally polarized supermode in straight and curved multicore microstructured fibres

Igor A. Goncharenko and Marian Marciniak

Abstract—We analyze the dependence of radiation loss, effective indices and difference of the effective indices of the two modes with similar field distribution propagating in dual-core microstructured fibres as well as their polarization behavior on fibre parameters (air hole diameter, hole separation, distance between guiding cores) and fibre bending. Optimization of the parameters of such fibres using as vector bend sensors is considered.

Keywords— multicore fibre, microstructured fibre, supermode, birefringence, mode dispersion, method of lines.

1. Introduction

Microstructured or holey fibres are single material fibres with a periodic array of air holes running along the length of the fibre [1, 2]. These fibres guide the light due to a defect (or defects) in the array using two different mechanisms: a photonic band-gap effect or an effective index difference between the defect region, which forms the core, and remainder of the periodic region, which acts as the cladding. Microstructured fibres (MFs) offer exciting new possibilities for guiding of light. They have enormous potential in admitting exotic microstructures with relative ease of manufacturing and can also be made single-mode over a wide range of wavelengths. For many applications, two or more guiding cores rather than just one are required. Examples of such applications include switching, vector bend sensors, phase-locked high-power lasers, fibre couplers and polarization splitters [3–5]. An interesting feature of multicore microstructured fibres (MCMFs) is the possibility to control and modify the shape of their modes by varying the diameter of air holes, hole separation, distance between guiding cores and fibre bends [5, 6].

In a dual-core MF shown in Fig. 1, two supermodes with similar field distribution but different propagation constants and confinement losses propagate equally in both cores [6]. The difference between parameters of both modes is dependent on the structure of MCMF. According to the theory of coupled fibres (see, for instance, [7]), one of the supermodes of the dual-core fibre formed by the sum of the fundamental solutions of separate fibres (separate cores) has propagation constant larger than the propagation constant of the separate fibre by the value of coupling coefficient of two cores. This supermode is called even mode. The second (odd) supermode is formed by subtraction of fundamental solutions and has the propagation constant lower then the separate fibre – by value of the coupling coefficient. In addition each mode exists in two polarization states. Because the cross-section of the dual-core MF with usual hexagonal lattice of air holes substantially differs for the x and y directions, it is natural to expect the difference of parameters and field distributions of modes with orthogonal polarizations.

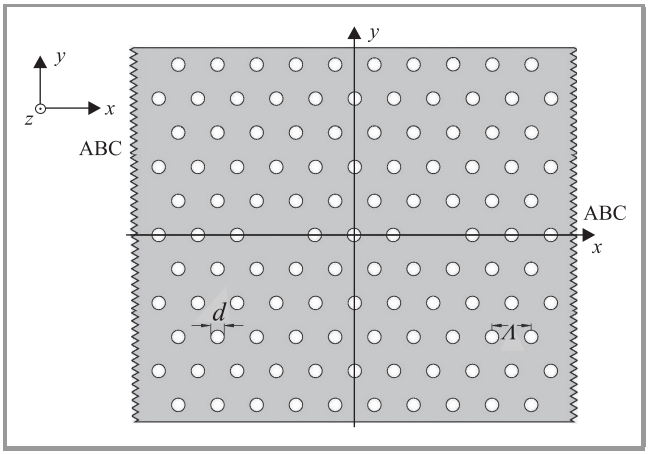

Fig. 1. Cross-section of dual-core microstructured fibre.

In this paper we analyse the mode dispersion in dual-core microstructured fibres in dependence on the MCMF structure and bending. Under the term "mode dispersion" we understand here not the difference of group velocities, but the difference of effective indices and radiation loss coefficients, both of orthogonally polarized modes (polarization mode dispersion or birefringence) and two supermodes of dual-core MF (supermode dispersion).

2. Theory

The cross-section of dual-core MF under investigation with hexagonal lattice is presented in Fig. 1. We use the algorithm based on the method of lines [8, 9] for calculation of mode field distribution, effective refractive indices and radiation loss in MCMF, as we have proven the efficiency of

that method for analysis of single-core MFs [10]. Following the method of lines we divide the structure under investigation into layers in y direction. In each layer the permittivity is assumed to be a function of the x coordinate only: $\varepsilon = \varepsilon(x)$. Wave propagation in z direction is described by $\exp(-jk_z z) = \exp(-j\sqrt{\varepsilon_{re}}\, z)$, ε_{re} being the propagation constant. Therefore, we have $\partial/\partial z = -jk_z = -j\sqrt{\varepsilon_{re}}$. From the Maxwell equations we derive two coupled generalized transmission line equations for the y direction for each layer, which have to be solved [8]:

$$\begin{aligned} \frac{\partial}{\partial \overline{y}} \begin{bmatrix} -\widetilde{H}_x \\ j\widetilde{H}_z \end{bmatrix} &= -\big[R_E\big] \begin{bmatrix} jE_z \\ E_x \end{bmatrix}, \\ \frac{\partial}{\partial \overline{y}} \begin{bmatrix} jE_z \\ E_x \end{bmatrix} &= -\big[R_H\big] \begin{bmatrix} -\widetilde{H}_x \\ j\widetilde{H}_z \end{bmatrix}, \end{aligned} \tag{1}$$

where

$$\begin{aligned} \big[R_E\big] &= \begin{bmatrix} D_{\overline{x}}\mu^{-1}D_{\overline{x}} + \varepsilon_z & -\sqrt{\varepsilon_{re}}D_{\overline{x}}\mu^{-1} \\ -\sqrt{\varepsilon_{re}}\,\mu^{-1}D_{\overline{x}} & \varepsilon_{re}\mu^{-1} - \varepsilon_x \end{bmatrix}, \\ \big[R_H\big] &= \begin{bmatrix} \varepsilon_{re}\,\varepsilon_y^{-1} - \mu & \sqrt{\varepsilon_{re}}\varepsilon_y^{-1}D_{\overline{x}} \\ \sqrt{\varepsilon_{re}}D_{\overline{x}}\varepsilon_y^{-1} & D_{\overline{x}}\varepsilon_y^{-1}D_{\overline{x}} + \mu \end{bmatrix}, \\ E_y &= \varepsilon_y^{-1}\Big[\sqrt{\varepsilon_{re}};\quad -D_{\overline{x}}\Big] \begin{bmatrix} -\widetilde{H}_x \\ j\widetilde{H}_z \end{bmatrix}, \\ \widetilde{H}_y &= \mu^{-1}\Big[D_{\overline{x}};\quad -\sqrt{\varepsilon_{re}}\Big] \begin{bmatrix} jE_z \\ E_x \end{bmatrix}, \end{aligned} \tag{2}$$

$\widetilde{H}_{x,y,z} = \sqrt{\varepsilon_0/\mu_0}\,H_{x,y,z}$, $E_{x,y,z}$ and $H_{x,y,z}$ are the electrical and magnetic field components, $D_{\overline{x}}$ is abbreviation for $\partial/\partial\overline{x}$. All coordinates and dimensions are normalized to the free space wave number k_0 according to $\overline{x} = k_0 x$, $\overline{y} = k_0 y$. The combination of two equations (1) yields wave equations for the electric and magnetic fields, which are completely equivalent

$$\begin{aligned} \frac{\partial^2}{\partial \overline{y}^2} \begin{bmatrix} E_z \\ E_x \end{bmatrix} - \big[R_H\big]\big[R_E\big] \begin{bmatrix} E_z \\ E_x \end{bmatrix} &= 0, \\ \frac{\partial^2}{\partial \overline{y}^2} \begin{bmatrix} -H_x \\ H_z \end{bmatrix} - \big[R_E\big]\big[R_H\big] \begin{bmatrix} -H_x \\ H_z \end{bmatrix} &= 0. \end{aligned} \tag{3}$$

For instance, for the product $[Q_H] = [R_E][R_H]$ we obtain four submatrices:

$$\begin{aligned} Q_{H11} &= -D_{\overline{x}}\mu^{-1}D_{\overline{x}}\mu + \varepsilon_{re}\,\varepsilon_z\,\varepsilon_y^{-1} - \varepsilon_z\mu\,, \\ Q_{H12} &= \sqrt{\varepsilon_{re}}\big(\varepsilon_z\varepsilon_y^{-1}D_{\overline{x}} - D_{\overline{x}}\big)\,, \\ Q_{H21} &= \sqrt{\varepsilon_{re}}\big(D_{\overline{x}} - \varepsilon_x D_{\overline{x}}\varepsilon_y^{-1}\big)\,, \\ Q_{H22} &= -\varepsilon_x D_{\overline{x}}\varepsilon_y^{-1}D_{\overline{x}} + \varepsilon_{re} - \varepsilon_x\mu\,. \end{aligned} \tag{4}$$

The partial differential equations (3) have to be discretized with respect to x coordinate in order to obtain ordinary differential equations, which can be solved analytically. In this case not only the field components but also the permittivities and the radial coordinate x have to be discretized. The discretization has to be done in two different line systems, yielding

$$\begin{aligned} &E_x, H_z, H_y \to \mathbf{E}_x, \mathbf{H}_z, \mathbf{H}_y \qquad H_x, E_z, E_y \to \mathbf{H}_x, \mathbf{E}_z, \mathbf{E}_y \\ &\varepsilon_x \to \boldsymbol{\varepsilon}_x \qquad\qquad \varepsilon_z, \varepsilon_y \to \boldsymbol{\varepsilon}_z, \boldsymbol{\varepsilon}_y \\ &\frac{\partial}{\partial \overline{x}} \to \overline{h}^{-1}\mathbf{D}_x^{\circ} = \overline{\mathbf{D}}_x^{\circ}\,, \qquad \frac{\partial}{\partial \overline{x}} \to \overline{h}^{-1}\mathbf{D}_x^{\bullet} = \overline{\mathbf{D}}_x^{\bullet}\,, \end{aligned} \tag{5}$$

where: $h = k_0 h$ is the normalized discretization distance, $\boldsymbol{\varepsilon}$ are diagonal matrices. The symbols $^{\circ}$ and $^{\bullet}$ indicate the discretization line system to which the quantities belong. In order to take into account the confinement and bend radiation losses, we introduce the absorbing boundary conditions (ABC) [11] on the outer boundaries of the structure.

Now the Eqs. (3) can be rewritten in the form

$$\frac{d^2}{d\overline{y}^2}\,\mathbf{F} - \mathbf{Q}\mathbf{F} = \mathbf{0}\,, \tag{6}$$

where $\mathbf{F} = \mathbf{E}$, $\mathbf{H}$; $\mathbf{E} = \begin{bmatrix} j\mathbf{E}_z \\ \mathbf{E}_x \end{bmatrix}$, $\mathbf{H} = \begin{bmatrix} \mathbf{H}_x \\ j\mathbf{H}_z \end{bmatrix}$ and, for instance,

$$\begin{aligned} Q_{H11} &= -\overline{\mathbf{D}}_x^{\circ}\overline{\mathbf{D}}_x^{\bullet} + \varepsilon_{re}\,\boldsymbol{\varepsilon}_z\boldsymbol{\varepsilon}_y^{-1} - \boldsymbol{\varepsilon}_z\mu\,, \\ Q_{H12} &= \sqrt{\varepsilon_{re}}\big(\boldsymbol{\varepsilon}_z\boldsymbol{\varepsilon}_y^{-1}\overline{\mathbf{D}}_x^{\circ} - \overline{\mathbf{D}}_x^{\circ}\big)\,, \\ Q_{H21} &= \sqrt{\varepsilon_{re}}\big(\overline{\mathbf{D}}_x^{\bullet} - \boldsymbol{\varepsilon}_x\overline{\mathbf{D}}_x^{\bullet}\boldsymbol{\varepsilon}_y^{-1}\big)\,, \\ Q_{H22} &= -\boldsymbol{\varepsilon}_x\overline{\mathbf{D}}_x^{\bullet}\boldsymbol{\varepsilon}_y^{-1}\overline{\mathbf{D}}_x^{\circ} + \varepsilon_{re} - \boldsymbol{\varepsilon}_x\mu\,. \end{aligned}$$

By transformation to main axes (diagonalization)

$$\mathbf{T}_H^{-1}\mathbf{Q}_H\mathbf{T}_H = \boldsymbol{\Gamma}^2, \quad \mathbf{T}_E = j\mathbf{R}_H\mathbf{T}_H\boldsymbol{\Gamma}^{-1}\,,$$

or

$$\begin{aligned} &\mathbf{T}_E^{-1}\mathbf{Q}_E\mathbf{T}_E = \boldsymbol{\Gamma}^2\,, \quad \mathbf{T}_H = j\mathbf{R}_E\mathbf{T}_E\boldsymbol{\Gamma}^{-1}\,, \\ &\mathbf{E} = \mathbf{T}_E\overline{\mathbf{E}}, \quad \mathbf{H} = \mathbf{T}_H\overline{\mathbf{H}} \end{aligned} \tag{7}$$

we obtain uncoupled equations in the transformed domain

$$\frac{d^2}{d\overline{y}^2}\,\overline{\mathbf{F}} - \boldsymbol{\Gamma}^2\overline{\mathbf{F}} = \mathbf{0} \tag{8}$$

with the general solution

$$\overline{\mathbf{F}} = \exp(-\boldsymbol{\Gamma}\overline{y})\,\overline{\mathbf{F}}^{f} + \exp(\boldsymbol{\Gamma}\overline{y})\,\overline{\mathbf{F}}^{b}\,. \tag{9}$$

By solving the eigenvalue problem in Eqs. (7) we obtain the transformation matrices $\mathbf{T}_{E,H}$ and eigenvectors $\boldsymbol{\Gamma}$ for each layer of the structure. In order to obtain the relation between fields at the layer boundaries at the planes $y = y_0$ and $y = y_0 + d$ we introduce a reflection coefficient $\mathbf{r}$ as

the ratio between the backward and forward propagating waves [9]

$$\overline{\mathbf{F}}^{b}(\overline{y}) = \mathbf{r}(\overline{y})\,\overline{\mathbf{F}}^{f}. \tag{10}$$

Inside the layer, the fields and reflection coefficient vary in accordance with

$$\begin{aligned} \overline{\mathbf{F}}^{f}(\overline{y}_0 + \overline{d}) &= \exp(-\boldsymbol{\Gamma}\overline{d})\,\overline{\mathbf{F}}^{f}(\overline{y}_o), \\ \overline{\mathbf{F}}^{b}(\overline{y}_0) &= \exp(-\boldsymbol{\Gamma}\overline{d})\,\overline{\mathbf{F}}^{b}(\overline{y}_0 + \overline{d}), \end{aligned} \tag{11}$$

$$\mathbf{r}(\overline{y}) = \exp(-\boldsymbol{\Gamma}\overline{d})\,\mathbf{r}(\overline{y}_0 + \overline{d})\exp(-\boldsymbol{\Gamma}\overline{d}). \tag{12}$$

where $\overline{d} = k_0 d$, d is the layer thickness.

The transformation of the reflection coefficient at the boundary between two layers II and I, where field components match in original domain (Fig. 2) can be done by using

$$\mathbf{p}_{\mathrm{II}} = (\mathbf{e}_{\mathrm{II}} - \mathbf{h}_{\mathrm{II}})(\mathbf{e}_{\mathrm{II}} + \mathbf{h}_{\mathrm{II}})^{-1} \tag{13}$$

with

$$\begin{aligned} \mathbf{e}_{\mathrm{II}} &= \left(\mathbf{T}_E^{\mathrm{I}}\right)^{-1}\mathbf{T}_E^{\mathrm{II}}(\mathbf{I} + \mathbf{p}_{\mathrm{II}}), \\ \mathbf{h}_{\mathrm{II}} &= \left(\mathbf{T}_H^{\mathrm{I}}\right)^{-1}\mathbf{T}_H^{\mathrm{II}}(\mathbf{I} - \mathbf{p}_{\mathrm{II}}), \end{aligned} \tag{14}$$

where $\mathbf{I}$ stands for the identity matrix.

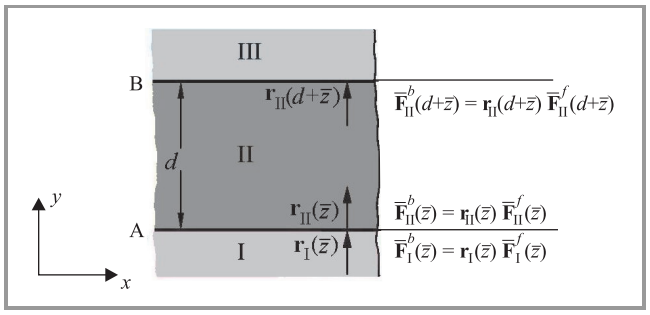

Fig. 2. Transformation of the reflection coefficient between two homogeneous layers.

Using this algorithm we successively transform the reflection coefficient from the top and bottom layers of the structure (where we have $\mathbf{r} = 0$) to a matching plane, which we place in the middle of the central layer (Fig. 3). Taking into account the direction of modes and assuming the symmetry of the structure with respect to the matching plane ($\mathbf{r}_l = \mathbf{r}_u = \mathbf{r}$), we obtain a system of equations:

$$\left[\mathbf{I} - \mathbf{r}^2(\varepsilon_{re})\right]\overline{\mathbf{F}}^{f} = \mathbf{0}, \tag{15}$$

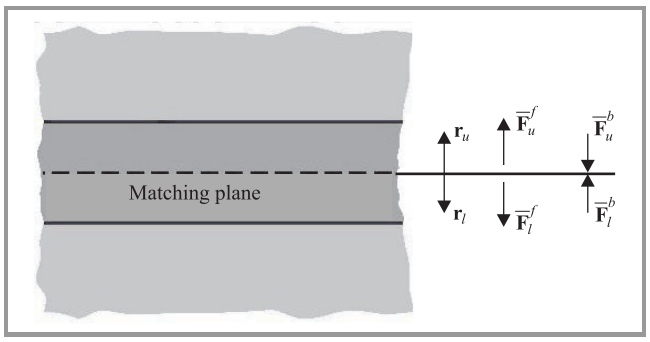

Fig. 3. Transformation of the reflection coefficient from the top and bottom to a matching plane.

from which the determinant equation

$$\det\left[\mathbf{I} - \mathbf{r}^2(\varepsilon_{re})\right] = \det\left[\mathbf{I} - \mathbf{r}(\varepsilon_{re})\right]\cdot\det\left[\mathbf{I} + \mathbf{r}(\varepsilon_{re})\right] = \mathbf{0} \tag{16}$$

can be derived. The solution of the determinant equation gives us the propagation constant ε_{re}, which is complex because of the radiation. The real part of the $\sqrt{\varepsilon_{re}}$ is the effective refractive index n_{eff}, while the imaginary one stands for the radiation loss coefficient $\alpha = 0.0868 \cdot \mathrm{Im}\left(\sqrt{\varepsilon_{re}}\right)$ dB/cm.

After determining ε_{re}, we can compute the modes in the matching plane, and consequently the field distribution in the whole structure.

The expression (16) is a quadratic equation and has two solutions. One of the solutions follows from the first factor $\det\left[\mathbf{I} - \mathbf{r}(\varepsilon_{re})\right]$ of the equation and corresponds to the x-polarized mode. Another root obtained from the second factor $\det\left[\mathbf{I} + \mathbf{r}(\varepsilon_{re})\right]$ describes the mode polarized in orthogonal y direction.

3. Results and discussion

3.1. Birefringence and supermode dispersion in straight MCMFs

We have applied the algorithm described above to calculate mode field distribution, propagation constants and radiation loss coefficients for dual-core MFs. The results are plotted in Figs. 4–7.

Figure 4 shows the electric field transverse component distribution of the orthogonally polarized odd and even modes in MF with two guiding cores separated by three air holes. The air hole diameter d of the MF equals to 0.64 μm in that case; the ratio of hole diameter to hole separation d/Λ is 0.2 and the wavelength of propagating radiation is 1.5 μm. The first ten and last five contour lines in the figure are spaced by 0.01 of the field maximum value, while others are spaced by 0.025. As one can see from the figure, the field distributions of modes of both polarizations look quite similar in high intensity region and slightly differ for low intensities nearby the fibre boundaries. This is because the MF structure is anisotropic in the cross-section. The same "slight but significant difference" in the field profiles of x- and y-polarized modes has been reported in [12]. The field distributions for odd and even supermodes are also similar for high intensity region, but even modes have additional low intensity components between cores.

Figures 5 and 6 show, respectively, the effective indices and the difference between effective indices of even and odd modes of dual-core MF and the orthogonal polarization states of these modes as a function of the ratio d/Λ

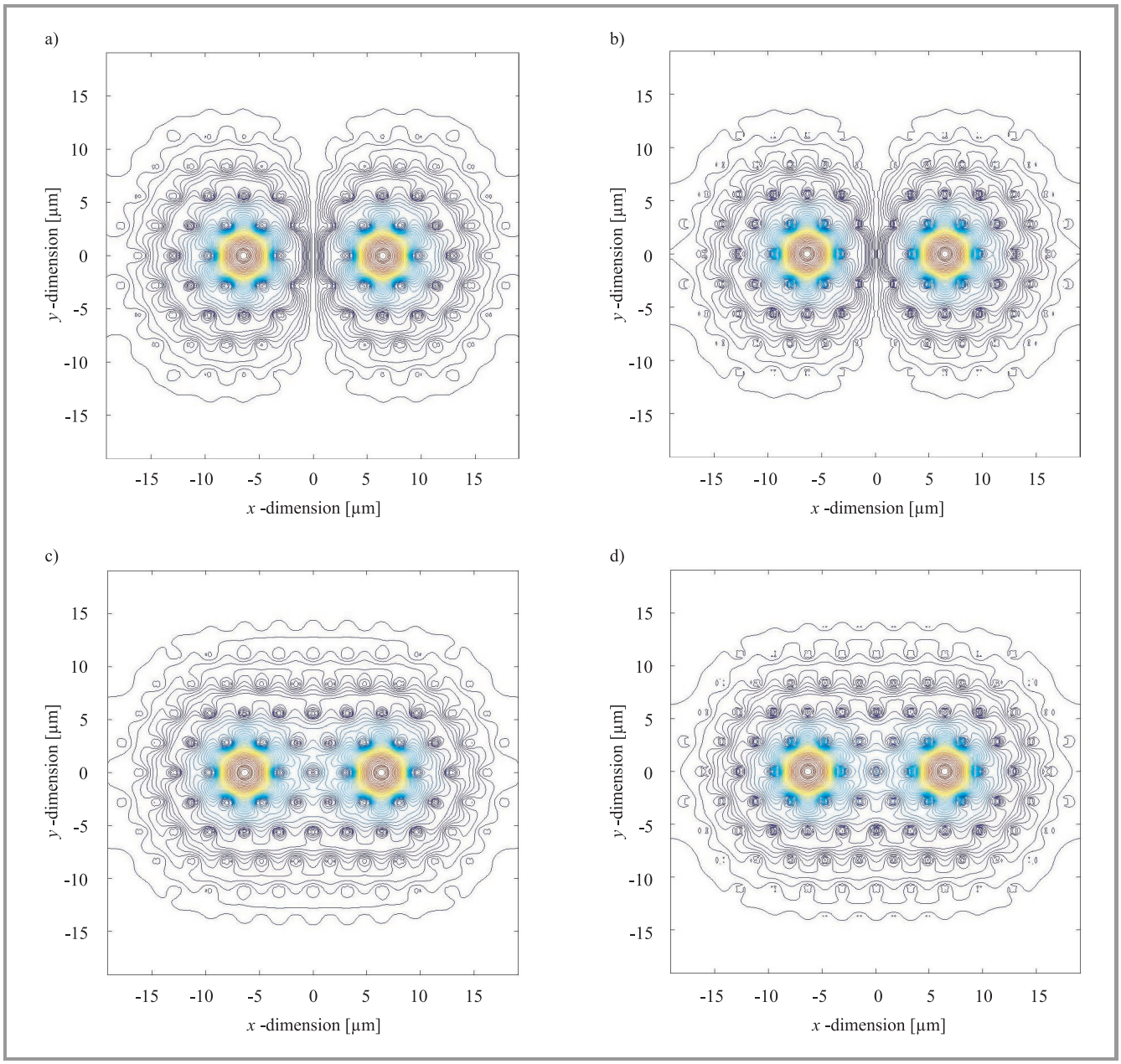

Fig. 4. Transverse electric field distribution of the orthogonally polarized modes: (a)$|E_x(x, y)|$ for x-polarized odd mode; (b) $|E_y(x, y)|$ for y-polarized odd mode; (c) $|E_x(x, y)|$ for x-polarized even mode; (d) $|E_y(x, y)|$ for y-polarized even mode.

for MF with 3 holes between cores and radiation wavelength $\lambda = 1.5$ μm (a), function of the number of holes between guiding cores (core separation) for $d/\Lambda = 0.2$ and $\lambda = 1.5$ μm (b), and function of normalized wavelength λ/Λ for $d/\Lambda = 0.2$ and 3 holes between cores (c). Plots for the effective indices of different MCMF supermodes on Fig. 5c coincide within printing resolution.

Figure 7 shows similar dependences for the radiation loss of the two modes in both polarization states. In Fig. 6, curves *1–4* present, respectively, the birefringence of the odd $n^x_{ef\,od} - n^y_{ef\,od}$ (curve *1*) and even $n^x_{ef\ ev} - n^y_{ef\,ev}$ (curve *2*) modes and supermode dispersion for x-polarized $n^x_{ef\,ev} - n^x_{ef\,od}$ (curve *3*) and y-polarized $n^y_{ef\,ev} - n^y_{ef\,od}$ (curve *4*) modes. In Figs. 5 and 7, the effective indices and radiation loss coefficient α are plotted: solid lines correspond to x-polarized modes and dashed lines represent y-polarized modes. Curves *1* and *2* describe effective indices and loss of the odd and even supermodes, respectively. In these calculations we take into account the dependence of the material refractive index on wavelength, using the Sellmeier equation.

As one can see, the effective indices of the all supermodes decrease with enlarging fibre air-filling fraction or reducing the radiation wavelength. As the core separation increases the effective indices of the orthogonally polarized odd and even supermodes correspondingly decrease and increase, approaching effective indices of the x- and y-polarized modes of the single-core MF. The difference

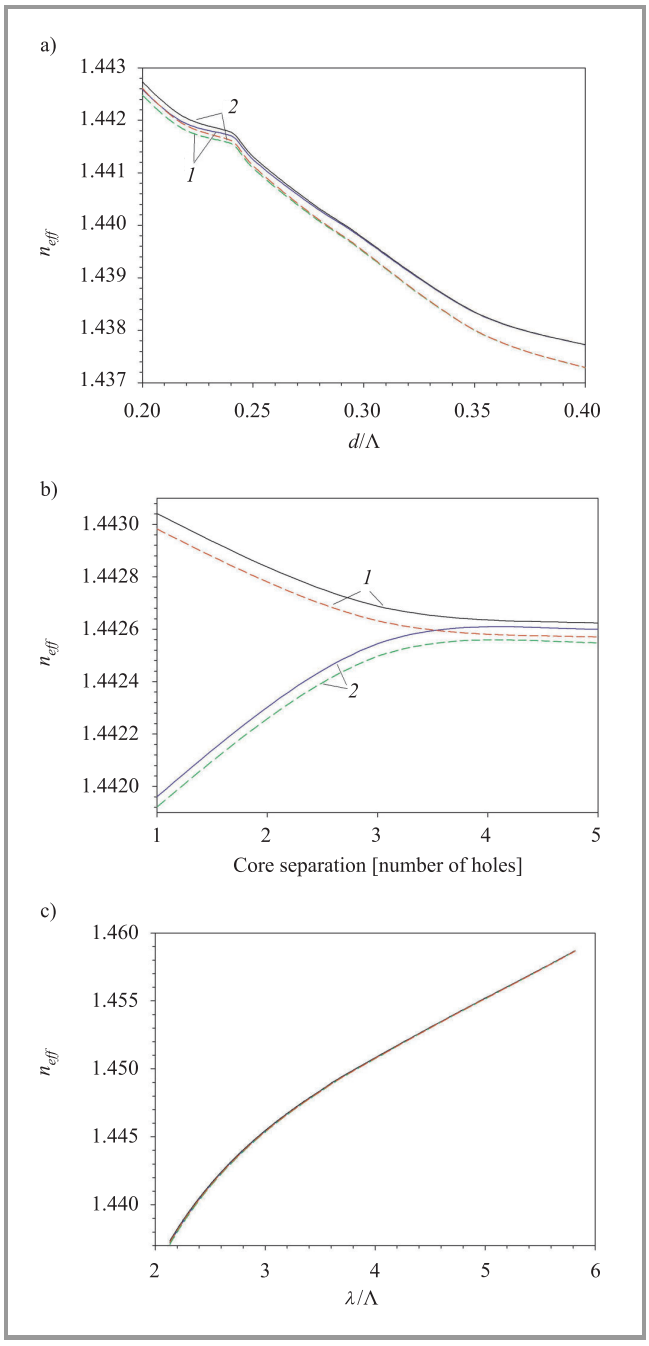

Fig. 5. Effective indices of the supermodes of dual-core MF as a function of (a) the ratio d/Λ; (b) core separation; (c) normalized wavelength λ/Λ. Solid and dashed lines correspond to the *x*- and the *y*-polarized modes. Curves *1* and *2* describe the effective indices of the odd and even supermode, respectively.

between effective indices of orthogonally polarized modes increases with enlarging the hole diameter or reducing hole separation. At the same time, the polarization birefringence has more flat dependence on the separation of fibre cores. With increasing core separation, birefringence of the odd and even supermodes decreases and increases correspondingly, converging to the birefringence value of the mode propagated in a single-core microstructured fibre with similar parameters (dashed line in Fig. 6b).

Similar small influence of microstructured fibre core separation on polarization beat length has been observed experimentally by the group of dr. J. Wojcik from the Lublin Maria Curie-Sklodowska University (UMCS) [13]. Increase of fibre air-filling fraction d/Λ or core separation leads to reduction the difference between effective indices of the odd and even modes of dual-core MF. For $d/\Lambda \geq 0.4$ (for $\lambda = 1.5$ μm) and/or separation of the cores in more than 5 holes, the effective indices of the both modes prac-

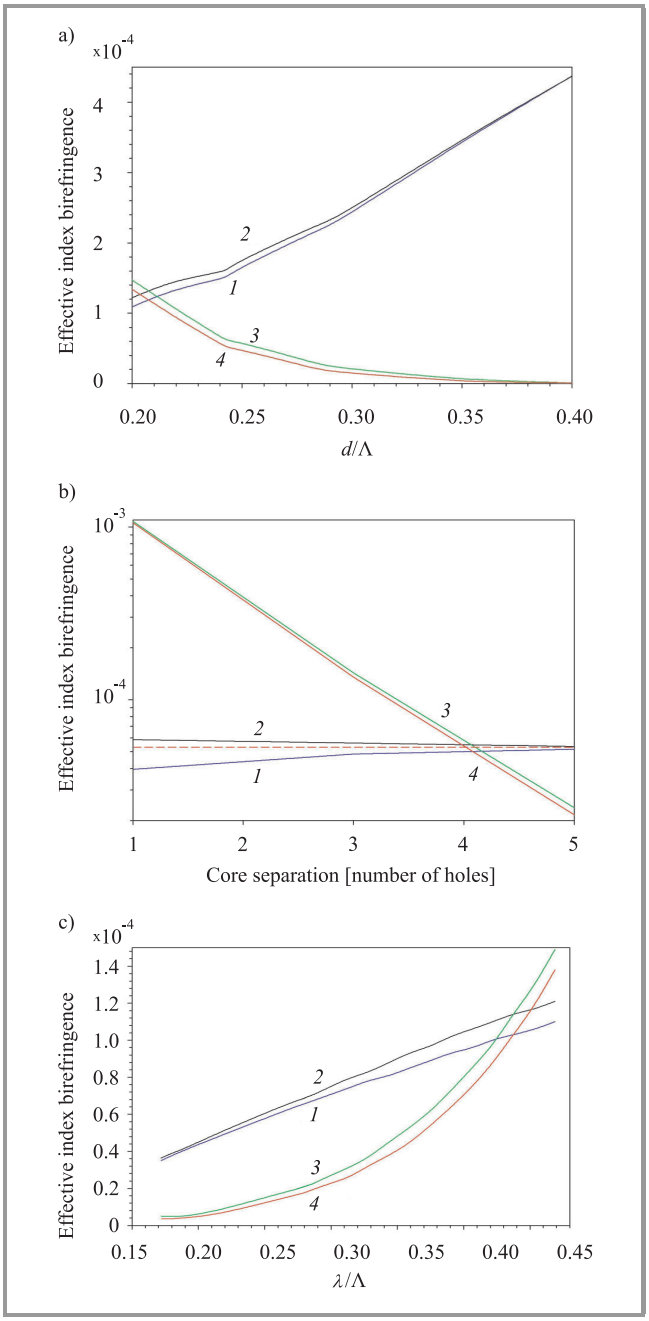

Fig. 6. Effective index birefringence and supermode dispersion of dual-core MF as a function of (a) the ratio d/Λ; (b) core separation; (c) normalized wavelength λ/Λ. The plot numbers indicate $n^x_{ef\,od} - n^y_{ef\,od}$ (*1*), $n^x_{ef\,ev} - n^y_{ef\,ev}$ (*2*), $n^x_{ef\,ev} - n^x_{ef\,od}$ (*3*), and $n^y_{ef\,ev} - n^y_{ef\,od}$ (*4*). Dashed line in (b) describes polarization birefringence of a single-core microstructured fibre.

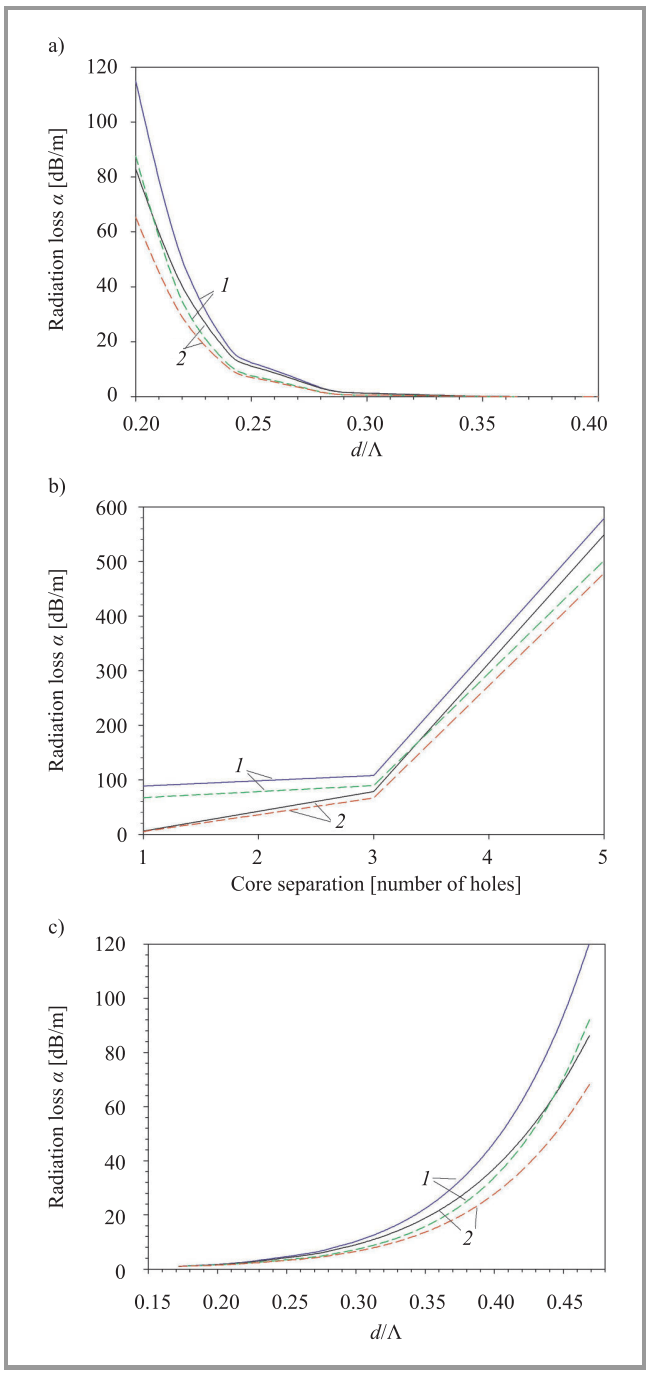

Fig. 7. Radiation loss coefficient of the modes of dual-core MF as a function of (a) the ratio d/Λ; (b) core separation; (c) normalized wavelength λ/Λ.

tically coincide. Thus, there is no coupling between cores and each core behaves as a separate fibre. Both supermode dispersion and polarization birefringence are reduced with decrease of radiation wavelength.

In such case, the difference between orthogonally polarized modes drops approximately linearly with decrease of wavelength, while the difference between even and odd modes has more sharp exponential wavelength dependence. In the short wavelength region ($\lambda/\Lambda \leq 0.18$ for $d/\Lambda = 0.2$) the difference between effective indices of even and odd modes is negligible and two cores are practically decoupled. Increasing the ratio d/Λ or decreasing core separation reduces the radiation loss in MCMFs. At that, the loss of *y*-polarized modes is lower, because the fields of these modes decay steeper to the fibre boundaries. Calculations of the influence of core separation have been done for fibres of identical size. Thus, the extension of distance between cores leads to reduction of distance from the cores to fibre outer boundaries (cladding thickness). As a result, the decay of mode field amplitudes on the fibre boundaries is insufficient; this explains the rise of calculated radiation loss for large core separation.

In calculation of MFs with some ratios d/Λ the *calculated* fibre dimension, which is an integer multiply of the discretization step, slightly differs from the *real* fibre dimension. This can explain the small kinks observed on the curves in Figs. 5a, 6a and 7a.

3.2. Curved dual-core MFs

Microstructured fibres being used, for instance, in communication lines can be subject to bending. Sensitivity to bends is also important issue for multicore MFs used as bend sensors and couplers. Therefore, the behavior of multicore MFs modes in bend region has to be investigated. For straight MF we used the Cartesian coordinate system whereas the cylindrical coordinate system where the angular coordinate φ corresponds to the bend is used for curved MF [6].

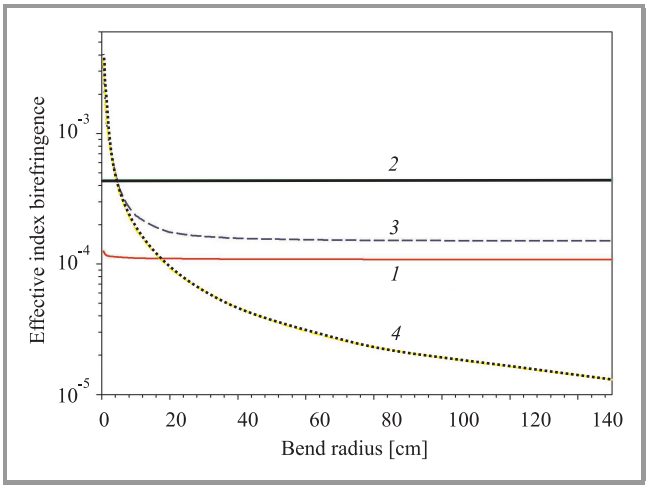

Fig. 8. Birefringence and supermode dispersion of the MF as a function of bend radius.

Figure 8 shows birefringence ($n^x_{ef\,od} - n^y_{ef\,od}$, solid lines *1* and *2*) and supermode dispersion ($n^x_{ef\,ev} - n^x_{ef\,od}$, dashed lines *3* and *4*) of the MF as a function of bend radius for different cores separation and air-filling fraction. Curves *1* and *3* correspond to MFs with $d/\Lambda = 0.2$ and curves *2* and *4* relate to $d/\Lambda = 0.4$. As one can see from plots *1* and *2*, the difference between effective indices of orthogonally polarized modes doesn't change with the bend. In opposite, the difference between effective indices of odd

and even supermodes increases with reducing bend radius. The supermode dispersion of the MCMFs with larger ratio d/Λ more sharply depends on the fibre bend.

Bending causes redistribution of optical power of two modes of dual-core MF between the cores and eliminates the first and second modes quasi-degeneracy. The power of the odd modes is concentrated mostly in the core on the inner side of the bend, and amplitude of the mode in outer core decreases [6]. The even mode field concentrates mostly in the outer core. The difference between mode amplitudes in left and right cores in dual-core MFs increases as the bend radius decreases (see Fig. 9). Thus, by comparing

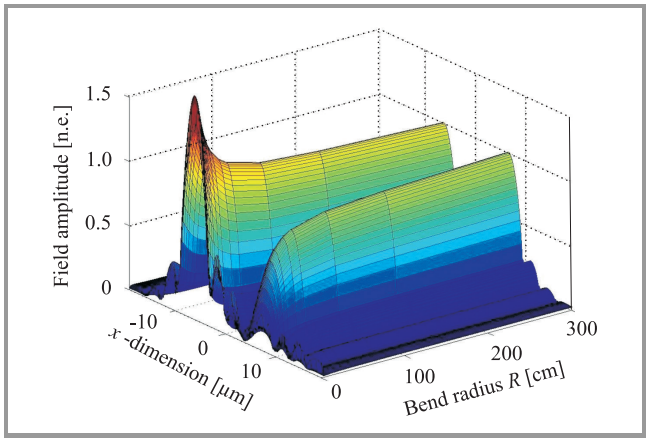

Fig. 9. Variation of the odd mode amplitude in both cores of the dual-core MF with the fibre bend radius.

the measured power in both cores of the MF it is possible to determine the value of fibre bend radius. Change of bend direction leads to opposite distribution of the mode fields. This feature allows using the dual-core MFs as vector bend sensors, i.e., sensors for determining both the bend value and direction.

4. Conclusions

We have calculated the field distribution, effective indices and radiation loss of two supermodes in both polarization states propagating in dual-core microstructured fibres with different parameters and analyzed the birefringence and supermode dispersion as a function of fibre parameters, wavelength and bend. This analyzis shows that the effective indices of the MCMF supermodes decrease with enlarging fibre air-filling fraction or reducing the radiation wavelength. As the core separation increases, the effective indices of the orthogonally polarized odd and even supermodes decrease and increase correspondingly and approach the values of effective indices of the x- and y-polarized modes of the single-core MF. The birefringence increases with enlarging the hole diameter, wavelength or reducing hole separation. The polarization birefringence exhibits more flat dependence on the separation of fibre cores. With increasing core separation the birefringence of the odd supermode slightly decreases and the one of the even mode increases; both tend to the birefringence of the mode of single-core fibre with similar parameters – from different sides. The supermode dispersion reduces with increasing fibre air-filling fraction, core separation or decreasing wavelength. For $d/\Lambda \geq 0.4$ (for $\lambda = 1.5$ μm) and/or separation of the cores in more than 5 holes the effective indices of the both supermodes practically coincide and each core behaves as a separate fibre. The same core decoupling is achieved for propagating radiation with short wavelength.

Fibre bending causes redistribution of optical power of two supermodes of dual-core MF between the cores. The power of the odd mode is concentrated mostly in the core, which is on inner side of the bend, and amplitude of the mode in the outer core decreases. The even mode concentrates mostly in outer core. The difference between mode amplitudes in both cores in dual-core MFs increases with reduction of the bend radius. At that, bending doesn't change the polarization birefringence. In opposite, the supermode dispersion increases as the bend radius reduces.

Acknowledgements

Igor A. Goncharenko thanks the Belarussian Fund of Fundamental Research for the financial support of this work. The authors thank the European Project COST Action P11 "Physics of linear, nonlinear and active photonic crystals" for stimulating interactions.

References

[1] J. C. Knight, J. Broeng, T. A. Birks, and P. St. J. Russell, "Photonic bandgap guidance in optical fibers", *Science*, vol. 282, pp. 1476–1478, 1998.

[2] T. M. Monro, D. J. Richardson, N. G. R. Broderick, and P. J. Bennet, "Holey optical fibers: an efficient modal model", *J. Lightw. Technol.*, vol. 17, pp. 1093–1102, 1999.

[3] P. J. Roberts and T. J. Shepherd, "The guidance properties of multicore photonic crystal fibres", *J. Opt. A.: Pure Appl. Opt.*, vol. 3, pp. S133–S140, 2001.

[4] L. Zhang and C. Yang, "A novel polarization splitter based on the photonic crystal fiber with nonidentical dual cores", *IEEE Photon. Technol. Lett.*, vol. 16, pp.1670–1672, 2004.

[5] A. Mafi and J. V. Moloney, "Shaping modes in multicore photonic crystal fibers", *IEEE Photon. Technol. Lett.*, vol. 17, pp. 348–350, 2005.

[6] I. A. Goncharenko, "Propagation constants and radiation loss of the modes in curved multi-core microstructure fibres", in *Proc. ICTON 2004*, Wrocław, Poland, 2004, vol. 2, pp. 107–110.

[7] A. W. Snyder and J. D. Love, *Optical Waveguide Theory*. London-N.Y.: Chapman and Hall, 1983.

[8] R. Pregla, "The method of lines as generalized transmission line technique for the analysis of multilayered structures", *Int. J. Electron. Commun. (AEÜ)*, vol. 50, pp. 293–300, 1996.

[9] S. F. Helfert and R. Pregla, "The method of lines: a versatile tool for the analysis of waveguide structures", *Electromagnetics*, vol. 22, pp. 615–637, 2002.

[10] I. A. Goncharenko, S. F. Helfert, and R. Pregla, "Radiation loss and mode field distribution in curved holey fibers", *Int. J. Electron. Commun. (AEÜ)*, vol. 59, pp. 185–191, 2005.

[11] R. Pregla, "MoL-BPM method of lines based beam propagation method", in *Methods for Modelling and Simulation of Guided-Wave Optoelectronic Devices*, Ed. W. P. Huang. Cambridge: EMW Publishing, 1995, pp. 65–70.

[12] F. Fogli, L. Saccomandi, P. Bassi, G. Bellanca, and S. Trillo, "Full vectorial BPM modeling of index-guiding photonic crystal fibers and couplers", *Opt. Expr.*, vol. 10, pp. 54–59, 2002.

[13] Private communication by dr. Jan Wojcik.

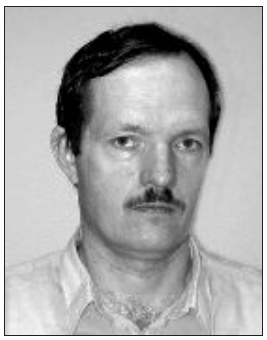

Igor A. Goncharenko graduated from the Physics Department of the Belarussian State University in 1981. He received the Ph.D. degree in physics and mathematics from the USSR Academy of Sciences (Moscow) in 1985 and Dr.Sci. degree from the National Academy of Sciences of Belarus (Minsk) in 2001. From 1985 until August 2007 he worked in Institute of Electronics of the National Academy of Sciences of Belarus. Last time he took up the positions of Chief Research Fellow at the Institute. In 1994 he was awarded a Royal Society Fellowship and worked with the Optoelectronics Research Centre, University of Southampton, UK. In 1996 he was awarded the Alexander von Humboldt Research Fellowship and carried out research at the FernUniversitaet in Hagen, Germany. In 2007 he carried out the analysis of waveguiding conditions in liquid crystal and investigated photonics switches on the base of LC waveguides in Hong Kong University of Science and Technology. Since September 2007 Dr. Goncharenko takes up the position of Professor of the Department of Natural Sciences in the Institute for Command Engineers of the Ministry of Emergencies of the Republic of Belarus. Also he has a part time Professor position in Belarussian National Technical University, department of laser technique and technology, where he gives special courses of lectures "Wave optics" and "Physical optics". At the same time he gives special course of lectures "Fibre optics" for students of Physics Department of Belarussian State University. His present scientific interests include the theory of optical fibres, microstructure (photonic crystal) fibres, active and passive fibre devices, tuneable fibre and waveguide lasers and amplifiers, multilayer waveguide structures, pulse propagation and nonlinear effects in optical fibres, optical information processing, optics logic elements and so on. He has contributed to a number of national and international conferences and published more than 180 papers in scientific journals including 38 patents. Doctor Goncharenko is a member of the IEEE. He participates in Program Committees of the *WSEAS International Conference on Global Optical & Wireless Network*, *SPIE Europe International Congress on Optics & Optoelectronics*, *Conference on Photonic Crystal & Fibers* and *International Conference for Young Scientists on Optics*. He serves as a reviewer for several international scientific journals. His biography has been cited in Marquis *Who's Who in Science and Engineering*, *Who's Who in America* and in the International Biographical Centre, Cambridge *2000 Outstanding Scientists of the 21st Century, Living Science Award* and *21st Century Awards for Achievement*.

e-mail: Igor02@tut.by
Institute for Command Engineers
of the Ministry of Emergencies of the Republic of Belarus
Department of Natural Sciences
25 Mashinostroiteley Str.
220118 Minsk, Belarus

Marian Marciniak Associate Professor has been graduated in solid state physics from Marie-Curie Sklodovska University in Lublin, Poland, in 1977. From 1985 to 1989 he performed Ph.D. studies in electromagnetic wave theory at the Institute of Fundamental Technological Research, Polish Academy of Sciences, followed linebreak by Ph.D. degree (with distinction) in optoelectronics received from Military University of Technology in Warsaw. In 1997 he received his Doctor of Sciences (habilitation) degree in physics/optics from Warsaw University of Technology. From 1978 to 1997 he held an academic position in the Military Academy of Telecommunications in Zegrze, Poland. In 1996 he joined the National Institute of Telecommunications in Warsaw, where he actually leads the Department of Transmission and Fibre Technology. Previous activities have included extended studies of optical waveguiding linear and nonlinear phenomena with analytic and numerical methods including beam-propagation methods. Actual research interests include photonic crystal technology and phenomena, optical packet-switched networks, and the future global optical and wireless network. Recently he has introduced and developed a concept of a hybrid real-time service end photonic packet network. He is an author or co-author of over 200 technical publications, including a number of conference invited presentations and 14 books authored, co-authored and/or edited by himself. He is a Senior Member of the IEEE – Lasers & Electro-Optics, Communications, and Computer Societies, a member of The New York Academy of Sciences, The Optical Society of America, SPIE – The International Society for Optical Engineering and its Technical Group on Optical Networks, and of the American Association for the Advancement of Science. In early 2001 he originated the IEEE/LEOS Poland Chapter and he has served as the Chairman of that Chapter until July 2003. He is widely involved in the European research for optical telecommunication networks, systems and devices. He was the originator of accession of Poland to European Research Programs in the optical telecommunications domain, in

chronological order: COST 240 *Modelling and Measuring of Advanced Photonic Telecommunication Components*, COST P2 *Applications of Nonlinear Optical Phenomena*, COST 266 *Advanced Infrastructure for Photonic Networks*, COST 268 *Wavelength-Scale Photonic Components for Telecommunications*, COST 270 *Reliability of Optical Components and Devices in Communications Systems and Networks*, COST 273 *Towards Mobile Broadband Multimedia Networks*, and very recently two new starting actions COST 288 *Nanoscale and Ultrafast Photonics* and COST P11 *Physics of Linear, Nonlinear and Active Photonic Crystals*. In all but two those projects he acted as one of the originators at the European level. He has been appointed to Management Committees of all those Projects as the Delegate of Poland. In addition, he has been appointed as the Evaluator of the European Union's 5th Framework Program proposals in the Action Line *All-Optical and Terabit Networks* and 6th FP *Research Networking Test-beds*. He is a Delegate to the International Telecommunication Union, Study Group 15: *Optical and Other Transport Networks*, and to the International Electrotechnical Commission, Technical Committee 86 *Fibre Optics* and its two sub-Committees. He served as a member of Polish Delegation to the World Telecommunication Standards Assembly WTSA 2000. From 2002 he participates in the work of the URSI – *International Union of Radio Science, Commission D – Electronics and Photonics*. In 2000 he originated and actually serves as the Chairman of the Technical Committee 282 on *Fibre Optics* of the National Committee for Standardisation. Since May 2003 he serves as the Vice-President of the Delegation of Poland to the Intergovernmental Ukrainian-Polish Working Group for Cooperation in Telecommunications. He is the originator and the main organiser of the *International Conference on Transparent Optical Networks* ICTON starting in 1999, and a co-located events the *European Symposium on Photonic Crystals* ESPC and *Workshop on All-Optical Routing* WAOR since 2002 and *Global Optical and Wireless GOWN Seminar* since 2004. He is the Technical Program Committee Co-Chair of the *International Conference on Advanced Optoelectronics and Lasers* CAOL, and he participates in Program Committees of the *Conference on the Optical Internet & Australian Conference on Optical Fibre Technology* COIN/ACOFT, the *International Conference on Mathematical Methods i*n Electromagnetic *Theory* MMET, the *International Workshop on Laser and Fiber-Optical Network Modeling* LFNM, and the *International School for Young Scientists and Students on Optics, Laser Physics and Biophysics/Workshop on Laser Physics and Photonics*. He serves as a reviewer for several international scientific journals, and he is a Member of the Editorial Board of *Microwave & Optoelectronics Technology Letters* journal, Wiley, USA, and the *Journal of Telecommunications and Information Technology*, National Institute of Telecommunications, Poland. Languages spoken: Polish (native), English, French, and Russian. His biography has been cited in Marquis *Who's Who in the World, Who's Who in Science and Engineering*, and in the *International Directory of Distinguished Leadership of the American Biographical Institute*.

e-mail: M.Marciniak@itl.waw.pl
e-mail: marian.marciniak@ieee.org
Department of Transmission and Fibre Technology
National Institute of Telecommunications
Szachowa st 1
04-894 Warsaw, Poland

Paper

Impact of the duration of speech sequences on speech quality

Peter Počta and Martin Vaculík

Abstract—This paper describes simulations of speech sequences transmission for intrusive measurement of voice transmission quality of service (VTQoS) in the environment of IP networks. The aim of the simulations was to investigate the impact of the different durations of speech sequences on speech quality from the jitter rate and packet loss point of view in IP networks. The ITU-T G.729 and ITU-T G.723.1 encoding schemes were used for the purpose of the simulations. The assessment of speech quality was realized by means of perceptual evaluation of speech quality (PESQ) algorithm. A comparison of the impact of different durations of speech sequences on speech quality and determination of the optimal duration of speech sequence for measurements of speech quality in telecommunication networks, is the aim of this paper.

Keywords— voice transmission quality of service, speech sequence, intrusive measurement, perceptual evaluation of speech quality, jitter rate, packet loss.

1. Introduction

Voice transmission quality of service (VTQoS) is one of the important parts of quality of service (QoS). It is very important for providers as well as for users. When communication networks incorporate more and more transmission technologies, an increase in complication and the complexity of networks is seen. Measurement of the voice transmission quality becomes only platform that is available for simultaneous comparison of different transmission technologies and that is the most relevant to the view of the users. Of course, it is possible to measure and evaluate the transmission parameters of the networks, but only the evaluation of end-to-end quality provides optimal results because of the complexity of network technologies. Thus, it is the evaluation by similar way as users do. Since voice service is the most wide-spread service, in which a user uses filter and predicative abilities of human brain, it is crucial to optimally evaluate a quality of such service.

Evaluation of a quality of the voice service may be performed using intrusive or non-intrusive methods, objectively or subjectively. Using non-intrusive method, we only monitor existing dialogue. The drawback of this method is that the evaluation algorithm cannot utilize an original sample of the primary signal. Thus, it is very difficult to detect some types of signal distortion that occure during transmission. In the intrusive methods, only a test voice sample is transmitted. These methods have been known since the beginning of the telecommunication technologies, when the special sequences of vowels (known as logathoms) were transmitted after the connection had been built-up. A receiver had to recognize these logathoms. This way of subjective evaluation has been used till nowadays (e.g., absolute category rating method).

Today's technical and software facilities provide an objectification of this measurement method by transmitting the voice sample defined beforehand, its receiving on the destination side, and a comparison of the transmission sample and the original sample using the suitable algorithm that imitates the way of perception and evaluation of the quality transmission opinion by an average listener. It is for example perceptual speech quality measurement (PSQM) algorithm defined in ITU-T Rec. P.861 [6] or perceptual evaluation of speech quality (PESQ) algorithm defined in ITU-T Rec. P.862 [7]. The PSQM algorithm is based on comparison of the power spectrum of the corresponding sections of the original and the received signals. The results of this algorithm more correlate with the results of listening tests, in comparison with E-model [1]. At present, this algorithm is no longer used because of a raw time alignment. Instead of it the PESQ algorithm is used. The PESQ algorithm facilitates with very fine time alignment and one single interruption are also taken into account in the calculation of mean opinion score (MOS). It is possible to use PESQ in mobile networks as well as in networks based on packet transmission. The disadvantages include impossibility to use it for codec with data rate lower than 4 kbit/s and higher calculation load what is caused by recursions in the algorithm.

The ITU-T Rec. P.862.3 [10] recommends to use the speech sequence in duration in the range from 8 s till 30 s for the purpose of speech quality measurement. Here we focus on the impact of different durations of speech sequences on speech quality from the point of view of jitter rate and packet loss in IP network. We want to compare two durations of speech sequences from the range that is recommend for purpose of speech quality measurements in the ITU-T Rec. P.862.3 [10]. The speech sequences in duration of 10 and 30 s are compared in this paper. The rest of paper is organized as follows: Section 2 describes simulation design. Section 3 presents the simulation results. Section 4 concludes the paper and suggests some future studies.

2. Simulation design

2.1. Experimental design

The transmission simulations were carried out on Gaoresearch's (freeware) online simulator [11]. The simulation model of transmission chain with codec ITU-T G.723.1 [2]

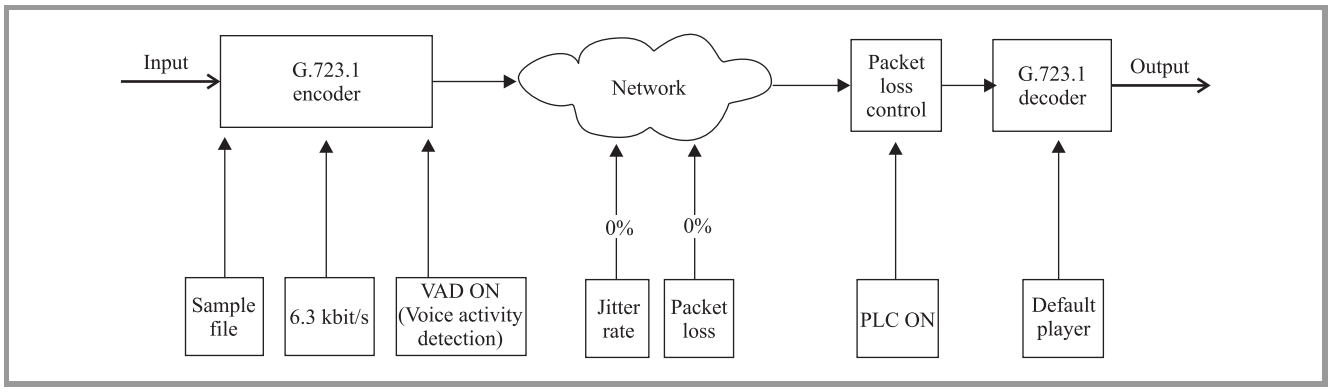

Fig. 1. The simulation model of transmission chain with codec ITU-T G.723.1.

is depicted in Fig. 1. The simulation model enables to change jitter rate and packet loss parameters in the range from 0% to 10%. The simulation model renders voice activity detection (VAD) and packet loss control (PLC) functions.

The speech sequences described in Subsection 2.2 were used for the simulations. The simulations were performed for different setting of packet loss and jitter rate parameters and by using these 2 encoding schemes:

- ITU-T G.723.1 (6.3 kbit/s) [2],
- ITU-T G.729 [3].

The simulations of jitter influence were done for the values of jitter rate in the range from 0% to 10%. Jitter rate is defined as percentual number of the packets, whose jitter value is above maximum tolerated jitter for given connection. Jitter is a measure of variation in latency over time. Jitter is caused by random variation of the momentary traffic load. This simulator tolerates the jitter below 90 ms. The packets delivered after this time are further not processed, they are also dropped out. The packets loss influence was investigated for the values of packet loss in the range from 0% to 10%. The packet loss parameter is defined as the percentual number of the packets that were lost during the transmission. Packets may lost, due to high bit error rate of the transmission channel and high traffic load. The VAD and PLC functions were activated for all the performed simulations. Finally, MOS was measured by PESQ algorithm.

2.2. Description of speech sequences

The speech sequences selection should follow the criteria given by ITU-T Rec. P.830 [5] and ITU-T Rec. P.800 [4]. The speech sequence should include bursts separated by silence periods, and are normally 1–3 s in duration. Also it should be active for 40–80% of the length. The speech sequences are composed from speech records. In our experiments, these speech records come from a Slovak database. In each set, two female and two male speech utterances were used. The speech sequences was stored in 16-bit, 8000 Hz linear PCM, and were 10 s in duration with 61.5% of active speech interval and 30 s in duration with 57% of active speech interval.

2.3. Assessment of speech quality

The MOS was measured by PESQ [7] metric, the most recent ITU-T standard for objective speech quality assessment. The PESQ combines merits of PAMS and PSQM99 (an updated version PSQM), and adds new methods for transfer function equalization and averaging distortions over time. It can be used in wider range of network conditions, and gives higher correlation with subjective tests and the other objective algorithms [7, 12]. In contrast to the conversational model; PESQ is a listening-only model, the degraded sample is time-aligned with the reference sample during pre-processing. The PESQMOS values do not reflect the effects of delay on speech quality.

3. Simulation results

The simulation was independently performed 3 times under the same testing conditions. The MOS results were averaged out and the standard deviation was kept within 0.0894 MOS for speech sequences in duration of 10 s and 0.0664 MOS for speech sequences in duration of 30 s. The values of standard deviation for both durations and types of speech sequences, and for both encoding schemes are summarized in Table 1.

Table 1
Standard deviation values

Encoding scheme	10 s		30 s	
	M	F	M	F
G.729 (jitter)	0.0792	0.0894	0.0553	0.0385
G.729 (packet loss)	0.0553	0.0701	0.0403	0.0448
G.723.1 (jitter)	0.0458	0.0727	0.0328	0.0664
G.723.1 (packet loss)	0.0339	0.0561	0.0288	0.0375

3.1. The simulation results of jitter influence on speech sequences transmission

The graphs (Figs. 2–5) represent the dependence of MOS values change on the percentual number of packets, whose

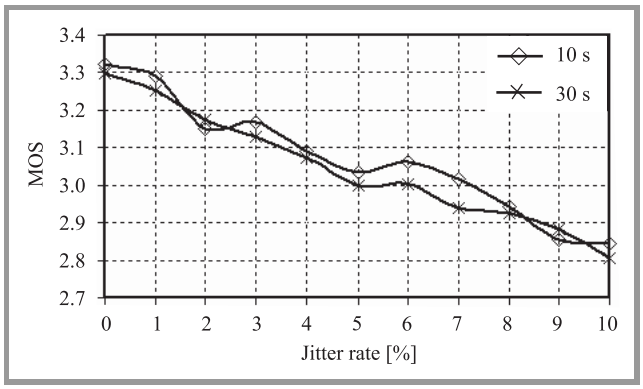

Fig. 2. Impact of jitter rate on speech quality of male speech sequences for ITU-T G.729.

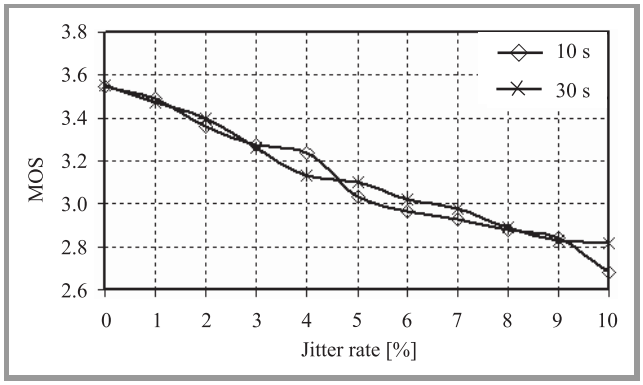

Fig. 3. Impact of jitter rate on speech quality of female speech sequences for ITU-T G.729.

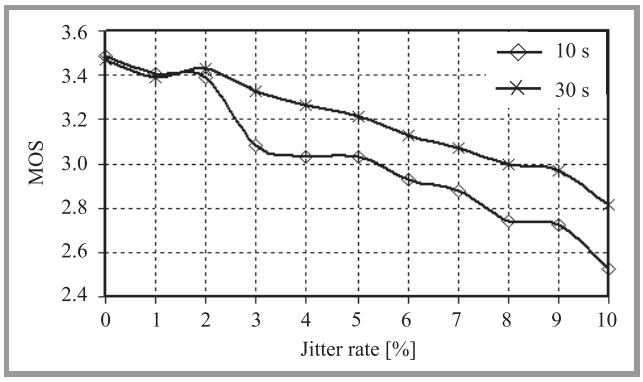

Fig. 4. Impact of jitter rate on speech quality of male speech sequences for ITU-T G.723.1 (6.3 kbit/s).

jitter overstepped the time of 90 ms. Every packet whose jitter overstepped the time of 90 ms is dropped. Non-uniform distribution of the dropped packets in both active speech and silence periods causes a smooth undulation

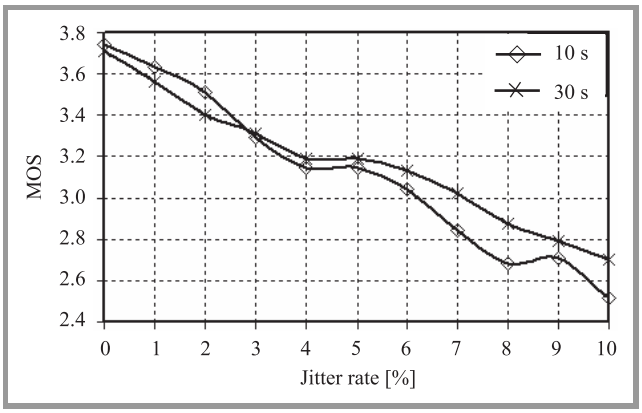

Fig. 5. Impact of jitter rate on speech quality of female speech sequences for ITU-T G.723.1 (6.3 kbit/s).

of the characteristics. In the case of zero jitter rate, MOS value change is cause only by encoding scheme. The graphs show only average values for female speech sequences and for male speech sequences, respectively.

3.2. The simulation results of packets loss influence on speech sequences transmission

The graphs (Figs. 6–9) represent the dependence of MOS values change on packets loss that means of percentual

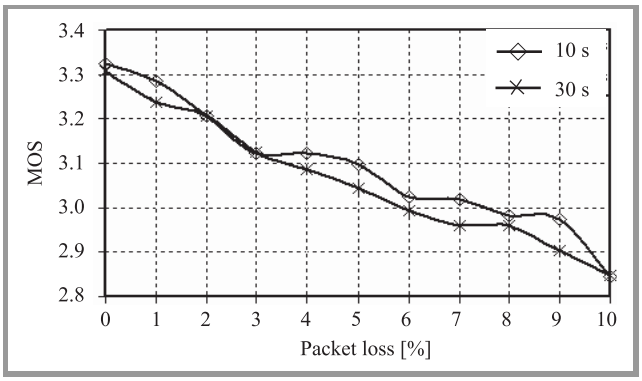

Fig. 6. Impact of packet loss on speech quality of male speech sequences for ITU-T G.729.

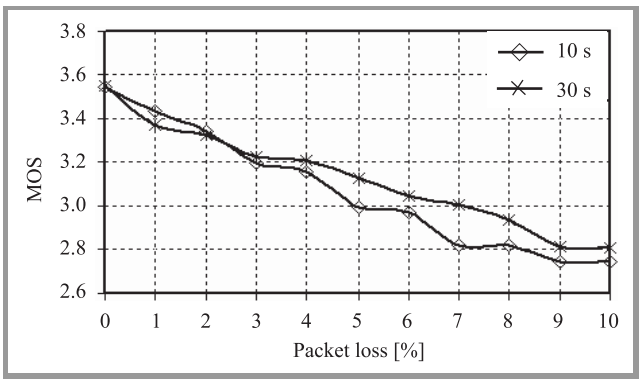

Fig. 7. Impact of packet loss on speech quality of female speech sequences for ITU-T G.729.

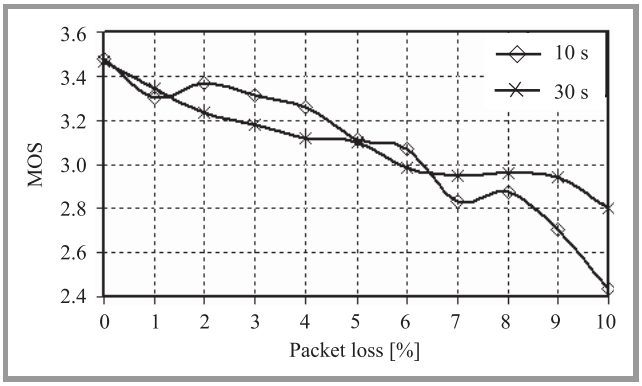

Fig. 8. Impact of packet loss on speech quality of male speech sequences for ITU-T G.723.1 (6.3 kbit/s).

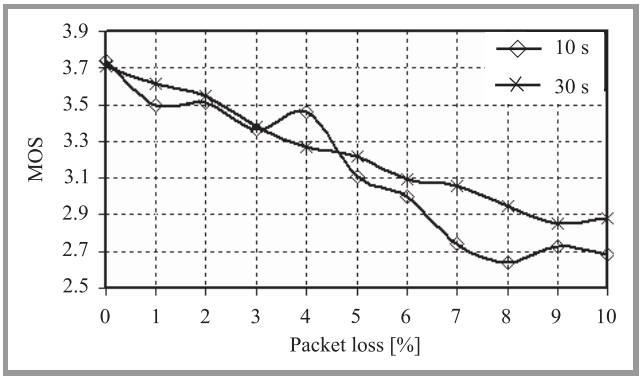

Fig. 9. Impact of packet loss on speech quality of female speech sequences for ITU-T G.723.1 (6.3 kbit/s).

number of the packets, which were not delivered. The smooth undulation of the characteristics is caused by non-uniform distribution of lost packets in both active speech and silence periods. In the case of zero packet loss, MOS value change is cause only by encoding scheme. The graphs show only average values for female speech sequences and for male speech sequences, respectively.

4. Conclusion

This paper has investigated the impact of the different durations of speech sequences for codecs ITU-T G.729 and ITU-T G.723.1 on speech quality from the jitter rate and packet loss point of view in IP networks. The results show that the difference in duration of speech sequences has the impact on speech quality. It is caused by more active speech and silence periods in sequences in duration of 30 s. A probability of impact of jitter rate and packet loss on speech quality is higher if more periods are available. It means that it is possible to capture more changes in speech quality in this case. The capture of more changes allows to realize the more precise measurements of speech quality in telecommunication networks. It was a first idea for the comparison of these two types of speech sequences from the duration point of view.

The speech sequences in duration of 30 s have the smoother characteristic than speech sequences in duration of 10 s. The values of the standard deviation (Table 1) are lesser for speech sequences in duration of 30 s than for speech sequences in 10 s duration. Therefore this type of speech sequences is better for speech quality measurements. The more precise results are obtained by means of longer speech sequences in 30 s duration.
In the future, this problem will be investigated in the converged network of the University of Žilina.

References

[1] "The E-model, a computational model for use in transmission planning", ITU-T Rec. G.107 (03/2005).

[2] "Dual rate speech coder for multimedia communications transmitting at 5.3 and 6.3 kbit/s", ITU-T Rec. G.723.1 (05/2006).

[3] "Coding of speech at 8 kbit/s using conjugate-structure algebraic-code-excited linear prediction (CS-ACELP)", ITU-T Rec. G.729 (03/1996).

[4] "Methods for subjective determination of transmission quality", ITU-T Rec. P.800 (08/1996).

[5] "Subjective performance assessment of telephone-band and wide-band digital codecs", ITU-T Rec. P. 830 (02/1996).

[6] "Objective quality measurement of telephone-band (300–3400 Hz) speech codecs", ITU-T Rec. P.861 (02/1998).

[7] "Perceptual evaluation of speech quality (PESQ): An objective method for end-to-end speech quality assessment of narrow-band telephone networks and peech codecs", ITU-T Rec. P.862 (02/2001).

[8] "Mapping function for transforming P.862 raw result scores to MOS-LQO", ITU-T Rec. P.862.1 (11/2003).

[9] "Wideband extension to Recommendation P.862 for the assessment of wideband telephone networks and speech codecs", ITU-T Rec. P.862.2 (11/2005).

[10] "Application guide for objective quality measurement based on Recommendations P.862, P.862.1 and P.862.2", ITU-T Rec. P.862.3 (11/2005).

[11] "Gaoresearch online simulator", http://www.gaoresearch.com/products/speechsoftware/speechsoftware.php

[12] A. W. Rix, J. G. Beerends, M. P. Hollier, and A. P. Hekstra, "Perceptual evaluation of speech quality (PESQ) a new method for speech quality assessment of telephone network and codecs", in *Proc. IEEE Int. Conf. Acoust., Speech Sig. Proces*., Salt Lake City, USA, 2001, pp. 749–752.

[13] L. Ding and R. A. Goubran, "Assessment of effects of packet loss on speech quality in VoIP", in *Proc. 2nd IEEE Int. Worksh. Hapt., Audio Visu. Env. Their Appl. 2003, HAVE 2003*, Ottawa, Canada, 2003, pp. 49–54.

[14] M. Varela, I. Marsh, and B. Gronvall, "A systematic study of PESQ's behavior", in *Proc. Conf. MESAQIN 2006*, Prague, Czech Republic, 2006.

[15] J. G. Beerends, E. Larsen, and N. Iyer, "Measurement of speech intelligibility based on the PESQ approach", in *Proc. Conf. MESAQIN 2004*, Prague, Czech Republic, 2004.

[16] J. Holub and A. Drozdová, "Proprietary low bit-rate radio-communication network – objective and subjective speech transmission quality assessment", in *Proc. Conf. MESAQIN 2006*, Prague, Czech Republic, 2006.

[17] W. A. Rix, "Comparison between subjective listening quality and P.862 PESQ score", in *Proc. Conf. MESAQIN 2003*, Prague, Czech Republic, 2003.

[18] J. Holub, R. Šmíd, and M. Bachtík, "Child listeners as the test subject – comparison with adults and P.862", in *Proc. Conf. MESAQIN 2003*, Prague, Czech Republic, 2003.

[19] S. Pennock, "Accuracy of the perceptual evaluation of speech quality (PESQ) algorithm", in *Proc. Conf. MESAQIN 2002*, Prague, Czech Republic, 2002.

Peter Počta was born in 1981, in Nové Zámky, Slovakia. He graduated from the University of Žilina, the Faculty of Electrical Engineering. He joined the Department of Telecommunications at the University of Žilina to obtain Ph.D. degree in telecommunications. His areas of interest include speech quality assessment, access networks, convergent networks, VoIP, VoWLAN, VoWiMAX.

e-mail: pocta@fel.uniza.sk
Faculty of Electrical Engineering
Department of Telecommunications
University of Žilina
Univerzitná st 1
010 26 Žilina, Slovakia

Martin Vaculík was born in 1951, in Žilina, Slovakia. He graduated from the University of Žilina as Dipl. Ing. in telecommunications in 1976. He received Ph.D. in 1987. The title of his thesis was "Some possibilities of dynamic routing control". He was with Siemens PSE Company, Optical Network Department in 2001–2002. Nowadays he works in the Department of Telecommunications at the University of Žilina as an Associate Professor. His areas of interest include switching, access networks and convergent networks. He is author of the book with the title "Access Networks" and co-author of 2 books: "ISDN" and "Broadband Networks".

e-mail: vaculik@fel.uniza.sk
Faculty of Electrical Engineering
Department of Telecommunications
University of Žilina
Univerzitná st 1
010 26 Žilina, Slovakia

Paper

Optimum receiver performance of TH-PPM ultra wideband system in multiple user interference

Mohammad Upal Mahfuz, Kazi M. Ahmed, and Nandana Rajatheva

Abstract—This paper demonstrates optimum receiver performance in terms of bit error rate (BER) for time hopping pulse position modulation (TH-PPM) ultra wideband (UWB) system in multiple user interference environment for indoor radio communication. Equal gain combining and selective gain combining have been demonstrated in terms of ideal RAKE (ARAKE), selective RAKE (SRAKE) and partial RAKE (PRAKE) receiver performances. The recently accepted IEEE 802.15.3a model of the UWB channel has been used to describe UWB propagation in indoor environment. Two channel scenarios named CM-1 and CM-3 for IEEE 802.15.3a channel model have been investigated principally. Finally, this paper concludes with an approximation of equivalence of number of fingers in SRAKE and PRAKE receivers as well as an indication of SNR gains achievable as the RAKE finger number is increased, especially with multiple user interference (MUI), for a 16.6 Mbit/s UWB system.

Keywords— optimum receiver performance, TH-PPM, ultra wideband, multiple user interference.

1. Introduction

Ultra wideband impulse radio (UWB-IR) is currently receiving a great deal of global attention because of its ability to provide higher data rate with low cost and relatively low power consumption. Impulse radio UWB communicates with baseband pulses of very short duration on the order of tenth of a nanosecond. According to the regulation of Federal Commission of Communications (FCC), a signal is defined as UWB signal if it has a –10 dB fractional bandwidth, F_{BW} greater than (or equal to) 0.20 or it occupies at least 500 MHz of the spectrum [1], the fractional bandwidth being expressed as

$$F_{BW} = 2\frac{f_H - f_L}{f_H + f_L} \geq 0.20\,, \tag{1}$$

where f_H and f_L correspond to the –10 dB upper and lower frequencies, respectively. The FCC has also regulated the spectral shape and maximum power spectral density (–41.3 dBm/MHz) of the UWB radiation in order to limit the interference with other communication systems like UMTS or WLAN [2]. The waveforms that are used for UWB radio are very short in duration, causing their energy to be spread across the frequency spectrum. With UWB signals the dense multipath can be resolved, allowing a RAKE receiver for signal demodulation. Multiple access in UWB communications is accomplished with traditional spread-spectrum techniques. Most of the research conducted so far is concerned with time hopping (TH) spread spectrum, associated with either binary pulse position modulation (TH-PPM) [3] or bipolar pulse amplitude modulation (TH-PAM) [4]. The performance of RAKE receivers operating with TH-PPM has been investigated in [5] in the absence of multiple user interference (MUI) and assuming perfect channel knowledge. The impact of MUI on the detection process is discussed in [3] with line-of-sight (LOS) propagation. Unfortunately, in the presence of MUI the question of optimum performance is so complex that physical intuition does not help and an analytical approach seems impossible [4]. Clearly, MUI plays a role both in channel estimation as well as in receiver performance.

In this paper we extend these results in various ways. We have compared the performances ideal, selective and partial RAKE receiver performances for TH-PPM UWB scheme in presence of low to moderate multiple user interference using two channel models named CM-1 and CM-2 as described recently by the IEEE 802.15.3a [6] standardization group for use in indoor UWB communications [7]. We have also shown how the system performance changes as the number of RAKE fingers varies. In particular, our research targets optimum receiver performance and comparison of the system performances between CM-1 and CM-3, which are 0–2 m LOS and 4–10 m NLOS channel conditions and are used very often in UWB system performance evaluation studies. Finally, since indoor radio communication is affected by a large number of multipaths, the equivalence between selective RAKE (SRAKE) and partial RAKE (PRAKE) finger numbers is another important aspect that this paper has addressed regarding TH-PPM UWB scheme. The paper is organized as follows: Section 2 provides with a brief description of the concept of multiuser interference. The discussion is followed by Section 3 describing the complete system model under investigation as well as detailed simulation environment. Section 4 briefly describes RAKE receiver principle regarding SRAKE and PRAKE operations, which is then followed by Section 5 discussing the results obtained with extensive simulation of the TH-PPM UWB system. Finally, Section 6 concludes the paper.

2. Concept of multiuser interference

Multiple user interference is modeled as signals coming from other UWB users having the same basic signal characteristics as those of the user of interest, but using different spreading codes. Assuming a total of N_u users, the received signal $r(t)$ can be written as

$$r(t) = s^{(1)}(t) \otimes h^{(1)}(t) + i(t) + n(t), \tag{2}$$

where $s^{(1)}(t)$ is the signal of interest at the output of the transmitting antenna, $h^{(1)}(t)$ represents the impulse response of the channel corresponding to the user of interest, $n(t)$ is the Gaussian noise and $i(t)$ is the interference coming from the other $(N_u - 1)$ users. Here the interference, $i(t)$ can be defined as

$$i(t) = \sum_{n=2}^{N_u} s^{(n)}(t - \tau_n) \otimes h^{(n)}(t), \tag{3}$$

where $h^{(n)}(t)$ for $n = 2, 3 \ldots, N_u$ are the impulse responses of the channels corresponding to the $(N_u - 1)$ interfering users and τ_n is the delay of the arrival time of the nth user from the user of interest, i.e., $s^{(1)}(t)$ for which $\tau_1 = 0$. Each user experiences the channel with a different channel realization so that the channel impulse response

$$h^{(n)}(t) \neq h^{(m)}(t),$$

where $n, m = 1, 2, \ldots N_u, n \neq m$.
Each MUI user has the same power as the user of interest. Interfering users are considered either synchronous or asynchronous with the user of interest. The "synchronous" condition refers to "frame synchronization" where the receiver is synchronized with all other users and can receive all users' data at the same time instant. On the other hand, in the asynchronous case, the interfering signals arrive at the receiver with resolution of a time sample. The asynchronism is performed between every interfering user and the user of interest, and also among the interfering users.

3. System model

In this paper, TH-PPM transmission has been used in the transmitter section. Time hopping is a widely used multiple access method for UWB radio communications. The most recent IEEE 802.15.3a UWB channel model has been chosen as the channel used for UWB propagation. Details of simulation parameters have been shown in Table 1.

3.1. The UWB pulse shape and modulation schemes

A typical energy normalized UWB TH-PPM signal can be modeled as follows:

$$s_{tr}^{(k)}\left(t^{(k)}\right) = \sum_{j=-\infty}^{\infty} w_{tr}\left(t^{(k)} - jT_f - c_j^{(k)}T_c - d_j^{(k)}\Delta\right), \tag{4}$$

where c_j is the distinct time hopping sequence, t is the transmitter clock time, w_{tr} is the transmitted monocycle

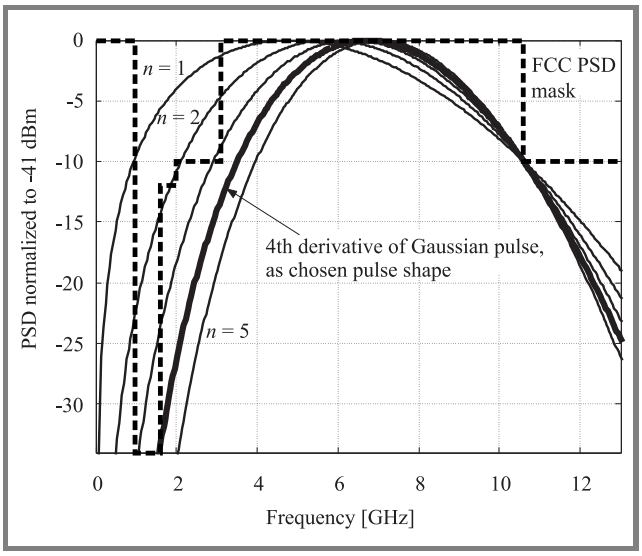

Fig. 1. PSD of 4th order derivative of Gaussian pulse fulfilling indoor UWB PSD requirement for indoor systems.

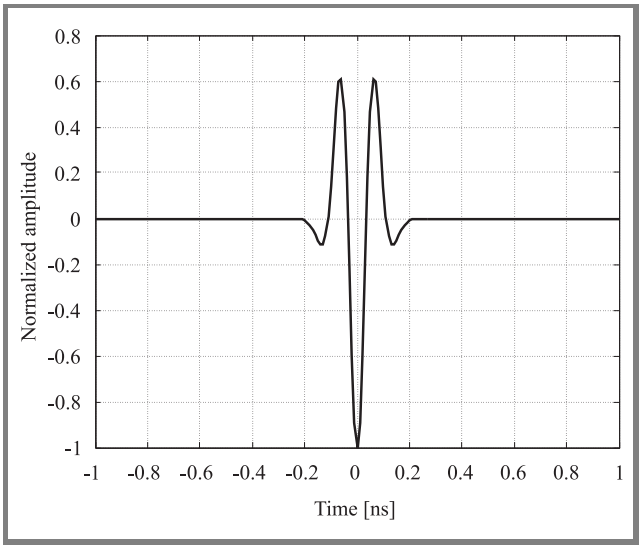

Fig. 2. Fourth order derivative of Gaussian pulse.

waveform, T_f is the pulse repetition time, T_c is the chip duration and d_j are the information symbols and Δ is the PPM pulse shift [3]. In this paper, a pulse position is shifted by 0.5 ns for a data bit 1 under PPM modulation scheme. The fourth derivative of Gaussian pulse that fits the FCC mask in a better manner can be chosen. Based on normalized power spectral density (PSD) of nth order Gaussian derivative pulse, applying bisection method as in [8], the fourth order derivative of Gaussian pulse with pulse shaping factor of 0.168 ns has been chosen in our simulations. The selection of appropriate pulse shape has been shown in Figs. 1 and 2.

3.2. IEEE 802.15.3a UWB channel model

In IEEE 802.15.3a UWB channel model (Fig. 3), a modified Saleh-Valenzuela (S-V) model has been proposed on

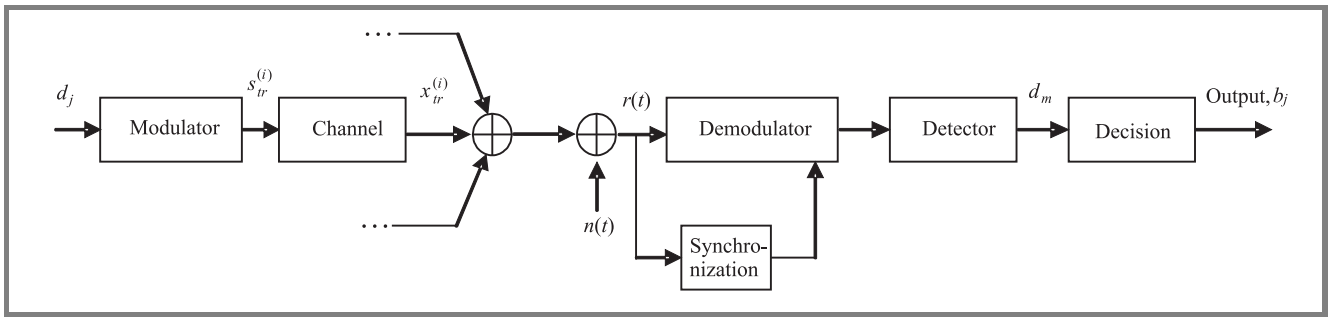

Fig. 3. The system model.

Table 1
Parameters used in simulation of the complete system

Parameters	Values used in simulation
Source data rate [Mbit/s]	16.6
Processing gain [dB]	20.79
Average transmitter power [dBm]	-30
Sampling frequency [GHz]	30
No. of pulse per bit	1
Frame time [ns]	60.1
Periodicity of the TH code	2000
Chip time [ns]	1
Multiuser interference	Single user and multiple user scenarios
Receiver	ARAKE SRAKE, PRAKE with 2, 4, 6, 8, 10, 12, 14, 16, 18, 20, 32 fingers
Channel model	IEEE 802.15.3a, CM-1: 0–2 m, LOS and CM-3: 4–10 m, NLOS
Modulation scheme	PPM
Multiple access	TH
Time shift for PPM [ns]	0.5
Pulse shape	Gaussian 4th derivative
Pulse width [ns]	0.5
Pulse decay factor [ns]	0.168
Code cardinality	5

the basis of observed clustering phenomenon in several channel measurements [7]. Lognormal distribution rather than Rayleigh distribution for the multipath gain magnitude has been recommended. In addition, independent fading is assumed for each cluster as well as each ray within the cluster. Therefore, the discrete impulse response of the multipath channel model (Fig. 4) can be described as [6]

$$h_i(t) = X_i \sum_{l=0}^{L} \sum_{k=0}^{K} \alpha_{k,l}^{i} \delta(t - T_l^i - \tau_{k,l}^i), \qquad (5)$$

where $\{\alpha_{k,l}^i\}$ are the multipath gain coefficients, $\{T_l^i\}$ is the delay of the lth cluster, $\{\tau_{k,l}^i\}$ is the delay of the kth multipath component relative to the lth cluster arrival time (T_l^i), $\{X_i\}$ represents the lognormal shadowing and i refers to the ith realization. So, according to the model, T_l represents the arrival time of the first path (ray) of the lth cluster; $\tau_{k,l}$ is the delay of the kth path (ray) within the lth cluster relative to the first path arrival time, T_l.

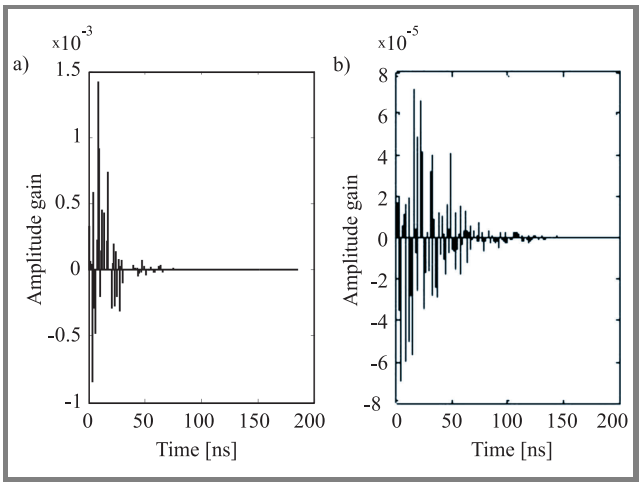

Fig. 4. Discrete time channel impulse response for: (a) CM-1: 0–2 m (LOS); (b) CM-3: 4–10 m (NLOS).

The IEEE 802.15.3a channel model has been explained for four special cases depending on transmitter to receiver distance and the availability of line of sight path be-

Table 2
Model parameters in IEEE 802.15.3a UWB channel [7]

Model parameters	CM-1 LOS at 0–2 m	CM-3 NLOS at 4–10 m
Cluster arrival rate, Λ [1/ns]	0.0233	0.0667
Ray arrival rate, λ [1/ns]	2.5	2.1
Cluster decay factor, Γ	7.1	14
Ray decay factor, γ	4.3	7.9
Std. dev. of cluster log-normal fading, σ_1 [dB]	3.3941	3.3941
Std. dev. of ray log-normal fading, σ_2 [dB]	3.3941	3.3941
Std. dev. of total multipath log-normal fading, σ_x [dB]	3	3

tween them. In this study, CM-1 (0–2 m, LOS) and CM-3 (4–10 m, NLOS) condition of the channel have been used and the corresponding channel parameters are shown in Table 2.

3.3. Receiver section

In the receiver section, selective RAKE receiver has been used. The received signal is the sum of replicas of the transmitted signals. The received signal is, therefore, expressed as

$$r(t) = X \sum_{l=1}^{L} \sum_{k=1}^{K} \alpha_{k,l} s_{tr}(t - T_l - \tau_{k,l}) + n(t) + i(t), \qquad (6)$$

where $s_{tr}(t)$ is the transmitted signal which suffers from attenuation and time delay in multipath propagation, $n(t)$ is zero mean additive white Gaussian noise (AWGN) and $i(t)$ is the multiple user interference signal. For simulation of this study RAKE receivers with 2, 4, 6, 8, 10, 12, 14, 16, 18, 20 and 32 fingers have been used and finding an optimum RAKE receiver finger number has been targeted. First arm is locked to the first multipath component, m_1. Multipath component, m_2 arrives τ_1 time units later than m_1 and is captured and so on. All decision statistics are weighted by a weighting factor, α to form overall decision statistics. The signals are then integrated over the entire period. The integrated signal is then compared with the appropriate threshold value to receive the better estimate of the transmitted signal. Since one pulse per bit of information transmitted is used all through, any of hard decision detection (HDD) or soft decision detection (SDD) can be used at the receiver, however, HDD has been adopted in this paper with TH-PPM UWB systems.

4. RAKE receiver principles

The goal of a RAKE receiver is to combine the energies of the useful signal components. Unfortunately, as a typical UWB channel has hundreds of resolvable paths, too many fingers would be necessary to capture all these energies. In practice, power consumption and channel estimation issues limit the number of fingers to ten or so. This prompts the notion of SRAKE [5], in which only the strongest paths are exploited. On the other hand, an ideal RAKE (ARAKE) is an ideal receiver in which all the non-zero resolvable multipaths are combined. Its performance establishes a benchmark for comparison of practical receivers. The operating principle of an SRAKE is as follows. Let $\{\alpha_q\}_{q=1}^{Q}$ be the gains of Q strongest paths and $\{\tau_q\}_{q=1}^{Q}$ the corresponding delays. Also let us assume that the receiver achieved perfect symbol synchronization for the desired signal. Then according to [4] the decision statistic for the symbol a_i is a weighted sum of the type (maximum ratio combining):

$$x_i = \sum_{q=1}^{Q} \hat{\alpha}_q \int_{iN_fT_f}^{(i+1)N_fT_f} r(t) v(t - iN_fT_f - \hat{\tau}_q) dt, \qquad (7)$$

where $\{\hat{\alpha}_q\}$ and $\{\hat{\tau}_q\}$ are the gain and delay estimates and $v(t)$ is a correlation template waveform depending on the signaling format, which for TH-PPM case, can be expressed as

$$v(t) = w_{tr}(t) - w_{tr}(t - \Delta). \qquad (8)$$

With TH-PPM a decision $\hat{a} = 0$ or $\hat{a}_i = 1$ is made according to whether x_i is positive or negative, respectively, the corresponding decision being $\hat{a}_i = 1$ or $\hat{a}_i = -1$.
The channel impulse response (CIR) is assumed to be known. The total number of non-zero multipath components is found. In the case of ARAKE, all of the non-zero multipath components of CIR vector are considered with equal weight for the weighting factor vector, whereas for SRAKE a predefined number of weighting coefficients are considered in the descending order of their magnitude and the weighting factor vector is formed giving weight proportional to the magnitude of the respective multipath component. On the other hand, in the case of PRAKE receivers, a predefined number of multipath components are considered according to their propagation delay, i.e., on first receive first take basis and not on the basis of descending order of the magnitude as in SRAKE.

5. Results

The bit error rate (BER) performance of UWB system varies significantly as the number of fingers of RAKE receiver in use varies, as shown in this paper in case of TH-PPM UWB system using IEEE 802.15.3a UWB channel

Table 3
Equivalence of PRAKE fingers at BER = 10^{-1}

No. of multi-users	CM-3		CM-1	
	SRAKE	Eqv. PRAKE	SRAKE	Eqv. PRAKE
0, i.e., single user	2	8	2	4
	4	12	4	10
	8	20	8	14
	16	32	16	16
5	2	8	2	6
	4	12	4	8
	8	20	8	14
	16	–32	16	20
10	2	8	2	6
	4	12	4	8
	8	18	8	14
	16	32	16	20
20	2	8	2	6
	4	14	4	10
	8	20	8	14
	16	32	16	20

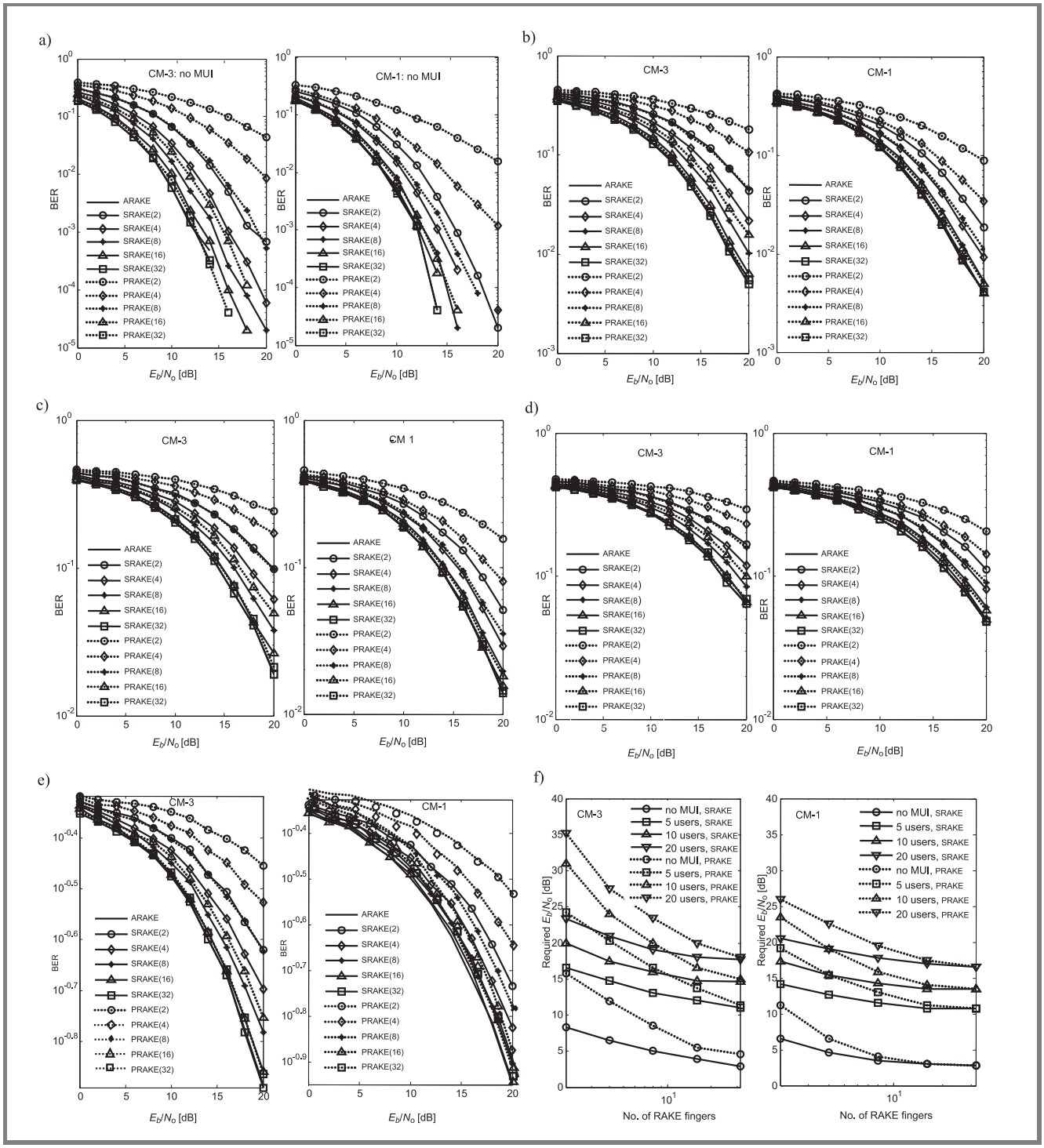

Fig. 5. Performance of TH-PPM UWB system under different multiple user scenarios: (a) single user; (b) 5; (c) 10; (d) 20; (e) 40 interfering users; (f) required SNR characteristics at desired BER of 10^{-1}.

model. In this paper, the equivalence of selective and partial RAKE finger performance has been investigated. As shown in Table 3, for a SRAKE receiver of 2 fingers, for a desired BER of 10^{-1}, as many as 8 PRAKE fingers are needed to achieve the same signal to noise ratio (SNR) requirement at all MUI scenarios. This implies that 4 times as many as SRAKE fingers are needed if PRAKE receiver is used. However, if the number of available SRAKE arms is doubled to 4, 8, 16 it has been found that the equivalent PRAKE arm number required to give the same performance as that of corresponding SRAKE receiver becomes 3, 2.5 and 2 times as many as the SRAKE fingers on an average,

Table 4

SNR gains at different MUI scenarios for variation of RAKE fingers

No. of multi users	CM-3				CM-1			
	SRAKE		PRAKE		SRAKE		PRAKE	
	SNR gain [dB/octave]	No. of fingers, N_f	SNR gain [dB/octave]	No. of fingers, N_f	SNR gain [dB/octave]	No. of fingers, N_f	SNR gain [dB/octave]	No. of fingers, N_f
0, i.e., single user	1.25	$2 \le N_f \le 32$	3.43	$2 \le N_f \le 16$	0.94	$2 \le N_f \le 32$	3.43	$2 \le N_f \le 8$
			1.5	$16 \le N_f \le 32$			1.1	$8 \le N_f \le 32$
5	1.75	$2 \le N_f \le 8$	3.8	$2 \le N_f \le 8$	1.17	$2 \le N_f \le 16$	3.8	$2 \le N_f \le 4$
	1	$8 \le N_f \le 32$	2.64	$8 \le N_f \le 32$	0	$16 \le N_F \le 32$	2.08	$4 \le N_F \le 16$
							0.55	$16 \le N_f \le 32$
10	2.5	$2 \le N_f \le 4$	7	$2 \le N_f \le 4$	1.9	$2 \le N_f \le 4$	3.85	$2 \le N_f \le 8$
	1.4	$4 \le N_f \le 16$	3.75	$4 \le N_f \le 16$	0.95	$4 \le N_f \le 16$	1.2	$8 \le N_f \le 32$
	0.14	$16 \le N_f \le 32$	1.5	$16 \le N_f \le 32$	0.06	$16 \le N_f \le 32$		
20	2.15	$2 \le N_f \le 8$	7.7	$2 \le N_f \le 4$	1.17	$4 \le N_f \le 16$	3.25	$2 \le N_f \le 8$
	0.67	$8 \le N_f \le 32$	3.75	$4 \le N_f \le 16$	0.44	$16 \le N_f \le 32$	1.47	$8 \le N_f \le 32$
			2	$16 \le N_f \le 32$				

respectively, in all MUI scenarios. It is found that increasing multiple users does not affect the ratio of SRAKE to equivalent PRAKE arms for a required SNR, although as shown in Fig. 5, the BER performance degrades severely if the number of multiple users increases. Figures 5a to 5e show the BER performances of the simulated TH-PPM system for different MUI scenarios for CM-3 and CM-1 cases of IEEE 802.15.3a UWB indoor channel model.

On the other hand, Fig. 5f shows the required SNR versus number of RAKE fingers characteristics at different MUI scenarios for a desired BER of 10^{-1}. Three things become clear from Fig. 5f. Firstly, increasing number of RAKE fingers requires comparatively less SNR in order to give the same bit error rate. This effect is desired and true for single user and multiple user scenarios. Secondly, increasing number of multiple users acting simultaneously implies a higher SNR requirement for the same bit error rate and for the same number of RAKE fingers used in the correlator receiver. Thirdly, as shown in Fig. 5f, the SNR requirement for SRAKE and PRAKE receivers changes at different fashions for different multiple user interference scenarios. For instance, as shown in Table 4, when 5 interfering users are present in the system, if the number of RAKE fingers is increased, SRAKE receiver provides an SNR gain at the rate of 1.75 dB/octave for up to 8 SRAKE fingers and 1 dB/octave from 8 fingers to 32 fingers, respectively, thus maintaining a two-slope straight-line relationship between required SNR and logarithm of SRAKE fingers. Whereas using PRAKE receiver we found a similar two-slope relationship but the required SNR decreases at the rates of 3.8 dB/octave and 2.64 dB/octave of the number of fingers of the PRAKE receiver in the same range of PRAKE arms as is shown for SRAKE condition mentioned previously. Table 4 ultimately shows the different SNR gains as a function of SRAKE and PRAKE fingers, especially in presence of multiple user interference. The results for 40 multiple users is omitted here because the BER performance degrades enormously at that condition as shown in Fig. 5e.

As a final note, the BER performance and SNR gains of IEEE channel models, CM-3 and CM-1, have been compared with special focus on different multiple user interference scenarios. The discrete time channel impulse responses of CM-3 and CM-1 have been shown in Fig. 4. As shown in Fig. 5, for single user and with 5, 10, 20 and 40 interfering users transmitting simultaneously, the BER performances for CM-1 have found to be better than those for CM-3 case. This implies the fact that CM-1 is especially for short LOS distances of up to 2 m and CM-3 is for distances greater than 4 m. As shown in Table 3, in case of CM-1, the required number of PRAKE fingers equivalent to given SRAKE fingers is comparatively lower than that required for the corresponding CM-3 case. This is also due to the fact that CM-1 case has less number of significant multipath components than in CM-3, or alternatively, the rays of significant energy are more or less in the first set of rays for PRAKE receiver, which in fact reduces the performance gap between SRAKE and PRAKE receiver of the same number of fingers in CM-1 than in CM-3. Figure 4 shows that for CM-3 some rays with significant energy content can come after a long delay of, for instance, 50 ns. Referring to Table 4, it is found that in single user

case and also in the presence of 5, 10, 20 multiple users, CM-3 provides more SNR gains than in CM-1 case if the number of SRAKE or PRAKE fingers is doubled in 2, 4, 8, 16, 32 fashion. It is found as well in all simulation results that any type of RAKE receiver with 32 fingers would perform as good as an ideal RAKE which has a finger number equal to the number of non-zero multipaths in the system.

Finally, considering that increasing fingers would severely increase receiver complexity, using an SRAKE of 8 fingers has been recommended in this paper, making a trade-off among BER performance, SNR gain and circuit complexity.

6. Conclusions

In this paper the BER performances of TH-PPM UWB system using SRAKE and PRAKE receivers have been compared. Performances of two channel conditions named CM-1 and CM-3 of IEEE 802.15.3a model of UWB channel have been particularly investigated. ARAKE receiver performance is also shown for comparison of performances of SRAKE and PRAKE.

Results obtained through simulations show that the equivalent PRAKE finger number required for maintaining same SNR requirement varies from 2 to 3 times the original SRAKE fingers. Increasing multiple users deteriorates BER performance severely but has no effect on the ratio of the number of PRAKE fingers to that of SRAKE receiver. Results also suggest that with MUI the SNR gains due to increasing number of RAKE fingers for CM-3 channel model are different and are different from CM-1 condition, the gains for CM-1 being slightly lower than those for CM-3. Using a maximum of 32 RAKE fingers, regardless of being of SRAKE or PRAKE type, the ARAKE performance can be achieved. Finally, it is recommended that the number of SRAKE fingers must be limited to 8–10 for getting realistically optimum BER performance.

References

[1] M.-G. Di Benedetto and G. Giancola, *Understanding Ultra Wide Band Radio Fundamentals*. First Edition. Upper Saddle River: Prentice Hall, 2004.

[2] D. Barras, F. Ellinger, and H. Jäckel, "A comparison between ultra-wideband and narrowband transceivers", in *IEEE Wirel. 2002 Conf.*, Calgary, Canada, 2002.

[3] M. Z. Win and R. A. Scholtz, "Ultra-wide bandwidth time hopping spread spectrum impulse radio for wireless multiple access communications", *IEEE Trans. Commun.*, vol. 48, pp. 679–691, 2000.

[4] A. A. D'Amico, U. Mengali, and L. Taponecco, "Performance comparisons between two signaling formats for UWB communications", in *Proc. IEEE Int. Conf. Commun. ICC'04*, Paris, France, 2004.

[5] D. Cassioli, M. Z. Win, F. Vatalaro, and A. F. Molish, "Performance of low-complexity Rake reception in a realistic UWB channel", in *Proc. IEEE Int. Conf. Commun. ICC'02*, New York, USA, 2002, pp. 763–767.

[6] "IEEE Standard for Information technology – Telecommunications and information exchange between systems – Local and metropolitan area networks – Specific requirements". Part 15.3: "Wireless Medium Access Control (MAC) and Physical Layer (PHY) Specifications for High Rate Wireless Personal Area Networks (WPANs)", IEEE Std 802.15.3^{TM}-2003.

[7] J. R. Foerster, M. Pendergrass, and A. F. Molisch, "A channel model for ultrawideband indoor communication", in *Proc. Wirel. Pers. Multimed. Commun. WPMC'03*, Kanagawa, Japan, 2003, vol. 2, pp. 116–120.

[8] H. Sheng, P. Orlik, A. M. Haimovich, L. J. Cimini Jr., and J. Zhang, "On the spectral and power requirements for ultra-wideband transmission", in *Proc. IEEE Int. Conf. Commun. ICC'03*, Anchorage, USA, 2003, pp. 738–742.

Mohammad Upal Mahfuz received his B.Sc. engineering degree in electrical and electronic engineering from Bangladesh University of Engineering and Technology (BUET), Dhaka, Bangladesh, in 2002 and Master of engineering degree in telecommunications from Asian Institute of Technology (AIT), Thailand, in 2005. Currently, he is working towards his doctorate degree at University of Calgary, Canada. His current research interests include ultra wideband wireless communications, mobile communications and satellite-based positioning and navigation systems.

e-mail: upal41@yahoo.com
Telecommunications Program
Asian Institute of Technology (AIT)
PO Box: 4, Khlongluang
Pathumthani 12120, Thailand

Kazi M. Ahmed received the M.Sc. Eng. degree in electrical engineering from the Institute of Communications, Leningrad, USSR, and the Ph.D. degree from the University of Newcastle, NSW, Australia, in 1978 and 1983, respectively. Currently, he is a Professor of telecommunications in the School of Engineering and Technology, Asian Institute of Technology, Pathumthani, Thailand. His current research interests include digital signal processing, antenna array processing, tropospheric and ionospheric propagation studies for microwave, very high frequency-ultra high frequency communications, and satellite communications.

e-mail: kahmed@ait.ac.th
Telecommunications Program
Asian Institute of Technology (AIT)
PO Box: 4, Khlongluang
Pathumthani 12120, Thailand

Nandana Rajatheva received the B.Sc. degree in electronic and telecommunication engineering (with first class honors) from the University of Moratuwa, Sri Lanka, and the M.Sc. and Ph.D. degrees from the University of Manitoba, Winnipeg, Canada, in 1987, 1991, and 1995, respectively. Currently, he is an Associate Professor of telecommunications in the School of Engineering and Technology, Asian Institute of Technology, Pathumthani, Thailand. Earlier, he was with the University of Moratuwa, Sri Lanka, where he became a Professor of electronic and telecommunication engineering in June 2003. From May 1996 to December 2001, he was with TC-SAT as an Associate Professor. His research interests include mobile and wireless communications, coding and modulation techniques, space time processing for multiple input-multiple output systems, and communication theory.

e-mail: rajath@ait.ac.th
Telecommunications Program
Asian Institute of Technology (AIT)
PO Box: 4, Khlongluang
Pathumthani 12120, Thailand